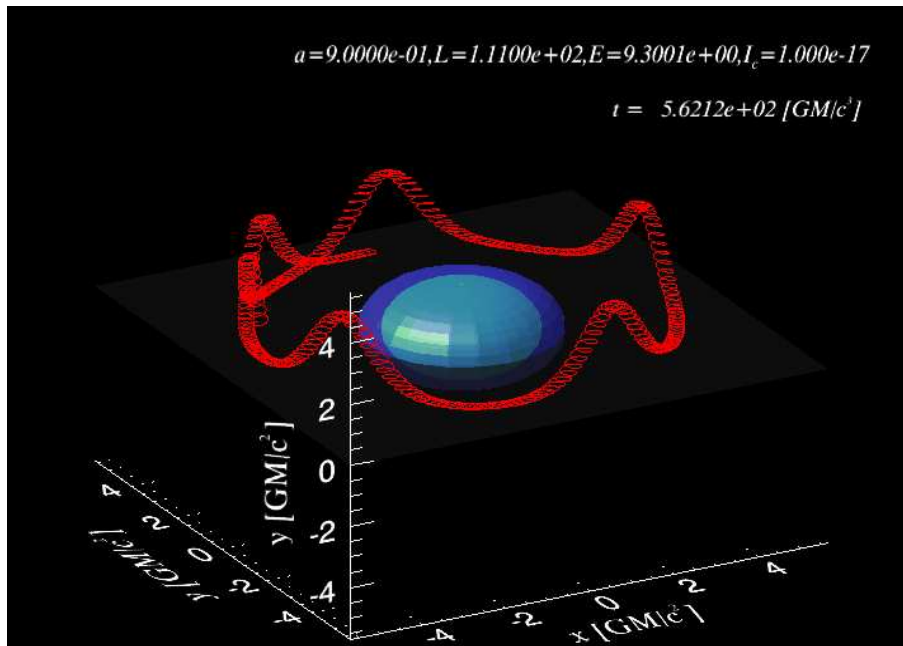


Dionysopoulou Kyriaki  
kdioni@physics.auth.gr

Diploma thesis  
Supervisor: Prof. N. Stergioulas  
niksterg@astro.auth.gr

# *Charged-Particles Orbits Near Magnetized Black Holes*



ARISTOTLE UNIVERSITY OF THESSALONIKI  
SCHOOL OF NATURAL SCIENCES  
DEPARTMENT OF PHYSICS  
16 November, 2008



# Acknowledgements

I want to thank my supervisor prof. Nikolaos Stergioulas who always encouraged me and provided me with valuable help and advice. Without him not a part of this work would have been completed. For my education in physics and astrophysics, I would also like to thank all my professors at the Aristotle University of Thessaloniki, and especially professors George Lalazisis, John H. Seiradakis, Nikolaos Spyrou. I have benefited significantly from the lectures taught by the late professor Symeon Ichtiaroglou. In addition, I acknowledge prof. Loukas Vlahos for introducing me to computational astrophysics and research and for any useful advice he gave me. Finally, prof. Kostas Kokkotas for the appreciable discussions we had.

I acknowledge all my friends, my family, especially my parents and brother Yianis, for their persistent support. Last but not least, I would like to thank Thanos, Vivi and Theodora for their patience and encouragement during my studies at the Aristotle University of Thessaloniki.



# Abstract

We examine the impact of external magnetic fields on the motion of charged particles in the neighborhood a Kerr black hole immersed in a uniform or dipolar magnetic field. In particular, we examine non-equatorial orbits and show three-dimensional presentations of the orbits that cross the equatorial plane. We find that there exist non-equatorial orbits that do not cross the equatorial plane for uniform magnetic fields and dipole magnetic fields. This kind of orbits could lead to observable effects. Finally, we investigate the motion of a group of particles which escape from the surface of a simple model of an accretion disk.



# Contents

|          |   |           |
|----------|---|-----------|
| <b>1</b> | <b>Introduction</b>   | <b>1</b>  |
| 1.1      | Description of Curved Spacetimes . . . . .                              | 2         |
| 1.2      | Units Employed . . . . .  | 3         |
| 1.3      | Kerr Geometry . . . . .   | 4         |
| 1.3.1    | The Kerr metric . . . . .   | 4         |
| 1.3.2    | Properties of the Kerr geometry . . . . .                               | 4         |
| 1.4      | Magnetic Fields in Astrophysics . . . . .                               | 5         |
| 1.5      | Motivation . . . . .  | 7         |
| <b>2</b> | <b>Theoretical Analysis</b>   | <b>9</b>  |
| 2.1      | Magnetic Fields Studied . . . . .                                       | 9         |
| 2.1.1    | Visualizing the Magnetic Field in GR . . . . .                          | 9         |
| 2.1.2    | Uniform Magnetic Field . . . . .  | 11        |
| 2.1.3    | Dipole Magnetic Field . . . . .   | 13        |
| 2.2      | Equations of Motion in a Kerr Background Geometry . . . . .             | 20        |
| 2.3      | The Effective potential . . . . .                                       | 21        |
| 2.4      | Guiding Center and Combined Gravitational and Magnetic Fields . . . . . | 23        |
| <b>3</b> | <b>Charged-Particle Motions</b>   | <b>25</b> |
| 3.1      | Numerical Analysis . . . . .  | 25        |
| 3.1.1    | Assumptions . . . . .   | 25        |
| 3.1.2    | Integral of Motions . . . . .   | 26        |
| 3.2      | Trajectories in the Equatorial Plane . . . . .                          | 26        |
| 3.2.1    | Uniform Magnetic Field . . . . .  | 27        |
| 3.2.2    | Dipole Magnetic Field . . . . .   | 27        |
| 3.3      | Trajectories including Lateral Motion . . . . .                         | 35        |
| 3.3.1    | Uniform Magnetic Field . . . . .  | 35        |
| 3.3.2    | Dipole Magnetic Field . . . . .   | 35        |
| 3.4      | Motion of a Group of Particles . . . . .                                | 37        |
| 3.4.1    | No magnetic field . . . . .   | 38        |
| 3.4.2    | Uniform magnetic field . . . . .  | 39        |
| 3.4.3    | Dipole magnetic field . . . . .   | 40        |
| <b>4</b> | <b>Halo Orbits</b>  | <b>41</b> |
| 4.1      | Introduction . . . . .  | 42        |
| 4.2      | Halo Orbits . . . . .   | 43        |
| 4.2.1    | Kerr Black hole . . . . .   | 44        |
| 4.2.2    | Kerr-Newman black hole . . . . .  | 52        |
| <b>5</b> | <b>Conclusions</b>  | <b>55</b> |

|                                    |           |
|------------------------------------|-----------|
| <b>APPENDIX</b>                    | <b>57</b> |
| <b>The Numerical Code</b>          | <b>59</b> |
| A.1 Equations of Motion . . . . .  | 60        |
| A.1.1 Fortran . . . . .            | 60        |
| A.1.2 IDL . . . . .                | 74        |
| A.2 Magnetic Field Lines . . . . . | 90        |
| A.2.1 Fortran . . . . .            | 90        |
| A.2.2 IDL . . . . .                | 91        |
| <b>Bibliography</b>                | <b>95</b> |

# List of Figures

|     |   |    |
|-----|---|----|
| 1.1 | The different regions of a Kerr black hole are shown. Two event horizons and the ergosphere of the Kerr black hole are illustrated. . . . .   | 5  |
| 2.1 | Magnetic field lines of a uniform magnetic field near a Kerr black hole as measured by a ZAMO observer. The blue surface indicates the boundaries of the ergosphere and the green one the outer event horizon. (a) The magnetic field lines thread the event horizon for an $a = 0$ Kerr black hole. (b) Magnetic field lines are expelled from the horizon for an $a = 0.9$ black hole. . . . .  | 12 |
| 2.2 | Magnetic field lines of a dipole magnetic field near a Kerr black hole as measured by ZAMO observer. The blue surface indicates the boundaries of the ergosphere and the green one the outer event horizon. (a) The magnetic field lines thread the event horizon for an $a = 0$ Kerr black hole. (b) Magnetic field lines are expelled from the horizon for an $a = 0.9$ black hole. . . . .   | 19 |
| 3.1 | (a,c) The motion of a proton in the field of Kerr black hole endowed in a uniform magnetic field is depicted for different initial conditions. (b,d) The effective potential is illustrated for this case (black solid line). The effective potential for the case without a magnetic field is shown is represented with the dotted line. Finally the red line corresponds to the particle's energy $E$ . . . . .   | 28 |
| 3.2 | (a,c) The motion of a proton in the field of Kerr black hole endowed in a uniform magnetic field is depicted for different initial conditions. In fig.(a) the particle performs a nearly-circular energetically bound orbit almost touching the horizon. In fig.(c) the particle "hits" the event horizon. (b,d) The effective potential is illustrated for this case (black solid line). The effective potential for the case without a magnetic field is shown is represented with the dotted line. Finally the red line corresponds to the particle's energy $E$ . . . . . | 29 |
| 3.3 | (a,c) The motion of a proton in the field of Kerr black hole endowed in a uniform magnetic field is depicted for different initial conditions. We observe that outside ergosphere the particle is allowed to gyrate, will inside circular motions are forbidden. (b,d) The effective potential is illustrated for this case (black solid line). The effective potential for the case without a magnetic field is shown is represented with the dotted line. Finally the red line corresponds to the particle's energy $E$ . . . . .   | 30 |
| 3.4 | (a,c) The motion of a proton in the field of Kerr black hole endowed in a uniform magnetic field is depicted for different initial conditions. (b,d) The effective potential is illustrated for this case (black solid line). The effective potential for the case without a magnetic field is shown is represented with the dotted line. Finally the red line corresponds to the particle's energy $E$ . For negative angular momentum the potential well appears in longer distances from the black hole something which is presumable. . . . .                             | 31 |

|      |   |    |
|------|---|----|
| 3.5  | (a,c) The motion of a proton in the field of Kerr black hole endowed in a uniform magnetic field is depicted for different initial conditions. (b,d) The effective potential is illustrated for this case (black solid line). The effective potential for the case without a magnetic field is shown is represented with the dotted line. Finally the red line corresponds to the particle's energy $E$ . . . . .   | 32 |
| 3.6  | (a,c) The motion of a proton in the field of Kerr black hole endowed in a dipole magnetic field (internal solution) is depicted for different initial conditions. (b,d) The effective potential is illustrated for this case (black solid line). The effective potential for the case without a magnetic field is shown is represented with the dotted line. We observe that a particle residing in the region $r < r_o$ can only escape if it has energy greater than the value of the effective potential at the limit $r = r_o$ . . . . .  | 33 |
| 3.7  | (a,c) The motion of an electron is depicted in the field of Kerr black hole endowed in a dipole magnetic field (external solution) is depicted. The Larmor motion of the particle has the opposite direction because of the negative charge of the electron. (b,d) The effective potential is illustrated for this case (black solid line). The effective potential for the case without a magnetic field is shown is represented with the dotted line. Finally the red line corresponds to the particle's energy $E$ . For negative angular momentum the potential well appears in longer distances from the black hole something which is presumable. . . . . | 34 |
| 3.8  | (a) The motion of a proton is depicted for the uniform magnetic field case. (b) The effective potential is illustrated for this case. The closed line corresponds to the bound orbit. . . . .   | 35 |
| 3.9  | (a) The motion of a proton is depicted for the magnetic dipole field case (internal solution). (b) The effective potential is illustrated for this case. The closed line corresponds to the bound orbit. . . . .  | 36 |
| 3.10 | The motion of a proton is depicted for the magnetic dipole field case (internal solution)   | 36 |
| 3.11 | The motion of an electron is depicted. . . . .  | 37 |
| 3.12 | The trajectories of protons (red dots) and electrons (green dots) are depicted. . . . .   | 38 |
| 3.13 | The trajectories of protons (red dots) and electrons (green dots) are depicted for the uniform magnetic field case. . . . .   | 39 |
| 3.14 | The trajectories of protons (red dots) and electrons (green dots) are depicted for the dipole magnetic field case. . . . .  | 40 |
| 4.1  | Effective potential $V_{eff}$ and its contours for motion of a charged particle in an extreme $a = 0.9$ Kerr black hole and an external uniform magnetic field. The axis of the magnetic field is parallel to the angular momentum of the black hole. The constants of motion are $L = 100$ , $E = 9.0999971$ and the magnetic field strength $B_o = 10^{-17}$ . The particle is a proton. . . . .  | 44 |
| 4.2  | The motion of a proton is depicted. The magnetic field forces the particle to execute Larmor motion of constant radius. The particle doesn't cross the equatorial plane. . . . .  | 45 |
| 4.3  | The motion of an electron is depicted. This motion is an intermediate step between the trajectories depicted in 3.8(a) and 4.2 . . . . .  | 45 |
| 4.4  | The dependence of $V_{eff}$ is shown in the pictures above. Roughly, increasing the angular momentum of the black hole, the lowest energy for a particle to participate in an off-equatorial circular motion is increased. Coinstantaneously the local minimum moves to a greater distance. As the angular momentum $L$ of the particle grows bigger, both the lowest energy and the distance of the local minimum from the black hole take greater values. Lastly, increasing the factor $k = qB_o/m_{part}$ , the lowest energy increases too, while the position of the local minimum moves towards $z = 0$ . . . . .  | 46 |

4.5 Effective potential  $V_{\text{eff}}$  and its contours for motion of charged particle in a  $a = 0.9$  Kerr black hole and an external dipole magnetic field. The internal solution of the magnetic dipole is considered. The axis of the magnetic field is parallel to the angular momentum of the black hole. The constants of motion are  $L = 70$  ,  $E = 5.3059152$  and the ring current that generates the magnetic field is  $I_c = 10^{-17}$ . The particle is a proton. . . . . 48

4.6 The dependence of  $V_{\text{eff}}$  is shown in the pictures above. (a) Roughly, increasing the angular momentum of the black hole, the lowest energy for a particle to participate in an off-equatorial circular motion is increased. Coinstantaneously the local minimum moves to a greater distance until it reaches a maximum and then moves towards the black hole. (b) As the angular momentum  $L$  of the particle grows bigger, both the lowest energy and the distance of the local minimum from the black hole take greater values. (c),(d) Lastly, increasing the current  $I_c$  and the factor  $q/m_{\text{part}}$ , the minimum energy increases too. The position of the local minimum moves away from the black hole in both graphs (c,d). . . . . 49

4.7 Effective potential  $V_{\text{eff}}$  and its contours for motion of charged particle in a  $a = 0.55$  Kerr black hole and an external dipole magnetic field. The external solution of the dipole magnetic field is considered. The axis of the magnetic field is parallel to the angular momentum of the black hole. The constants of motion are  $L = 1$  ,  $E = 0.95608159$  and the ring current that generates the magnetic field is  $I_c = 10^{-21}$ . The particle is a an electron. . . . . 50

4.8 The motion of an electron is depicted. The magnetic field forces the particle to execute Larmor motion of variable radius. The particle doesn't cross the equatorial plane. . . . . 50

4.9 The dependence of  $V_{\text{eff}}$  is shown in the pictures above. Roughly, increasing the angular momentum of the black hole, the minimum energy for a particle to participate in an off-equatorial circular motion is decreased. Coinstantaneously the local minimum moves to a greater distance from the black hole. As the angular momentum  $L$  of the particle grows bigger, the minimum energy increases while the local minimum approaches  $z = 0$ . For  $L = 3.5 - 6.0$  there are no halo orbits. The local minimum, for these values of  $L$ , corresponds to circular orbits exactly at the equatorial plane. Increasing  $I_c$  and  $q/m$  the local minima occur for greater values of energy. In addition, they move away from the black hole. . . . . 51

4.10 The contours of the effective potential for motion of charged particle in a  $a = 0.9$ ,  $Q = 5 \times 10^{-17}$  Kerr-Newman black hole and an external uniform magnetic field. The axis of the magnetic field is parallel to the angular momentum of the black hole. The constants of motion are  $L = 500$  ,  $E = 48.866846$  and the magnetic field  $B_o = 1.0 \times 10^{-16}$ . The particle is a proton. . . . . 52

4.11 The dependence of  $V_{\text{eff}}$  is shown in the pictures above. Roughly, increasing the net charge of the black hole, the minimum energy for a particle to participate in an off-equatorial circular motion is decreased. Coinstantaneously the position of the local minimum moves to larger  $z$ . As the magnetic field strength  $B_o$  grows bigger, the minimum energy takes greater values. The particle now moves towards the black hole. Lastly, increasing the factor  $q/m$ , the lowest energy increases too, while the particle moves towards  $z = 0$ . . . . . 53

4.12 (a) Contour plots of the effective potential  $V_{\text{eff}}$  for motion of charged particle in a  $a = 0.25$ ,  $Q = 3 \times 10^{-22}$  Kerr-Newman black hole and an external dipole magnetic field (external solution). The constants of motion are  $L = 1$ ,  $E = 0.98837041$  and the value of the ring current is  $I_c = 1.0 \times 10^{-21}$ . The particle is an electron. (b) Contour plots of the effective potential  $V_{\text{eff}}$  for motion of a proton in a  $a = 0.9$ ,  $Q = 3 \times 10^{-18}$  Kerr-Newman black hole and an external dipole magnetic field (internal solution). The constants of motion are  $L = 70$ ,  $E = 4.513327310$  and the value of the ring current is  $I_c = 1.0 \times 10^{-17}$ . . . . . 54

4.13 The dependence of  $V_{\text{eff}}$  is shown in the pictures above. (a) Increasing the net charge of the black hole, the minimum energy for a particle to participate in an off-equatorial circular motion is increased. Coinstantaneously the position of local minimum moves to a greater distance (external solution). (b) The local minima occur for lower values of energy while the net charge of the hole increases. In addition it moves towards  $z = 0$  (internal solution). . . . . 54

# Chapter 1

## Introduction

Magnetic fields play a crucial role in astrophysics. The importance of their study arises from the fact that compact objects, e.g. neutron stars and black holes, can possess strong electromagnetic fields. In the neighborhood of these objects is where astrophysically significant phenomena occur. Near rotating bodies, the field lines are deformed by gravity in the vicinity of the objects.

The work done on this paper refers to space, time, gravity, magnetic fields and how all of the previous quantities can be coupled to each other. The basic idea in general theory of relativity is that gravitation originates from the curvature of spacetimes (4-D), the coupling of space (3D) and time (1-D). It is due to the presence of mass or energy in the background geometry that spacetime becomes deformed. In particular, the curvature depends on the total density of a given spot. Gravity is directly related to the geometry of the region under investigation. In order to describe gravity in terms of mathematics it is essential to employ differential geometry.

In general relativity, black holes are created whenever mass, under specific circumstances, is condensed into a sphere with radius less than twice its mass (in gravitational units), and gravitational forces are so large that none of the other known forces can counterbalance their effect. A consequence of this fact is the gravitational collapse of the astrophysical object to a singularity surrounded by an event horizon. The gravitational forces are so strong in the neighborhood of the black hole that trajectories of both particles and light are strongly affected, compared to the Newtonian limit.

Newtonian mechanics gives us a first estimate of the escape velocity  $V_{\text{esc}}$  for a particle located at a distance  $R$  to escape the black hole.

$$\frac{1}{2}mV_{\text{esc}}^2 = \frac{GMm}{R}$$

When particle's velocity is greater than the velocity  $V_{\text{esc}}$  then the particle escapes, otherwise it's sucked into the hole. Escape velocity equals the speed of light when:

$$\frac{2GM}{c^2R} = 1 \tag{1.0.1}$$

which defines the Schwarzschild radius  $R = R_S$ .

Although the Newtonian approach is not suitable in this case, due to the appearance of relativistic effects, the result (1.0.1) is the same as the one obtained using relativity. The surface  $r = R_S$  is called the event horizon from within which nothing can escape the gravitational attraction of the object.

Black holes of several solar masses have been detected in binary systems. Supermassive black holes, of several million to billion solar masses have been detected in the center of galaxies. There is evidence that almost every large galaxy contains a supermassive black hole at its center. In particular, at the center of our galaxy, the Milky Way, there is a supermassive black hole of 3 million solar masses.

Bearing in mind the initial angular momentum of the protostellar cloud that formed the black hole, it is impossible for the black hole to have zero angular momentum. It is indeed so, because of the small radius of the black hole that its angular momentum would take an extremely high value. Presence of remaining matter in its surroundings or matter accreted from a companion allow for the formation of an accretion disc around the compact object. Plasma circling around the black hole creates a hot disk. Particles colliding with each other can become a source of X-ray radiation. Despite the fact that black holes are “dark”, the extremely distorted spacetime around them is an “arena” of the most wonderful, yet eruptive, phenomena of astrophysics. Ionized matter in the disk is also responsible for the generation of electromagnetic fields.

Even if the precise mechanism of radiation emission from the accretion disk is not yet fully understood, it is generally believed that plasma, consisting the accretion disk, is accountable for X-ray emission. A small fraction of this radiation, after traveling through space, becomes detectable. This radiation makes the black hole “visible” in X-rays and gamma-rays<sup>1</sup>. Thus, it is necessary to construct a theory adequate to predict and explain the formation and evolution of the accretion disk.

It is well known that moving charges account for a magnetic field. The exact structure of the electromagnetic fields produced by the accretion disk is difficult to be determined. Simulations using an ideal MHD approach are useful for this task, but can only yield estimates because ideal MHD is based on some assumptions that are likely to break near a black hole. The phenomena occurring in the disk are far more complex and compelling than this approximation describes. So, what happens near a black hole immersed in the magnetic field generated by an accretion disk surrounding it? We know that magnetic field lines are nearly frozen in the accretion disk and in a way follow the rotation of the disk. Does a magnetic field, generated by a current loop, affect the background geometry of the strongly gravitating object? How does the background geometry affect the structure of the magnetic fields? What is the topology of these magnetic fields? What is the structure of the charged magnetosphere around the black hole?

The answer to the above questions is not simple. An exact theory is difficult to be achieved. Consequently, one has to rely on some approximate models. Two main options are available. The single particle motion and the magnetohydrodynamics. The first theory considers the motion of charged test particles in the field of a black hole endowed in a magnetic field, while the second one neglects the individual motion of charged particles and accounts only for the advection of magnetic fields in a magnetized fluid. Sometimes it is suggestive that one uses both approaches, depending on the specific problem one examines.

## 1.1 Description of Curved Spacetimes

In general, spacetime is described by its metric, expressed through:

$$ds^2 = g_{\alpha\beta} dx^\alpha dx^\beta \quad (1.1.1)$$

where  $g_{\alpha\beta}$  is a symmetric tensor and  $x^a$  are the coordinates.

The metric is determined by the Einstein equations relating spacetime curvature to energy density of matter fields or electromagnetic fields. The Einstein equations are:

$$R_{\mu\nu} - \frac{1}{2} R g_{\mu\nu} = 8\pi G T_{\mu\nu} \quad (1.1.2)$$

The expression on the left hand side is a measure of the curvature of spacetime, while the right hand side of (1.1.2) is, apart from a constant, the energy-momentum tensor. The effects on particle’s trajectory can be summarized by the following sentence:

---

<sup>1</sup>Gamma-rays are emitted in places where the gravitational energy density is very high. Therein particle creation is allowed. Creation of pairs and their annihilation supply a mechanism for gamma-rays emission.

Free particles move along such trajectories, that they travel in the shortest distance. These trajectories are called geodesics. In the case of flat spacetime, particles move in straight lines. Conversely, when spacetime is curved there are no straight lines. Therefore, particles tend to follow the shortest path.

There is a more elegant definition of a geodesic line. Extremal proper time world lines are called geodesics, and the equations of motion that determine them comprise the geodesic equation.

The geodesic equations are:

$$\frac{d^2 x^\mu}{d\lambda^2} + \Gamma^\mu_{\rho\sigma} \frac{dx^\rho}{d\lambda} \frac{dx^\sigma}{d\lambda} = 0 \quad (1.1.3)$$

where  $\lambda$  is an affine parameter which depends on the nature of the particle<sup>2</sup>. Concerning  $\Gamma^\mu_{\rho\sigma}$ , this is one of the Christoffel symbols and is given by  $\Gamma^\mu_{\rho\sigma} = 1/2 g^{\mu\nu} (g_{\nu\rho,\sigma} + g_{\nu\sigma,\rho} - g_{\rho\sigma,\nu})$ . The indices run from 1 to 4.

On the right hand side of equation (1.1.3) we can add other forces

$$\frac{d^2 x^\mu}{d\tau^2} + \Gamma^\mu_{\rho\sigma} \frac{dx^\rho}{d\tau} \frac{dx^\sigma}{d\tau} = \frac{f^\mu}{m} \quad (1.1.4)$$

Henceforth, the only extra force we will consider will be the Lorentz force. In this case, the previous equation takes the form:

$$\frac{d^2 x^\mu}{d\tau^2} + \Gamma^\mu_{\rho\sigma} \frac{dx^\rho}{d\tau} \frac{dx^\sigma}{d\tau} = \frac{q}{m} F^\mu_{\nu} \frac{dx^\nu}{d\tau} \quad (1.1.5)$$

Where  $F^\mu_{\nu} = g^{\mu\kappa} F_{\kappa\nu}$  and  $F_{\mu\nu} = A_{\nu,\mu} - A_{\mu,\nu}$ , with  $A_\mu$  being the electromagnetic vector potential and  $q$  is the particle's charge and  $m$  is its mass.

Placing a charged particle in an electromagnetic field, it will start gyrating around the magnetic field lines. It's motion is a helical. The radius of the helica is finite and given by the relation  $r_L = mv_\perp c / |q|B \approx (0.2cm)(B/10^4G)^{-1}$ . However, the concept of Larmor radius is somewhat different in general relativity because of the distortion of spacetime. From classical electrodynamics we know that accelerated charged particles emit radiation. In the context of this work and for simplicity we will neglect this phenomenon.

Geodesic equations or equations of motion can be derived by investigating the Lagrangian of the system. The Lagrangian of the system we describe is given by:

$$\mathcal{L} = \frac{1}{2} g_{\mu\nu} u^\mu u^\nu + \frac{q}{m} A_\mu u^\mu \quad (1.1.6)$$

and the equations of motion are then derived from:

$$\frac{d}{d\tau} \left( \frac{\partial \mathcal{L}}{\partial u^\mu} \right) - \frac{\partial \mathcal{L}}{\partial x^\mu} = 0 \quad (1.1.7)$$

## 1.2 Units Employed

For the theoretical analysis we adopt the geometrized units in which  $G = c = 1$ . For the computational analysis we will adopt the dimensionless units for which  $G = c = M = 1$ . The conversion to the Gauss-cgs system is performed using the dimensionless quantities with following fundamental

---

<sup>2</sup>If the particle is classical then  $\lambda$  represents the proper time  $\tau$ . If the particle is a tachyon, a particle with superluminal velocity, then  $\lambda$  represents the proper length  $s$ . In the case that the particle is a photon,  $\lambda$  is neither the proper length nor the proper time, but simply parametrizes the geodesic line

length ( $L$ ), time ( $T$ ), mass ( $M$ ), charge ( $q$ ) and magnetic field strength ( $B$ ):

$$L = \frac{G M_{bh}}{c^2} \quad (1.2.1)$$

$$T = \frac{G M_{bh}}{c^3} \quad (1.2.2)$$

$$M = M_{bh} \quad (1.2.3)$$

$$q = \sqrt{G} M_{bh} \quad (1.2.4)$$

$$B = \frac{c^4}{G^{3/2} M_{bh}} \quad (1.2.5)$$

## 1.3 Kerr Geometry

### 1.3.1 The Kerr metric

Except of the non-rotating black holes (Schwarzschild), there is a more realistic. A rotating sphere assigned with the properties of a black hole. This is the Kerr black hole. The metric that describes spacetime around that object reads,

$$ds^2 = - \left( 1 - \frac{2Mr}{\Sigma} \right) dt^2 - \frac{4Mra}{\Sigma} \sin^2 \theta dt d\phi + \frac{\Sigma}{\Delta} dr^2 + \Sigma d\theta^2 + \frac{B}{\Sigma} \sin^2 \theta d\phi^2 \quad (1.3.1)$$

where

$$\begin{aligned} \Sigma &= r^2 + a^2 \cos^2 \theta, \quad \Delta = r^2 + a^2 - 2Mr \\ B &= (r^2 + a^2)^2 - \Delta a^2 \sin^2 \theta, \quad a = J/M \end{aligned}$$

In addition  $J =$  Komar angular momentum and measures the angular momentum of the black hole. It is obvious that for  $a = 0$  the above metric reduces to a Schwarzschild black hole, namely a solution of the Einstein equations that describe a static non-rotating black hole. The coordinate  $(t, \rho, \theta, \phi)$  are that of Boyer-Lindquist and the mapping to the Euclidean space is performed by the conversion:

$$\begin{aligned} x &= (r^2 + a^2)^{1/2} \sin \theta \cos \phi \\ y &= (r^2 + a^2)^{1/2} \sin \theta \sin \phi \\ z &= r \cos \theta \end{aligned}$$

### 1.3.2 Properties of the Kerr geometry

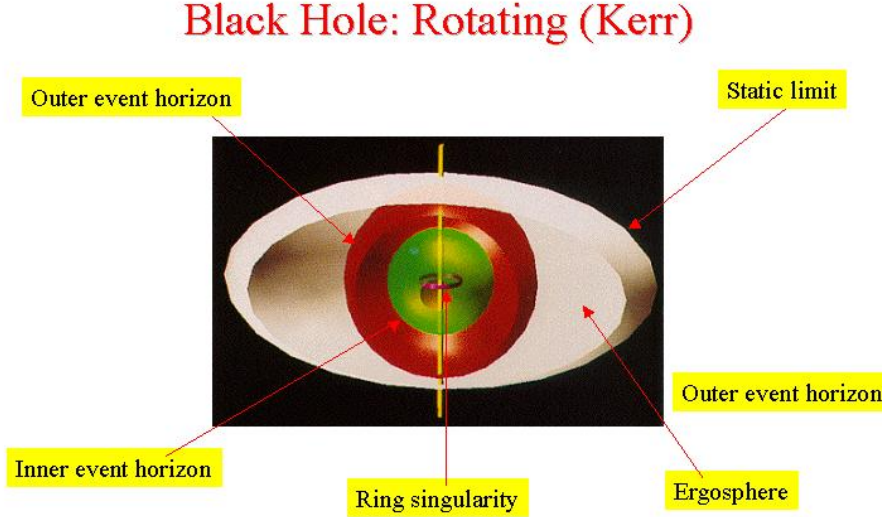
The solution of Einstein equations for a rotating black hole is a solution of stationary, but not static, black hole. Stationarity implies that its angular momentum is the same as time passes by. Alternatively, we could say that a Kerr black hole is not static because it's independent of time inversion. Changing the sign of time  $t \rightarrow -t$  in equations would result to a reversed sign of black hole's angular momentum.

Boyer-Lindquist coordinates are not suitable for the study of motion inside the horizon. Some of the metric components expressed in these coordinates become undetermined for specific values of  $r$  and  $\theta$  when  $a \leq M$ . The quantity  $\Delta$  is nullified when:

$$r_{\pm} = M \pm \sqrt{M^2 - a^2} \quad (1.3.2)$$

which infers that there are two event horizons because the term  $r^2/\Delta dr^2$  becomes zero. It can be shown that the outer event horizon is nothing more than an irregularity of the coordinates chosen. For the places where  $r = 0$  and  $\theta = \pi/2$  this irregularity is real. At that point spacetime curvature

becomes infinite and this anomaly of the coordinates cannot be eliminated. The conclusion is that passing even through the outer event horizon there is no turning back. We can easily deduce from (1.3.2), that for  $a > M$  the event horizons disappear, meaning that the existence of a black hole with  $a > M$  is impossible.



From *Black Holes - A Traveller's Guide*, by Clifford Pickover (Wiley 1996).

**Figure 1.1:** The different regions of a Kerr black hole are shown. Two event horizons and the ergosphere of the Kerr black hole are illustrated.

Additionally to the above surfaces there is one more. This surface provides the static limit for a particle that enters the gravitational potential of a black hole. On that surface the term  $g_{tt} = 1 - 2mr/\Sigma$  is zero. Consequently,

$$R_+ = m + \sqrt{m^2 - a^2 \cos^2 \theta} \quad (1.3.3)$$

The equation (1.3.3) defines a surface that surrounds the outer event horizon and is the locus of points that allow for a static observer.

Fig. 1.1 illustrates the ergosphere, which is the space between the outer event horizon and the static limit. When a particle resides inside the ergosphere it can only corotate with the black hole. However, the particle can approach or escape the black hole. The concept is that no matter how much energy we give to a particle located inside the ergosphere, it is not possible for the particle to remain still therein. The dragging of inertial frames is so strong that the particle is dragged along by the black holes rotation. Ergosphere is of great importance because it allows for energy extraction from the black hole (Penrose process and Blandford-Znajek mechanism). Furthermore no circular orbits are allowed inside the ergosphere even in the presence of the magnetic field. A charged particle executing a circular orbit inside the ergosphere will corotate only for half of the motion and then counterrotate.

## 1.4 Magnetic Fields in Astrophysics

In classical electrodynamics magnetic fields are governed by Maxwell's equations. These are first order differential equations for the electric and magnetic field vectors. In general relativity, the

mutually coupled electric and magnetic field can be combined in terms of the electromagnetic tensor  $F_{\mu\nu}$  (or Faraday tensor), comprising both components of the electromagnetic field in a single quantity.

Here, we will consider only a Kerr black hole as the gravitational source. This is done so because the Kerr black hole is stationary and axially symmetric and corresponds to one of the simpler, yet close to reality, cases. As for the magnetic field, we will investigate the cases of an external asymptotically uniform magnetic field and a dipole magnetic field generated by a ring current placed at the equatorial plane.

Generally magnetic fields are represented by their lines of force. According to our intuitive definition, a uniform field would be characterized by field lines which are parallel to each other. This is not always the case in general relativity. Magnetic field lines are observer dependent. Though Maxwell's equations don't couple with newtonian gravity, general relativity comes to change this fact. In particular, the magnetic energy density, as the energy density of any other field, contributes to the Einstein's equations, which describe the spacetime structure. As of that fact, Einstein's and Maxwell equations must be considered simultaneously. We will see that near rapidly rotating and strong gravitating sources spacetime is deformed and dragged along with the hole. This deformation and dragging also affects the structure of the magnetic field. The magnetic field lines do reflect the presence of the body.

In order to calculate the magnetic field around these astronomical objects, we either have to solve the coupled Einstein-Maxwell equations or at least adopt an approximation which allows us to regard strong gravity. In the latter approximation, which will be adopted herein, the metric is determined by solving the Einstein equations as if the magnetic field was not present, and then solve the Maxwell equations considering the backreaction of spacetime curvature on them neglecting the impact of the magnetic energy density on Einstein equations. We thus focus on effects of strong gravity to electromagnetic fields. The above approach account only for the vacuum solutions of the Einstein and Maxwell equations. In reality, under astrophysically realistic conditions, space near a black hole is not vacuum. A realistic model would have to consider the non-vacuum solution of the Einstein equations and it can only be treated by numerical techniques.

As mentioned before, towards a mathematically correct description of the spacetime around a black hole surrounded by an accretion disk, one has to carry out complicated calculations for the coupled Maxwell-Einstein equations. Fortunately, the energy density contribution that come from the electromagnetic fields of the disk turns out to be far low to influence spacetime's structure. Therefore, test-fields are adequate for describing weak electromagnetic fields. We'd like to point out that the magnetic density of  $10^{12}$ Gauss sounds an enormous amount, compared to the ones we are used to find near earth. In neutron stars, the energy density of their magnetic fields corresponds to matter density of the order of  $1000 \text{ gr/cm}^3$ .

The magnetic fields we come across in astrophysics are of very weak intensity, but they get amplified inside gravitating bodies, such as stars, nuclei of galaxies etc. during their formation and subsequent evolution. Matter consists charged particles, e.g. electrons, protons, ions etc. When matter enters a strong gravitational field it gets attracted by the source and compressed. This may lead to the ionization of matter, as happens in neutron stars. Plasmas that come from the ionization of matter are responsible for the magnetic fields encountered near or inside compact objects. For stellar black holes with mass almost  $10 M_{\odot}$  the magnetic fields we observe are of the order of  $10^{12} \text{ Gauss}$  and for supermassive black holes (galactic) of almost  $10 M_{\odot}$  are of the order of  $10^5 \text{ Gauss}$ . There is a linear correlation between the mass of the black hole and the magnetic field strengths of the accretion disks surrounding the hole. So there is no difference in examining stellar black holes with magnetic fields of the order of  $10^{12} \text{ Gauss}$  and supermassive black holes with magnetic fields of the order of  $10^5 \text{ Gauss}$ , the results will be the same.

Processes involving turbulent plasma motions are often too complicated to be described. Usually, assumptions have to be made in order to create a model that explains them. Often, a qualitative explanation is sufficient. The study of charged particles orbits in the neighborhood of a black hole yields some answers and sometimes is a very good approximation of what happens there.

For example when plasma density around a hole is so low that any effects due to conductivity or pressure can be eliminated.

The production of magnetic fields around a rotating body yields the creation of electric fields due to its rotation. Electric fields play an important role in astrophysical processes. These electric fields allow for the acceleration of charged particles to relativistic velocities near a magnetized neutron star.

## 1.5 Motivation

Like said, gaseous thick or thin accretion disks can reside in the region of a black hole. The rapid phenomena occurring in these objects suggest the formation of extended magnetospheres around the accretion disks. What we wish to do here is to study charged particles, possibly ejected from the accretion disk due to the connection of magnetic field lines and turbulent phenomena, and their motion in a space where the gas pressure of the disk can be neglected. We have wished to find some interesting orbits that would tell us about the black hole itself. These orbits have been found. They are the so called "halo orbits" or "Stormer orbits". Off-equatorial potential traps are responsible for the confinement of charged particles for  $z > 0$  or  $z < 0$ . This is the same phenomenon as that occurring in earth's magnetosphere. The existence of two mutually detached off-equatorial lobes can have profound consequences for plasma oscillations near compact objects [22]. These oscillations could be observed in the detected X-ray spectrum.

In addition to the previous, jets are also astrophysically important processes. The most common approach for studying jet formation is ideal or resistive MHD. But as argued by Ardavan (1976) the ideal MHD condition from the standard Ohm's law suggest that around a black hole there should be regions in which standard Ohm's law is a poor approximation [20]. The plasma can only be described as a single fluid if its components are cold. By this we mean that the internal energy density and pressure can be omitted compared to the rest-mass energy density. The applicability or not of the MHD approach for astrophysical objects is restricted to the above case. Another constraint in the MHD approach is that approaching the horizon we cannot describe plasma as a fluid, because plasma particles become collisionless. A question posed by Elsässer [17] is whether MHD is consistent with a rotating black hole. He argues that the non-diagonal component of a Kerr metric couples the components  $A_t$  and  $A_\phi$  in Ampere's law, which contradicts the strong coupling of  $A_t$  and  $A_\phi$  obtained by MHD models. In fact, in ideal MHD models  $A_t$  and  $A_\phi$  are usually a function of each other.

As mentioned above, for particles near the horizon and away from the accretion disk the collision rates are very low. Thus charged particles can be considered as test particles carrying a charge. The energy-momentum tensor describing a perfect-fluid immersed in a magnetic field is given by

$$T_{\mu\nu} = (\rho + p)u_\mu u_\nu + p g_{\mu\nu} + F^{\mu\lambda} F_\nu{}^\lambda - \frac{1}{4}g_{\mu\nu} F_{\rho\sigma} F^{\rho\sigma}$$

where  $F_{\mu\nu}$  the electromagnetic field tensor,  $\rho$  the mass density of the perfect fluid and  $p$  the gas pressure. For collisionless plasma we have to set  $p = 0$ . In addition we consider that the magnetic energy density is small compared to the rest-mass energy density, so any terms including the Faraday tensor are neglected. Finally we are left with

$$T_{\mu\nu} = \rho u_\mu u_\nu$$

which describes matter. The dynamical evolution of the fluid is governed by the vanishing divergence of the stress-energy tensor,

$$\nabla_\beta T^{\alpha\beta} = 0$$

and by conservation of baryons and charge. The projection of the energy-momentum tensor along  $u^\alpha$  yields an energy conservation law,

$$u^\alpha \nabla_\beta T^{\alpha\beta} \simeq \rho u_\mu u_\nu \rightarrow \nabla_\beta (\rho u^\beta) = 0$$

while the projection orthogonal to  $u^\alpha$  yields the relativistic Euler equation

$$q^\alpha_\gamma \nabla_\beta T^{\beta\gamma} = 0$$

where  $q^{\alpha\beta} = g^{\alpha\beta} + u^\alpha u^\beta$  is the projection operator orthogonal to  $u^\alpha$ . The equation above describes the equations of motion  $u^\beta \nabla_\beta u^\alpha = q F_{\alpha\beta} u^\beta$  of single charged particles in the gravitational field of a black hole immersed in a magnetic field. Throughout our analysis we will employ this approach, which is only valid for particles moving away from the accretion disk.

## Chapter 2

# Theoretical Analysis

The theoretical analysis that follows concerns the investigation of charged particles trajectories near a Kerr and Kerr-Newman black hole immersed in a test-magnetic field.

In order to determine the parameters that affect the orbit of a particle we will make use of the effective potential of the magnetized black hole. The effective potential of a black hole corresponds to the minimum kinetic energy required for a particle to escape the combined gravitational and magnetic field of the magnetized hole. Following the analysis of Misner, Thorne, and Wheeler [24] in p.909 we will evaluate the potential of a Kerr and Kerr-Newman black hole including any effects from external magnetic fields. In addition we will demonstrate a visualization of the magnetic field lines as measured by a ZAMO observer. This will give us a hint on how axisymmetric magnetic fields react to strong gravitational fields. Finally we will refer to the guiding center approach and deduce the drifts exerted upon it.

### 2.1 Magnetic Fields Studied

At this point we will describe how one can visualize the magnetic field in general relativity. We will perform the calculations necessary to express mathematically the magnetic field lines near a strong gravitating object such as a black hole. Two cases of external test-magnetic fields will be studied, the uniform magnetic field [39] and the dipole magnetic field [25; 7]. and

The second part concerns the computation of the magnetic field and its derivatives. The cases of study are: a) an asymptotically uniform magnetic field and b) the dipole magnetic field produced by a ring current placed at the equatorial plane near a Kerr black hole. Finally, some estimates of the possibility of selective charge accretion onto the black hole are considered.

#### 2.1.1 Visualizing the Magnetic Field in GR

The visualization of the magnetic field is carried out by the use of magnetic field lines. In Newtonian physics the calculation of the magnetic field lines is straightforward. However, in general relativity things are slightly different. Bearing in mind that spacetime is curved around a black hole, we sense that the equations of lines of force have to involve the components of the black hole's metric.

Thus, the equations for the magnetic field lines read,

$$\frac{dr}{dl} = \frac{B^r}{|\mathbf{B}|} \quad (2.1.1)$$

$$\frac{d\theta}{dl} = \frac{B^\theta}{|\mathbf{B}|} \quad (2.1.2)$$

where  $l$  is the length of the magnetic field line.

What remains to be done in order to finally visualize the magnetic lines is to determine the contravariant components ( $B^r$ ,  $B^\theta$ ) and the magnitude of the magnetic field ( $|\mathbf{B}|$ ). According to Teukolsky [36] the magnetic field as measured by a ZAMO observer is given by,

$$B_a = \frac{1}{2} \varepsilon_{a\mu\nu} F^{\mu\nu} u^\beta \quad (2.1.3)$$

where  $a$ ,  $\beta$ ,  $\mu$ ,  $\nu$  are running through all of the spatial components.

As mentioned above, the covariant magnetic field in (2.1.3) is measured by a ZAMO observer, for whom  $u^k = (u^t, 0, 0, u^\phi)$  and  $\Omega = u^\phi/u^t$ . As a consequence the non-zero covariant components of the magnetic field are of the form:

$$B_r = - (F^{\theta\phi} u^t + F^{\theta t} u^\phi) \quad (2.1.4a)$$

$$B_\theta = F^{r\phi} u^t + F^{rt} u^\phi \quad (2.1.4b)$$

In the previous calculation we have used the antisymmetric property of the Faraday tensor  $F^{\mu\nu}$ . In addition,

$$F^{\mu\nu} = g^{\kappa\mu} g^{\lambda\nu} F_{\kappa\lambda}$$

and

$$F_{\mu\nu} = A_{\nu,\mu} - A_{\mu,\nu}$$

leading eq. (2.1.4a) and (2.1.4b) to:

$$\left. \begin{aligned} B_r &= - (g^{\kappa\theta} g^{\lambda\phi} F_{\kappa\lambda} u^t + g^{\kappa\theta} g^{\lambda t} F_{\kappa\lambda} u^\phi) \\ B_\theta &= g^{\kappa r} g^{\lambda\phi} F_{\kappa\lambda} u^t + g^{\kappa r} g^{\lambda t} F_{\kappa\lambda} u^\phi \end{aligned} \right\} \Rightarrow$$

$$B_r = -g^{\theta\theta} u^t \left[ (g^{\phi\phi} F_{\theta\phi} + g^{\phi t} F_{\theta t}) + g^{tt} F_{\theta t} \frac{u^\phi}{u^t} \right] \quad (2.1.5a)$$

$$B_\theta = g^{rr} u^t \left[ (g^{\phi\phi} F_{r\phi} + g^{\phi t} F_{rt}) + g^{tt} F_{rt} \frac{u^\phi}{u^t} \right] \quad (2.1.5b)$$

Knowing that for a ZAMO observer  $l = 0$ ,  $\Omega$  takes the form,

$$\Omega = u^\phi/u^t = -\frac{g_{t\phi} + l g_{tt}}{g_{\phi\phi} + l g_{t\phi}} = -\frac{g_{t\phi}}{g_{\phi\phi}}$$

Hence equations (2.1.5a) (2.1.5b) may be rewritten as follows,

$$B_r = -g^{\theta\theta} u^t \left[ (g^{\phi\phi} F_{\theta\phi} + g^{\phi t} F_{\theta t}) - g^{tt} \frac{g_{t\phi}}{g_{\phi\phi}} F_{\theta t} \right]$$

$$B_\theta = g^{rr} u^t \left[ (g^{\phi\phi} F_{r\phi} + g^{\phi t} F_{rt}) - g^{tt} \frac{g_{t\phi}}{g_{\phi\phi}} F_{rt} \right]$$

Therefore for the magnetic field we obtain,

$$B^r = -\frac{g^{\theta\theta}}{g^{rr}} u^t \left[ (g^{\phi\phi} F_{\theta\phi} + g^{\phi t} F_{\theta t}) - g^{tt} \frac{g_{t\phi}}{g_{\phi\phi}} F_{\theta t} \right] \quad (2.1.6a)$$

$$B^\theta = \frac{g^{rr}}{g^{\theta\theta}} u^t \left[ (g^{\phi\phi} F_{r\phi} + g^{\phi t} F_{rt}) - g^{tt} \frac{g_{t\phi}}{g_{\phi\phi}} F_{rt} \right] \quad (2.1.6b)$$

The only unknown in equations (2.1.6) is the velocity  $u^t$  which can be defined from the normalization condition for a ZAMO observer,

$$u^t u_t + u^\phi u_\phi = -1 \Rightarrow$$

$$\begin{aligned}
u^t u_t \left( 1 + \frac{u^\phi u_\phi}{u^t u_t} \right) &= -1 \Rightarrow \\
u^t u_t (1 - \Omega l) &= -1 \Rightarrow \\
g_{tt} (u^t)^2 &= -1 \\
\boxed{u^t = (-g_{tt})^{-1/2}}
\end{aligned}$$

Replacing the above relation for  $u^t$  in eq. (2.1.6),

$$B^r = -\frac{g^{\theta\theta}}{g^{rr}} (-g_{tt})^{-1/2} \left[ g^{\phi\phi} A_{\phi,\theta} + g^{\phi t} A_{t,\theta} - \frac{g^{tt} g_{t\phi}}{g_{\phi\phi}} A_{t,\theta} \right] \quad (2.1.7a)$$

$$B^\theta = \frac{g^{rr}}{g^{\theta\theta}} (-g_{tt})^{-1/2} \left[ g^{\phi\phi} A_{\phi,r} + g^{\phi t} A_{t,r} - \frac{g^{tt} g_{t\phi}}{g_{\phi\phi}} A_{t,r} \right] \quad (2.1.7b)$$

Following the previous analysis we will demonstrate, in the following paragraph, the form of both the dipole and uniform magnetic fields near a Kerr black hole. To do so, we have employed a fourth-order Runge Kutta algorithm [29] in order to integrate eq. (2.1.1), (2.1.2) and find the expression that describes the magnetic field lines.

### 2.1.2 Uniform Magnetic Field

The solution of an electromagnetic field occurring when a stationary and axisymmetric black hole is immersed in a uniform magnetic field aligned along the symmetry axis of the black hole as expressed in [39] reads,

$$A_t = -aB_o \left( 1 - \frac{Mr}{\Sigma} (2 - \sin^2 \theta) \right) \quad (2.1.8)$$

$$A_\phi = \frac{B_o \sin^2 \theta}{2\Sigma} (B - 4Ma^2 r) \quad (2.1.9)$$

In order to study the motion of charged particles in the field of a black hole endowed in a magnetic field we will have to evaluate the partial derivatives of the vector potential along  $r$  and  $\theta$ .

$$A_{t,r} = -aMB_o (1 + \cos^2 \theta) \left( \frac{r^2 - a^2 \cos^2 \theta}{\Sigma^2} \right) \quad (2.1.10a)$$

$$A_{t,\theta} = \frac{-2MraB_o \cos \theta \sin \theta}{\Sigma^2} (r^2 - a^2) \quad (2.1.10b)$$

$$A_{\phi,r} = \frac{B_o \sin^2 \theta}{\Sigma} \left[ (1 + \cos^2 \theta)(a^2 r - a^2 M + 2r^3) - \frac{r(-4a^2 Mr + B)}{\Sigma} \right] \quad (2.1.10c)$$

$$A_{\phi,\theta} = \left( \frac{B_o \cos \theta \sin \theta}{\Sigma} \right) \left( \frac{(-4a^2 Mr + B)}{\Sigma} (r^2 + a^2) - \Delta a^2 \sin^2 \theta \right) \quad (2.1.10d)$$

Replacing (2.1.10) in (2.1.7) we obtain the magnetic field lines for the uniform magnetic field. Fig. 2.1 shows the structure of the magnetic field (2.1.8), (2.1.9) near a Kerr black hole.

It is obvious from fig. 2.1 that in the extreme Kerr black hole very few magnetic field lines are allowed to thread the outer event horizon. The black hole seems to behave like a superconductor in vacuum electrodynamics. The phenomenon is known as the ‘‘Meissner effect’’. The expulsion of magnetic flux from the horizon of a rapidly rotating black hole seem to undermine the role of the Blandford-Znajek mechanism, as the black hole becomes unmagnetized [6].

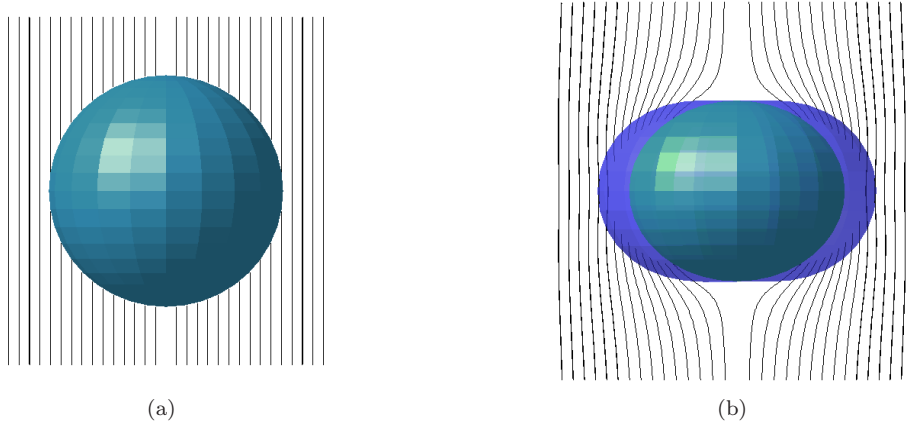


**Figure 2.1:** Magnetic field lines of a uniform magnetic field near a Kerr black hole as measured by a ZAMO observer. The blue surface indicates the boundaries of the ergosphere and the green one the outer event horizon. (a) The magnetic field lines thread the event horizon for an  $a = 0$  Kerr black hole. (b) Magnetic field lines are expelled from the horizon for an  $a = 0.9$  black hole.

However Komissarov and McKinney [21] express a different opinion about the phenomenon. In their work they have pointed out that this behavior of the magnetic field is not observed in the MHD description of the system. The difference between the two descriptions is that the MHD approach considers any effects due to the conductivity and inertia of plasma surrounding the black hole while the vacuum electrodynamics approximation ignores them.

Even approaching the fact from the vacuum electrodynamics point of view we can deduce that the “Meissner effect” cannot be dominant near extreme black holes. Taking the Wald problem for example into consideration. In such a configuration, the rotation of the hole will induce an electric field near the horizon. Therefore charges of different sign will move in opposite directions, bringing about the screening of the electric component. The screening that charges provide for the electric component is not perfect. In order to be able to observe marginal screening, a poloidal component of the electric current must flow through the ergosphere. This, in turn, contribute to the magnetic field by creating an azimuthal component, which we have not regarded before. Consequently the magnetic field is pulled inwards by the black hole. Finally, the black hole can selectively accrete charged particles of the same sign until it’s net charge reaches a maximum value. The net charge that the black hole has obtained through this process will be responsible for the creation of a dipolar magnetic field (Kerr-Newman black hole). In a sense, charged particles have to be present in the vicinity of the black hole. Hence, conductivity is sufficient to negate the “Meissner effect” even for extreme Kerr black holes. In the present study we ignore any effects of conductivity or any interactions between charged particles. This analysis goes for any axisymmetric field.

Wald in [39] proves that a black hole in a magnetic field will selectively accrete charged particles. Consequently the black hole will become charged. As stated previously, the accretion of charged particles will continue until the net charge of the black hole becomes  $Q = 2B_oJ$ , where  $B_o$  is the magnetic field strength and  $J$  the angular momentum of the black hole. Therefore, the maximum net charge that a black hole can carry in the background geometry described above is,

$$Q = 2aMB_o \quad (2.1.11)$$

### 2.1.3 Dipole Magnetic Field

#### Vector Potential Calculation

The spherical harmonic expansion for the vector potential of a stationary ring current situated axisymmetrically and equatorially with respect to a Kerr black hole is given analytically by Peterson [25]; Znajek [40]. In our study we will keep only the  $l = 0, 1$  multipole terms and assume that the ring current is placed at  $r = r_o$ ,  $\theta = \pi/2$  and carries zero net charge ( $b_o^i = 0$  and  $a_o^i = 0$ ). Therefore, in our case, the vector potential is given by the following equations:

For  $r > r_o$

$$A_{t_2}^1 = -2 \left\{ b_1^i \left[ -a \cos \theta \frac{\Delta}{\Sigma} \frac{dQ_1(u)}{du} \frac{du}{dr} P_1(\cos \theta) + \frac{ra \sin \theta}{\Sigma} Q_1(u) P_1^1(\cos \theta) \right] \right\} + C_> \quad (2.1.12)$$

and

$$A_{\phi_2}^1 = 2 \left\{ b_1^i \left[ -a^2 \sin^2 \theta \cos \theta \frac{\Delta}{\Sigma} \frac{dQ_1(u)}{du} \frac{du}{dr} P_1(\cos \theta) + r \sin \theta \frac{(r^2 + a^2)}{\Sigma} Q_1(u) P_1^1(\cos \theta) - \frac{\Delta \sin \theta}{2} \frac{dQ_1(u)}{du} \frac{du}{dr} P_1^1(\cos \theta) \right] \right\} \quad (2.1.13)$$

For  $r < r_o$

$$A_{t_1}^1 = -2 \left\{ a_1^i \left[ -a \cos \theta \frac{\Delta}{\Sigma} \frac{dP_1(u)}{du} \frac{du}{dr} P_1(\cos \theta) + \frac{ra \sin \theta}{\Sigma} P_1(u) P_1^1(\cos \theta) \right] \right\} + C_< \quad (2.1.14)$$

and

$$A_{\phi_1}^1 = 2 \left\{ a_1^i \left[ -a^2 \sin^2 \theta \cos \theta \frac{\Delta}{\Sigma} \frac{dP_1(u)}{du} \frac{du}{dr} P_1(\cos \theta) + r \sin \theta \frac{(r^2 + a^2)}{\Sigma} P_1(u) P_1^1(\cos \theta) - \frac{\Delta \sin \theta}{2} \frac{dP_1(u)}{du} \frac{du}{dr} P_1^1(\cos \theta) \right] \right\} \quad (2.1.15)$$

where  $\gamma = \sqrt{M^2 - a^2}$ ,  $u = (r - M)/\gamma$ . Moreover  $C_>$  and  $C_<$  are integration constants. The constants  $b_1^i$  and  $a_1^i$  are defined by the subsequent equations, given the ring current is placed at  $r = r_o$  and  $\theta = \theta_o = \pi/2$  ( $a_l^r = b_l^r = 0$ ).

$$b_1^i = \frac{3I}{4r_o\gamma} \left[ \sin \theta_o (r_o^2 + a^2) P_1^1(\cos \theta_o) P_1(u_o) - \frac{r_o \Delta_o \sin \theta_o P_1^1(\cos \theta_o)}{2\gamma} P_1'(u_o) \right] \quad (2.1.16)$$

and

$$a_1^i = \frac{3I}{4r_o\gamma} \left[ \sin \theta_o (r_o^2 + a^2) P_1^1(\cos \theta_o) Q_1(u_o) - \frac{r_o \Delta_o \sin \theta_o P_1^1(\cos \theta_o)}{2\gamma} Q_1'(u_o) \right] \quad (2.1.17)$$

However  $a_l^i = 0$  for all  $l$  when  $r > r_o$  and  $b_l^i = 0$  for all  $l$  when  $r < r_o$ .

At this point we will use the expressions of the associated Legendre polynomials of the first and second kind (see Abramowitz and Stegun [2]) to obtain a simplified formula for the vector potential.

$$P_1(u) = \frac{r - M}{\gamma}, \quad P_1(\cos \theta) = \cos \theta, \quad P_1^1(\cos \theta) = -\sin \theta, \quad P_1'(u) = 1$$

$$Q_1(u) = -1 + \frac{r - M}{2\gamma} \ln \left( \frac{r - M + \gamma}{r - M - \gamma} \right)$$

$$Q_1'(u) = \frac{1}{2} \ln \left( \frac{r - M + \gamma}{r - M - \gamma} \right) - \frac{2(r - M)}{2\gamma(r - M + \gamma)(r - M - \gamma)} = \frac{1}{2} \ln \left( \frac{r - M + \gamma}{r - M - \gamma} \right) - \frac{(r - M)\gamma}{\Delta}$$

Consequently,

For  $r > r_o$

$$A_{t_2}^1 = -2 \left\{ b_1^i \left[ -a \cos^2 \theta \frac{\Delta}{\Sigma \gamma} \left( \frac{1}{2} \ln \left( \frac{r-M+\gamma}{r-M-\gamma} \right) - \frac{(r-M)\gamma}{\Delta} \right) - \frac{ra \sin^2 \theta}{\Sigma} \left( -1 + \frac{r-M}{2\gamma} \ln \left( \frac{r-M+\gamma}{r-M-\gamma} \right) \right) \right] \right\} + C_>$$

$$A_{t_2}^1 = \frac{2ab_1^i}{\Sigma} \left[ \frac{1}{2\gamma} \ln \left( \frac{r-M+\gamma}{r-M-\gamma} \right) (\Delta \cos^2 \theta + r(r-M) \sin^2 \theta) - \cos^2 \theta (r-M) - r \sin^2 \theta \right] + C_>$$

$$\boxed{A_{t_2}^1 = \frac{2ab_1^i}{\Sigma} \left[ \frac{1}{2\gamma} \ln \left( \frac{r-M+\gamma}{r-M-\gamma} \right) [r(r-M) + \cos^2 \theta (a^2 - Mr)] - (r-M \cos^2 \theta) \right] + C_>} \quad (2.1.18)$$

and

$$\begin{aligned} A_{\phi_2}^1 &= 2b_1^i \left\{ -a^2 \sin^2 \theta \cos^2 \theta \frac{\Delta}{\Sigma \gamma} \left[ \frac{1}{2} \ln \left( \frac{r-M+\gamma}{r-M-\gamma} \right) - \frac{(r-M)\gamma}{\Delta} \right] - r \sin^2 \theta \frac{(r^2 + a^2)}{\Sigma} \right. \\ &\quad \cdot \left. \left[ -1 + \frac{r-M}{2\gamma} \ln \left( \frac{r-M+\gamma}{r-M-\gamma} \right) \right] + \frac{\Delta \sin^2 \theta}{2\gamma} \left[ \frac{1}{2} \ln \left( \frac{r-M+\gamma}{r-M-\gamma} \right) - \frac{(r-M)\gamma}{\Delta} \right] \right\} \\ &= \frac{2b_1^i \sin^2 \theta}{\Sigma} \left\{ \frac{1}{2\gamma} \ln \left( \frac{r-M+\gamma}{r-M-\gamma} \right) \left[ \frac{-2a^2 \cos^2 \theta \Delta - 2r(r^2 + a^2)(r-M) + \Sigma \Delta}{2} \right] \right. \\ &\quad \left. + a^2 \cos^2 \theta (r-M) + r(r^2 + a^2) - \frac{\Sigma}{2}(r-M) \right\} \\ &= \frac{2b_1^i \sin^2 \theta}{2\Sigma} \left\{ \frac{1}{2\gamma} \ln \left( \frac{r-M+\gamma}{r-M-\gamma} \right) [(\Sigma - 2a^2 \cos^2 \theta) \Delta - 2r(r^2 + a^2)(r-M)] \right. \\ &\quad \left. + 2a^2 \cos^2 \theta (r-M) + 2r(r^2 + a^2) - \Sigma(r-M) \right\} \\ &= \frac{2b_1^i \sin^2 \theta}{2\Sigma} \left\{ \frac{1}{2\gamma} \ln \left( \frac{r-M+\gamma}{r-M-\gamma} \right) [\Delta(r^2 - a^2 \cos^2 \theta) - 2r(r-M)(r^2 + a^2)] \right. \\ &\quad \left. - (r^2 - a^2 \cos^2 \theta)(r-M) + 2r(r^2 + a^2) \right\} \\ &= \frac{2b_1^i \sin^2 \theta}{2\Sigma} \left\{ \frac{1}{2\gamma} \ln \left( \frac{r-M+\gamma}{r-M-\gamma} \right) [-\Delta a^2 \cos^2 \theta + r^4 + a^2 r^2 - 2Mr^3 - 2r^4 + 2r^3 M \right. \\ &\quad \left. - 2r^2 a^2 + 2ra^2 M] - r^3 + r^2 M + a^2 \cos^2 \theta r - Ma^2 \cos^2 \theta + 2r^3 + 2ra^2 \right\} \\ &= \frac{2b_1^i \sin^2 \theta}{2\Sigma} \left\{ \frac{1}{2\gamma} \ln \left( \frac{r-M+\gamma}{r-M-\gamma} \right) [-\Delta a^2 \cos^2 \theta - r^4 - r^2 a^2 + 2ra^2 M] + r^3 + r^2 M \right. \\ &\quad \left. + 2ra^2 + a^2 \cos^2 \theta (r-M) \right\} \end{aligned}$$

$$A_{\phi_2}^1 = \frac{b_1^i \sin^2 \theta}{\Sigma} \left\{ \frac{1}{2\gamma} \ln \left( \frac{r-M+\gamma}{r-M-\gamma} \right) [-\Delta a^2 \cos^2 \theta - r(r^3 + ra^2 - 2a^2M)] \right. \\ \left. + r(r^2 + Mr + 2a^2) + a^2 \cos^2 \theta (r-M) \right\} \quad (2.1.19)$$

The only thing that is left to be defined is the constant  $b_l^i$  for  $l = 0, 1$ .

$$b_1^i = \frac{3I}{4r_o\gamma} \left[ -\sin^2 \theta_o (r_o^2 + a^2) \frac{(r_o - M)}{\gamma} + \frac{r_o \Delta_o \sin^2 \theta_o}{2\gamma} \right]$$

For a ring current placed at  $r = r_o$  and  $\theta = \theta_o = \pi/2$ :

$$b_1^i = \frac{3I}{8r_o\gamma^2} [-2(r_o^2 + a^2)(r_o - M) + r_o \Delta_o] \\ b_1^i = \frac{3I}{8r_o\gamma^2} [(-2r_o + 2M + r_o)(r_o^2 + a^2) - 2Mr_o^2] \\ b_1^i = \frac{3I}{8r_o\gamma^2} [-(r_o - 2M)(r_o^2 + a^2) - 2Mr_o^2]$$

$$b_1^i = -\frac{3I}{8r_o\gamma^2} [r_o(r_o^2 + a^2) - 2a^2M] \quad (2.1.20)$$

For  $r < r_o$

$$A_{t_1}^1 = -2 \left\{ a_1^i \left[ -a \cos^2 \theta \frac{\Delta}{\Sigma\gamma} - \frac{ra \sin^2 \theta (r-M)}{\Sigma\gamma} \right] \right\} + C_{<} \\ = \frac{2a_1^i}{\Sigma\gamma} [\Delta a \cos^2 \theta + ra \sin^2 \theta (r-M)] + C_{<} \\ = \frac{2a}{\Sigma\gamma} a_1^i [r^2 - Mr \cos^2 \theta - Mr + a^2 \cos^2 \theta] + C_{<}$$

$$A_{t_1}^1 = 2a_1^i \frac{a}{\gamma} \left[ 1 - \frac{Mr(1 + \cos^2 \theta)}{\Sigma} \right] + C_{<} \quad (2.1.21)$$

and

$$A_{\phi_1}^1 = 2 \left\{ a_1^i \left[ -a^2 \sin^2 \theta \cos^2 \theta \frac{\Delta}{\Sigma\gamma} - r \sin^2 \theta \frac{(r^2 + a^2)}{\Sigma\gamma} (r-M) + \frac{\Delta \sin^2 \theta}{2\gamma} \right] \right\} \\ = 2a_1^i \sin^2 \theta \left[ -a^2 \cos^2 \theta \frac{\Delta}{\Sigma\gamma} - r \frac{(r^2 + a^2)}{\Sigma\gamma} (r-M) + \frac{\Delta}{2\gamma} \right] \\ = \frac{2a_1^i \sin^2 \theta}{2\Sigma\gamma} [\Delta(-2a^2 \cos^2 \theta + \Sigma) - 2r(r^2 + a^2)(r-M)] \\ = \frac{2a_1^i \sin^2 \theta}{2\Sigma\gamma} [\Delta(r^2 - a^2 \cos^2 \theta) - 2r(r^2 + a^2)(r-M)]$$

$$A_{\phi_1}^1 = \frac{2a_1^i \sin^2 \theta}{2\Sigma\gamma} [r^4 - r^2 a^2 \cos^2 \theta + a^2 r^2 - a^4 \cos^2 \theta - 2Mr^3 + 2Mra^2 \cos^2 \theta - 2r^4 \\ + 2r^3 M - 2r^2 a^2 + 2ra^2 M] \\ = \frac{2a_1^i \sin^2 \theta}{2\Sigma\gamma} [-r^4 - r^2 a^2 - r^2 a^2 \cos^2 \theta + 2ra^2 M + 2Mra^2 \cos^2 \theta - a^4 \cos^2 \theta]$$

$$\boxed{A_{\phi_1}^1 = -\frac{a_1^i \sin^2 \theta}{\gamma} \left[ (r^2 + a^2) - 2Mra^2 \frac{(1 + \cos^2 \theta)}{\Sigma} \right]} \quad (2.1.22)$$

We now need to define the constant  $a_1^i$  for  $l = 1$ .

$$a_1^i = \frac{3I}{4\Sigma_o\gamma} \left[ -\sin^2 \theta_o r_o (r_o^2 + a^2) \left[ -1 + \frac{r_o - M}{2\gamma} \ln \left( \frac{r_o - M + \gamma}{r_o - M - \gamma} \right) \right] \right. \\ \left. + \frac{\Sigma_o \Delta_o \sin^2 \theta_o}{2\gamma} \left[ \frac{1}{2} \ln \left( \frac{r_o - M + \gamma}{r_o - M - \gamma} \right) - \frac{(r_o - M)\gamma}{\Delta_o} \right] \right]$$

For a ring current placed at  $r = r_o$  and  $\theta = \theta_o = \pi/2$ :

$$a_1^i = \frac{3I}{4r_o\gamma} \left[ -(r_o^2 + a^2) \left[ -1 + \frac{r_o - M}{2\gamma} \ln \left( \frac{r_o - M + \gamma}{r_o - M - \gamma} \right) \right] \right. \\ \left. + \frac{r_o \Delta_o}{2\gamma} \left[ \frac{1}{2} \ln \left( \frac{r_o - M + \gamma}{r_o - M - \gamma} \right) - \frac{(r_o - M)\gamma}{\Delta_o} \right] \right] \\ = \frac{3I}{4r_o\gamma} \left[ (r_o^2 + a^2) - \frac{(r_o - M)\gamma}{2\gamma\Delta_o} \Delta_o r_o + \frac{1}{2\gamma} \ln \left( \frac{r_o - M + \gamma}{r_o - M - \gamma} \right) \left[ \frac{r_o \Delta_o}{2} - (r_o - M)(r_o^2 + a^2) \right] \right]$$

$$a_1^i = \frac{3I}{8r_o\gamma} \left[ 2(r_o^2 + a^2) - (r_o - M)r_o + \frac{1}{2\gamma} \ln \left( \frac{r_o - M + \gamma}{r_o - M - \gamma} \right) [r_o \Delta_o - 2(r_o - M)(r_o^2 + a^2)] \right] \\ = \frac{3I}{8r_o\gamma} \left[ 2r_o^2 + 2a^2 - r_o^2 + Mr_o + \frac{1}{2\gamma} \ln \left( \frac{r_o - M + \gamma}{r_o - M - \gamma} \right) [-2Mr_o^2 + (r_o - 2r_o + 2M)(r_o^2 + a^2)] \right] \\ = \frac{3I}{8r_o\gamma} \left[ r_o(r_o + M) + 2a^2 + \frac{1}{2\gamma} \ln \left( \frac{r_o - M + \gamma}{r_o - M - \gamma} \right) [-2Mr_o^2 - (r_o - 2M)(r_o^2 + a^2)] \right]$$

$$\boxed{a_1^i = \frac{3I}{8r_o\gamma} \left[ r_o(r_o + M) + 2a^2 - \frac{1}{2\gamma} \ln \left( \frac{r_o - M + \gamma}{r_o - M - \gamma} \right) [r_o(r_o^2 + a^2) - 2Ma^2] \right]} \quad (2.1.25)$$

### Vector Potential at the Limit $r = r_o$

In order to see the behavior of the dipole magnetic field at the limit  $r = r_o$  we will calculate the difference in the vector potential between the external ( $r > r_o$ ) and the internal region ( $r < r_o$ ). In our calculation we will keep only the  $l = 0, 1$  terms of the multipoles expansion.

The integration constant in equations (2.1.13) and (2.1.15) is zero, because of  $\sin \theta \rightarrow 0$  when  $\theta \rightarrow 0$ .

By subtraction of eq. (2.1.14) from eq. (2.1.12) and eq. (2.1.15) from eq. (2.1.13) we get:

$$A_{t_2} - A_{t_1} = \frac{2a \cos^2 \theta \Delta}{\Sigma \gamma} [b_1^i Q_1'(u) - a_1^i P_1'(u)] + \frac{2ra \sin^2 \theta}{\Sigma} [b_1^i Q_1(u) - a_1^i P_1(u)] + C_> - C_< \quad (2.1.26)$$

$$A_{\phi_2} - A_{\phi_1} = \left[ \frac{-2a^2 \sin^2 \theta \cos^2 \theta \Delta}{\Sigma \gamma} + \frac{2\Delta \sin^2 \theta}{2\gamma} \right] [b_1^i Q_1'(u) - a_1^i P_1'(u)] \\ - 2r \sin^2 \theta \frac{(r^2 + a^2)}{\Sigma} [b_1^i Q_1(u) - a_1^i P_1(u)] \quad (2.1.27)$$

We will now derive a simpler formula for the terms  $[b_1^i Q_1(u) - a_1^i P_1(u)]$  and  $[b_1^i Q_1'(u) - a_1^i P_1'(u)]$  and replace  $r$  with  $r_o$  wherever it appears:

$$\begin{aligned} Q_1(u_o)P_1'(u_o) - P_1(u_o)Q_1'(u_o) &= -1 + \ln\left(\frac{r_o - M + \gamma}{r_o - M - \gamma}\right) \left(\frac{r_o - M}{2\gamma}\right) \\ &\quad - \left(\frac{r_o - M}{\gamma}\right) \left[\frac{1}{2} \ln\left(\frac{r_o - M + \gamma}{r_o - M - \gamma}\right) - \frac{(r_o - M)\gamma}{\Delta_o}\right] \\ &= \frac{-\Delta_o + r_o^2 + M^2 - 2Mr_o}{\Delta_o} \\ &= \frac{M^2 - a^2}{\Delta_o} \end{aligned}$$

$$\begin{aligned} b_1^i Q_1'(u_o) - a_1^i P_1'(u_o) &= -\frac{3I}{4r_o\gamma} \left\{ (r_o^2 + a^2)[Q_1'(u_o)P_1(u_o) - P_1'(u_o)Q_1(u_o)] \right. \\ &\quad \left. - \frac{r_o\Delta_o}{2\gamma}[P_1'(u_o)Q_1'(u_o) - Q_1'(u_o)P_1'(u_o)] \right\} \\ &= \frac{3I}{4r_o\gamma} \left\{ (r_o^2 + a^2) \left(\frac{M^2 - a^2}{\Delta_o}\right) \right\} \\ &= \frac{3I\gamma(r_o^2 + a^2)}{4r_o\Delta_o} \end{aligned} \tag{2.1.28}$$

$$\begin{aligned} b_1^i Q_1(u_o) - a_1^i P_1(u_o) &= -\frac{3I}{4r_o\gamma} \left\{ (r_o^2 + a^2)[Q_1(u_o)P_1(u_o) - P_1(u_o)Q_1(u_o)] \right. \\ &\quad \left. - \frac{r_o\Delta_o}{2\gamma}[P_1'(u_o)Q_1(u_o) - Q_1'(u_o)P_1(u_o)] \right\} \\ &= \frac{3I}{4r_o\gamma} \frac{r_o\Delta_o}{2\gamma} \frac{M^2 - a^2}{\Delta_o} \\ &= \frac{3I}{8} \end{aligned} \tag{2.1.29}$$

Replacing equations (2.1.28) and (2.1.29) in (2.1.26) and (2.1.27) we arrive at:

$$\begin{aligned} A_{t_2} - A_{t_1} &= \frac{2a \cos^2 \theta \Delta_o}{\Sigma \gamma} \frac{3I\gamma(r_o^2 + a^2)}{4r_o\Delta_o} + \frac{6r_o a I \sin^2 \theta}{8\Sigma} + C_{>} - C_{<} \\ &= \frac{6Ia}{8\Sigma r_o} [2r_o^2 \cos^2 \theta + 2a^2 \cos^2 \theta + r_o^2 \sin^2 \theta] + C_{>} - C_{<} \\ &= \frac{6Ia}{8\Sigma r_o} (r_o^2 + r_o^2 \cos^2 \theta + 2a^2 \cos^2 \theta) + C_{>} - C_{<} \\ &= \frac{6Ia}{8r_o} \left( 1 + \frac{r_o^2 + a^2}{\Sigma} \cos^2 \theta \right) + C_{>} - C_{<} \end{aligned} \tag{2.1.30}$$

$$\begin{aligned} A_{\phi_2} - A_{\phi_1} &= \left[ \frac{-2a^2 \sin^2 \theta \cos^2 \theta \Delta_o}{\Sigma \gamma} + \frac{\Delta_o \sin^2 \theta}{\gamma} \right] \frac{3I\gamma(r_o^2 + a^2)}{4r_o\Delta_o} - r_o \sin^2 \theta \frac{6I(r_o^2 + a^2)}{8\Sigma} \\ &= \frac{3I \sin^2 \theta (r_o^2 + a^2)}{4\Sigma r_o} (-2a^2 \cos^2 \theta + r_o^2 + a^2 \cos^2 \theta - r_o^2) \\ &= -\frac{3Ia^2 \cos^2 \theta \sin^2 \theta (r_o^2 + a^2)}{4\Sigma r_o} \end{aligned} \tag{2.1.31}$$

Equation (2.1.30) can be further simplified if we choose  $C_> = 0$ , so that  $A_t \rightarrow 0$  as  $r$  approaches infinity, and  $C_< = \frac{aI}{r_o}$  (Znajek [40]).

$$A_{t_2} - A_{t_1} = \frac{6Ia}{8r_o} \left( 1 + \frac{r_o^2 + a^2}{\Sigma} \cos^2 \theta \right) - \frac{aI}{r_o} \quad (2.1.32)$$

Equations (2.1.31), (2.1.32) indicate that the form of the vector potential for the dipole magnetic field case is not continuous at the limit  $r \rightarrow r_o$ . This discontinuity is due to the fact that we have only regarded the  $l = 0, 1$  terms of the multipole expansion of the vector potential. We can easily see from eq. (2.1.31) that the differences between the two solutions is of much lower order than that of  $I_c$ . This is why when we plot the magnetic field lines, the magnetic field seems continuous. An extra discontinuity is expected to arise for  $r = r_o$  and  $\theta = \pi/2$ , where the source is located. The  $l > 1$  terms of the multipole expansion we have neglected are not accountable for this type of discontinuity.

Calculating the partial derivatives of the vector potential using Mathematica and replacing them in eq. (2.1.7) we obtain the magnetic field lines for the dipole magnetic field. Fig. 2.2 shows the form of the dipole magnetic field near the black hole.

It is obvious from fig. 2.1 that in the extreme Kerr black hole few magnetic field lines are allowed to thread the outer event horizon. Again the black hole seems to behave like a superconductor, it exhibits the so-called ‘‘Meissner effect’’. The discontinuity of the vector potential at the limit  $r = r_o$  is apparent.

As argued by Znajek, if we allow selective accretion to operation between the hole and infinity then the maximum net charge that a black hole can carry is,

$$Q = \frac{2aMI}{r_o - 2M} \quad (2.1.33)$$

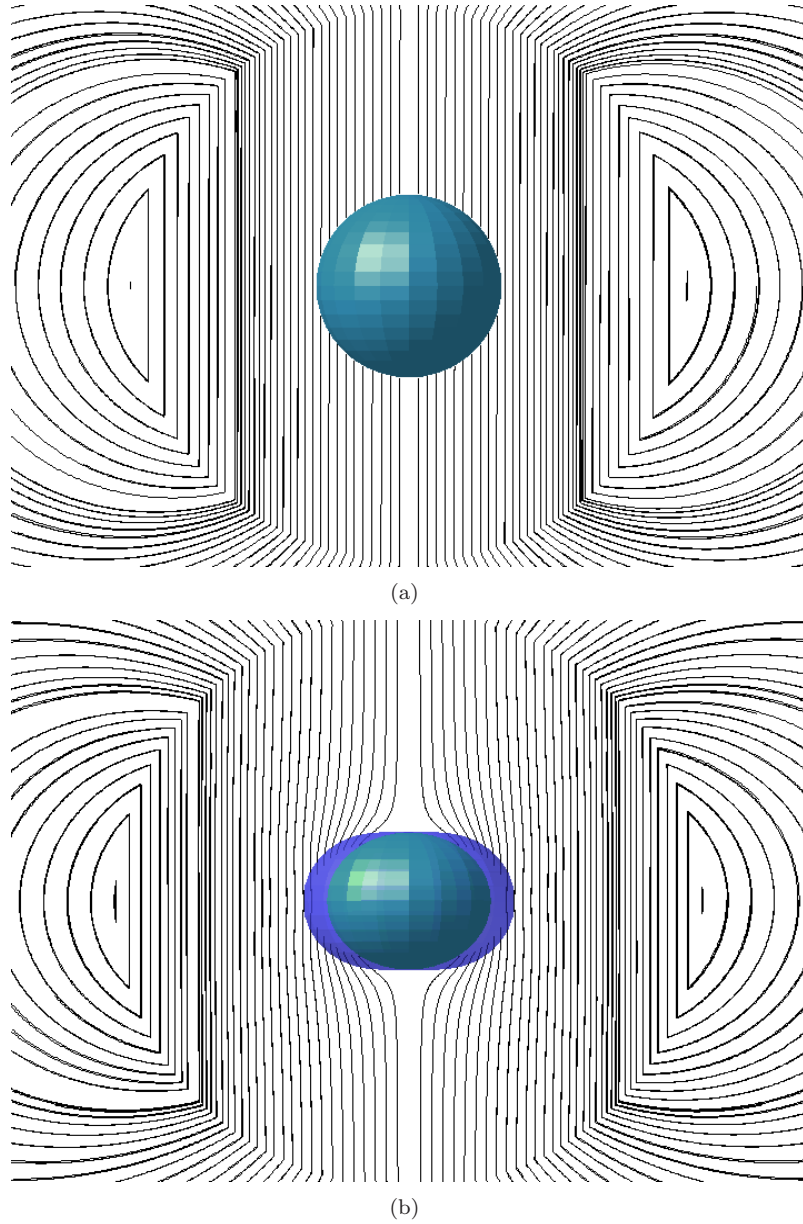


**Figure 2.2:** Magnetic field lines of a dipole magnetic field near a Kerr black hole as measured by ZAMO observer. The blue surface indicates the boundaries of the ergosphere and the green one the outer event horizon. (a) The magnetic field lines thread the event horizon for an  $a = 0$  Kerr black hole. (b) Magnetic field lines are expelled from the horizon for an  $a = 0.9$  black hole.

## 2.2 Equations of Motion in a Kerr Background Geometry

After painstaking calculations we derived the equations of motion for a charged particle in the gravitational potential of a Kerr black hole endowed in a magnetic field.

$$\begin{aligned}
\frac{d^2 t}{d\tau^2} = & - \frac{2M}{\Sigma^2 \Delta} (r^2 - a^2 \cos^2 \theta) (r^2 + a^2) \dot{t} \dot{r} \\
& - \frac{2Ma \sin^2 \theta}{\Sigma \Delta} \left[ (a^2 - r^2) - \frac{2r^2(r^2 + a^2)}{\Sigma} \right] \dot{\phi} \dot{r} \\
& + \left( \frac{4Mra^2 \sin \theta \cos \theta}{\Sigma^2} \right) \dot{\theta} \dot{t} - \left( \frac{4Ma^3 r \sin^3 \theta \cos \theta}{\Sigma^2} \right) \dot{\theta} \dot{\phi} \\
& + \frac{q}{m} \left[ \frac{2Mra}{\Sigma \Delta} (A_{\phi, r} \dot{r} + A_{\phi, \theta} \dot{\theta}) + \frac{B}{\Sigma \Delta} (A_{t, r} \dot{r} + A_{t, \theta} \dot{\theta}) \right] \quad (2.2.1)
\end{aligned}$$

$$\begin{aligned}
\frac{d^2 r}{d\tau^2} = & \frac{1}{\Delta \Sigma} (M(r^2 - a^2 \cos^2 \theta) - ra^2 \sin^2 \theta) \dot{r}^2 \\
& + \frac{2a^2 \sin \theta \cos \theta}{\Sigma} \dot{r} \dot{\theta} + \frac{r\Delta}{\Sigma} \dot{\theta}^2 - \frac{M\Delta}{\Sigma^3} (r^2 - a^2 \cos^2 \theta) \dot{t}^2 \\
& + \frac{\Delta \sin^2 \theta}{\Sigma^3} [r^5 + 2r^3 a^2 \cos^2 \theta - Mr^2 a^2 \sin^2 \theta + (M - r)a^4 \sin^2 \theta \cos^2 \theta \\
& + ra^4 \cos^2 \theta] \dot{\phi}^2 \\
& + \frac{2\Delta a M \sin^2 \theta}{\Sigma^3} (r^2 - a^2 \cos^2 \theta) \dot{\phi} \dot{t} + \frac{q}{m} \frac{\Delta}{\Sigma} (A_{\phi, r} \dot{\phi} + A_{t, r} \dot{t}) \quad (2.2.2)
\end{aligned}$$

$$\begin{aligned}
\frac{d^2 \theta}{d\tau^2} = & - \frac{1}{\Sigma \Delta} (a^2 \sin \theta \cos \theta) \dot{r}^2 - \frac{2r}{\Sigma} \dot{r} \dot{\theta} + \frac{a^2 \sin \theta \cos \theta}{\Sigma} \dot{\theta}^2 \\
& - \frac{4Mra}{\Sigma^3} (r^2 + a^2) \sin \theta \cos \theta \dot{\phi} \dot{t} + \frac{2Mr}{\Sigma^3} a^2 \sin \theta \cos \theta \dot{t}^2 \\
& + \frac{\sin \theta \cos \theta}{\Sigma^3} [(r^2 + a^2)^3 - (r^2 + a^2 + \Sigma)\Delta a^2 \sin^2 \theta] \dot{\phi}^2 \\
& + \frac{q}{m} \frac{1}{\Sigma} (A_{\phi, \theta} \dot{\phi} + A_{t, \theta} \dot{t}) \quad (2.2.3)
\end{aligned}$$

$$\begin{aligned}
\frac{d^2 \phi}{d\tau^2} = & - \frac{2aM}{\Delta \Sigma^2} (r^2 - a^2 \cos^2 \theta) \dot{t} \dot{r} + \frac{4aMr \cos \theta}{\Sigma^2 \sin \theta} \dot{t} \dot{\theta} \\
& - \frac{2}{\Sigma^2 \Delta} [r\Sigma \Delta - a^2 \sin^2 \theta (r\Sigma + M(r^2 - a^2 \cos^2 \theta))] \dot{\phi} \dot{r} \\
& - \frac{2 \cos \theta}{\sin \theta} \left[ 1 + \frac{2a^2 Mr \sin^2 \theta}{\Sigma^2} \right] \dot{\theta} \dot{\phi} \\
& + \frac{q}{m} \left[ \frac{2Mra}{\Sigma \Delta} (A_{t, r} \dot{r} + A_{t, \theta} \dot{\theta}) - \left( 1 - \frac{2Mr}{\Sigma} \right) \frac{1}{\Delta \sin^2 \theta} (A_{\phi, r} \dot{r} + A_{\phi, \theta} \dot{\theta}) \right] \quad (2.2.4)
\end{aligned}$$

where  $m_{part}$  is particle's mass. We have adopted geometrized units.

Replacing equations (2.1.10a)-(2.1.10d) in eq. (2.2.1)-(2.2.4) we obtain the equations of motion for a charged particle.

## 2.3 The Effective potential

We consider the more general Kerr-Newman metric so we can describe mathematically a black hole of mass  $M$ , net charge  $Q$  and angular momentum  $a = J/M$  [24],

$$ds^2 = - \left( 1 - \frac{2Mr - Q^2}{\Sigma} \right) dt^2 - 2a \sin^2 \theta \frac{2Mr - Q^2}{\Sigma} dt d\phi + \frac{\Sigma}{\Delta + Q^2} dr^2 + \Sigma d\theta^2 + \frac{B - Q^2 a^2 \sin^2 \theta}{\Sigma} \sin^2 \theta d\phi^2 \quad (2.3.1)$$

where  $m, q$  the mass and charge of the charged particle respectively and

$$\begin{aligned} \Sigma &= r^2 + a^2 \cos^2 \theta \\ \Delta &= r^2 - 2Mr + a^2 \\ B &= (r^2 + a^2)^2 - \Delta a^2 \sin^2 \theta \end{aligned}$$

The associated one-form potential of the black hole has nonvanishing components

$$A_t = \frac{Qr}{\Sigma}, \quad A_\phi = \frac{-Qar \sin^2 \theta}{\Sigma} \quad (2.3.2)$$

The mapping between the Boyer-Lindquist coordinates<sup>1</sup> and the Cartesian coordinates is performed by the following relations:

$$x = \sqrt{r^2 + a^2} \cos \phi \sin \theta \quad (2.3.3a)$$

$$y = \sqrt{r^2 + a^2} \sin \phi \sin \theta \quad (2.3.3b)$$

$$z = r \cos \theta \quad (2.3.3c)$$

An external magnetic field is superimposed to the geometry (2.3.1). The magnitude of the magnetic field is such that it doesn't affect the metric. As stated before, the best way to find a relation for the magnetic field, in curved spacetime, is by perturbing the Maxwell equations [36]. Our intention is to deduce an analytical expression for the effective potential of the composite system described above. For generality's sake we will not replace the vector potential for a specific field, but keep a general formula for the effective potential.

The generalized momenta (per particle's mass) for a charged particle traveling near the black hole (2.3.1) and through a magnetic field are obtained from the Lagrangian, ( $\mathcal{L} = \frac{1}{2}g_{\mu\nu}u^\mu u^\nu + \frac{q}{m}A_\mu u^\mu$ ).

$$\begin{aligned} \mathcal{L} = \frac{1}{2} \left[ - \left( 1 - \frac{2Mr - Q^2}{\Sigma} \right) \dot{t}^2 - 2a \sin^2 \theta \left( \frac{2Mr - Q^2}{\Sigma} \right) \dot{t} \dot{\phi} + \left( \frac{\Sigma}{\Delta + Q^2} \right) \dot{r}^2 + \Sigma \dot{\theta}^2 \right. \\ \left. + \frac{B}{\Sigma} \sin^2 \theta \dot{\phi}^2 \right] + \frac{q}{m} A_t \dot{t} + \frac{q}{m} A_\phi \dot{\phi} \end{aligned}$$

It is obvious that the Lagrangian is independent of the generalized coordinates  $t$  and  $\phi$ , so their conjugate quantities have to be conserved.

$$\tilde{p}_t = p_t + \frac{q}{m} A_t = - \left( 1 - \frac{2Mr - Q^2}{\Sigma} \right) \dot{t} - a \sin^2 \theta \left( \frac{2Mr - Q^2}{\Sigma} \right) \dot{\phi} + \frac{q}{m} A_t = -E \quad (2.3.4)$$

$$\tilde{p}_\phi = p_\phi + \frac{q}{m} A_\phi = -a \sin^2 \theta \left( \frac{2Mr - Q^2}{\Sigma} \right) \dot{t} + \frac{B - Q^2 a^2 \sin^2 \theta}{\Sigma} \dot{\phi} + \frac{q}{m} A_\phi = L_z \quad (2.3.5)$$

<sup>1</sup>The coordinates we have used to describe the spacetime.

Solving the previous system of equations in terms of  $\dot{t}$  and  $\dot{\phi}$  we arrive at:

$$\dot{t} = -a \frac{2Mr - Q^2}{\Sigma(\Delta + Q^2)} \left( L_z - \frac{q}{m} A_\phi \right) + \frac{B - Q^2 a^2 \sin^2 \theta}{\Sigma(\Delta + Q^2)} \left( E + \frac{q}{m} A_t \right) \quad (2.3.6)$$

$$\dot{\phi} = a \frac{2Mr - Q^2}{\Sigma(\Delta + Q^2)} \left( E + \frac{q}{m} A_t \right) + \frac{1}{(\Delta + Q^2) \sin^2 \theta} \left( L_z - \frac{q}{m} A_\phi \right) \quad (2.3.7)$$

To simplify further our problem, we will make use of the normalization condition<sup>2</sup>

$$p^\alpha p_\alpha = -1 \quad (2.3.8)$$

This way we find a relation that involves only the conserved quantities, the generalized coordinates and the components of the vector potential. Expressing  $u_\alpha u^\alpha$  in terms of the generalized angular momentum and energy yields the desired equation.

Thereby, replacing  $p_t$  and  $p_\phi$  from eq. (2.3.4), (2.3.5) and using (2.3.6), (2.3.7) in (2.3.8)

$$\begin{aligned} p^\alpha p_\alpha = & - \left( E + \frac{q}{m} A_t \right)^2 \frac{B - Q^2 a^2 \sin^2 \theta}{\Sigma(\Delta + Q^2)} + \frac{2a(2Mr - Q^2)}{\Sigma(\Delta + Q^2)} \left( E + \frac{q}{m} A_t \right) \left( L_z - \frac{q}{m} A_\phi \right) \\ & + \left( L_z - \frac{q}{m} A_\phi \right)^2 \left( 1 - \frac{2Mr - Q^2}{\Sigma} \right) \frac{1}{\sin^2 \theta} + \Sigma \dot{\theta}^2 + \frac{\Sigma}{\Delta + Q^2} \dot{r}^2 = -1 \end{aligned} \quad (2.3.9)$$

Expanding some of the terms of equation (2.3.9), changing signs and placing  $\dot{r} = 0$  and  $\dot{\theta} = 0$  we get,

$$\begin{aligned} E^2(B - Q^2 a^2 \sin^2 \theta) + 2E \frac{q}{m} A_t (B - Q^2 a^2 \sin^2 \theta) + \frac{q^2}{m^2} A_t^2 (B - Q^2 a^2 \sin^2 \theta) \\ - 2a(2Mr - Q^2) E \left( L_z - \frac{q}{m} A_\phi \right) - 2a \frac{q}{m} A_t (2Mr - Q^2) \left( L_z - \frac{q}{m} A_\phi \right) \\ - \frac{\Sigma}{\sin^2 \theta} \left( L_z - \frac{q}{m} A_\phi \right)^2 \left( 1 - \frac{2Mr - Q^2}{\Sigma} \right) - \Sigma^2 (\Delta + Q^2) \dot{\theta}^2 - \Sigma^2 \dot{r}^2 - (\Delta + Q^2) \Sigma = 0 \end{aligned} \quad (2.3.10)$$

The previous equation can be reduced to a quadratic equation of the type

$$\alpha E^2 - 2\beta E + \gamma = 0 \quad (2.3.11)$$

The root  $E$  of equation (2.3.11), which satisfies eq. (2.3.10) and additionally  $\dot{r} = 0$  and  $\dot{\theta} = 0$ , corresponds to the effective potential of the hole. By placing  $\dot{r} = 0$  and  $\dot{\theta} = 0$  in equation (2.3.11) we determine  $\alpha'$ ,  $\beta'$  and  $\gamma'$  for the effective potential through equations

$$\alpha' = B - Q^2 a^2 \sin^2 \theta \quad (2.3.12a)$$

$$\beta' = -\frac{q}{m} A_t (B - Q^2 a^2 \sin^2 \theta) + a(2Mr - Q^2) \left( L_z - \frac{q}{m} A_\phi \right) \quad (2.3.12b)$$

$$\begin{aligned} \gamma' = & \frac{q^2}{m^2} A_t^2 (B - Q^2 a^2 \sin^2 \theta) - \frac{2q}{m} A_t a (2Mr - Q^2) \left( L_z - \frac{q}{m} A_\phi \right) \\ & - \frac{\Sigma}{\sin^2 \theta} \left( L_z - \frac{q}{m} A_\phi \right)^2 \left( 1 - \frac{2Mr - Q^2}{\Sigma} \right) - (\Delta + Q^2) \Sigma \end{aligned} \quad (2.3.12c)$$

In conclusion, the effective potential reads

$$V_{\text{eff}} = \frac{\beta' \pm \sqrt{\beta'^2 - \alpha' \gamma'}}{\alpha'}$$

<sup>2</sup>The four-momenta  $p^\alpha$ , angular momentum  $L$  and energy  $E$  are expressed per unit mass.

and because of the fact that the four-momentum must point toward the future (and not toward the past) we will keep only the positive sign

$$V_{\text{eff}} = \frac{\beta' + \sqrt{\beta'^2 - \alpha'\gamma'}}{\alpha'} \quad (2.3.13)$$

Eq. (2.3.13) displays the dependence of charged particle's motion on the formula of the magnetic field. Hereupon we study two different cases for the vector potential. The first one corresponds to a uniform magnetic field. You might think that this is not a very realistic magnetic field. Though, the uniform magnetic field is a good approximation, close to the black hole, to the internal solution of a ring current (magnetic dipole). Moreover, we remind you that galaxies are percolated by a uniform magnetic field. Hence, this case is not astrophysically irrelevant. Lastly we replace the magnetic field by that of a magnetic dipole, generated by an ideal toroidal current at the equatorial plane. The key point is to understand the physics of an accretion disc and the surrounding environment through the employment of simpler models.

## 2.4 Guiding Center and Combined Gravitational and Magnetic Fields

In addition to the already derived analysis for the effective potential, we will present some relations concerning the motion of the guiding center. For a more detailed and strict approach see [4; 5; 14]. This approach will help us to understand better the motion of charged particles around a black hole immersed in magnetic fields.

The electric and magnetic fields  $\mathbf{E}$ ,  $\mathbf{B}$  and the gravitational acceleration  $\mathbf{g}$  are defined by the forces they exert on particles. Expressing velocity  $\mathbf{v}$  of a moving particle as measured by a FIDO observer in terms of the star-fixed spatial coordinates ( $dx^j/dt_{\text{part}}$ )

$$v^j = \frac{dt}{d\tau} \left[ \left( \frac{dx^j}{dt} \right)_{\text{part}} - \left( \frac{dx^j}{dt} \right)_{\text{FIDO}} \right] = \frac{1}{\alpha} \left[ \left( \frac{dx^j}{dt} \right)_{\text{part}} + \beta^j \right]$$

where  $\alpha = \Sigma\Delta/B$ ,  $\beta^r = \beta^\theta = 0$  and  $\beta^\phi = -2aMr/B$ ,  $\mathbf{E}$ ,  $\mathbf{B}$ ,  $\mathbf{v}$  are all 3-dimensional vectors,  $\mathbf{v} = v^j(\partial/\partial x^j)$  and  $d\tau$  refers to the FIDO proper time. Now, we can define the momentum of a particle of mass  $m$  and velocity  $\mathbf{v}$

$$\mathbf{p} = m \frac{\mathbf{v}}{\sqrt{1 - \mathbf{v}^2}}$$

The FIDO defines the electric and magnetic fields by the Lorentz force exerted on the charged particle  $q$

$$\left( \frac{d\mathbf{p}}{d\tau} \right)_{\text{Lorentz}} = q(\mathbf{E} \times \mathbf{B}) \quad (2.4.1)$$

and they define the gravitational acceleration  $\mathbf{g}$  as

$$\left( \frac{d\mathbf{p}}{d\tau} \right)_{\text{grav}} = \frac{m}{\sqrt{1 - \mathbf{v}^2}} \mathbf{g} \quad (2.4.2)$$

For a rotating black hole the gravitational acceleration due to the gradient of the lapse function is given in [31]

$$\mathbf{g} = -\nabla \ln \alpha = -\frac{M\Sigma(r^4 - a^4) + 2Mr^2a^2\Delta \sin^2 \theta}{B\Sigma\sqrt{\Sigma}\Delta} \mathbf{e}_{\hat{r}} + \frac{2Mr a^2(r^2 + a^2)}{B\Sigma\sqrt{\Sigma}} \cos \theta \sin \theta \mathbf{e}_{\hat{\phi}} \quad (2.4.3)$$

In addition to the gravitational field  $\mathbf{g}$  there is one extra field called the gravitomagnetic field, which arises due to the gradient of the shift function  $\beta$ . The components of the gravitomagnetic field are

$$\mathbf{H} = \frac{\nabla\beta}{\alpha} = -\frac{2aM}{\Sigma^2\sqrt{\Sigma}} \left[ (r^2 - a^2 \cos^2 \theta) \sin \theta \mathbf{e}_{\hat{\theta}} + \frac{2r(r^2 + a^2)}{\sqrt{\Delta}} \cos \theta \mathbf{e}_{\hat{r}} \right] \quad (2.4.4)$$

Because  $\beta_j$  drops as  $\sim J/r^3$  we can neglect the contribution of the gravitomagnetic field to the guiding center motion as we move away from the event horizon.

Now, considering a non-relativistic particle eq. (2.4.1), (2.4.2) reduce to,

$$m\mathbf{g} + q(\mathbf{E} \times \mathbf{B}) = 0$$

We have omitted the  $m d\mathbf{v}/dt$  term because it contributes only to the circular Larmor motion. Assuming a general magnetic field the observed drifts of the guiding center are the following,

$$v_{gc\perp} = \frac{m \mathbf{g} \times \mathbf{B} + \mathbf{E} \times \mathbf{B}}{q B^2} \quad (2.4.5)$$

The drift described above is the sum of the contributions of the electric and gravitational force. It is perpendicular to the force acting upon the particle (the electric or gravitational) but these differ from each other in one thing. The gravitational drift changes sign with respect to the particle's charge. Due to the gravitational force protons and electrons drift in opposite directions. The reason for this drift is the change in Larmor radius as it gains or loses energy in the gravitational field.

Another drift is related to the gradient and curvature of the magnetic field. These can be combined in one relation [13].

$$v_{gc} = \frac{m \mathbf{R}_c \times \mathbf{B}}{q R_c^2 B^2} \left( v_{\parallel}^2 + \frac{1}{2} v_{\perp}^2 \right) \quad (2.4.6)$$

where  $R_c$  is the curvature of the magnetic field lines. These drifts do not add. This means that if one bends the field lines into a torus, the particles will drift out of the torus.

# Chapter 3

## Charged-Particle Motions

This chapter focuses on a single charged particle's motion around a black hole endowed in a magnetic field. We will separate our results in mainly two categories, a) orbits for which  $\theta = 0$  and b) orbits including lateral motion. A comparison between the effective potential of a black hole with no external magnetic fields and one with magnetic fields is made.

### 3.1 Numerical Analysis

The equations of motion for charged particles near a magnetized rotating black hole are:

$$\frac{dx^\mu}{d\tau} = p^\mu \tag{3.1.1a}$$

$$\frac{dp^\mu}{d\tau} = -\Gamma^\mu_{\rho\sigma} p^\rho p^\sigma \tag{3.1.1b}$$

or alternatively equations (2.2.1)-(2.2.4) can be directly integrated. We have assembled the data in an 8-dimensional vector  $R = [p^\mu, x^\mu]$  and integrated the system of equations (1.1.5), (3.1.1a) implementing the fourth order Runge-Kutta adaptive stepsize scheme found in [29]. The code we have created in order to perform the above calculations is given in Ap. 5. The quantities in the code are all dimensionless. The dimensionless version of eq. (2.2.1)-(2.2.4) integrated numerically is obtained by placing  $M = 1$  everywhere. All quantities in the code are expressed in L-T-M units.

#### 3.1.1 Assumptions

The assumptions we have made so far in our theoretical analysis are the following:

- space around the black hole is considered void, in other words there is no matter or charges surrounding the black hole. Which of course is not true. What is true is that plasma forms a magnetosphere around the black hole. The proper approach would be to solve the full GRMHD equations (especially near the horizon) in order to take into account any effects of conductivity, magnetic pressure etc, that the surrounding plasma exerts on the particle under examination. As mentioned in Chap.1 plasma density and pressure around the black hole, apart from the accretion disk, is so low that can be neglected in MHD equations. Consequently, we are “allowed” to study the single particle approach and study its equations of motion considering that it doesn't interact with matter in the neighborhood of the black hole.
- the magnetic fields we employ, do not bend spacetime. We are aware that magnetic fields contribute to the energy density of the energy-momentum tensor  $T_{\mu\nu}$  in Einstein field equations. As discussed before the magnetic fields we encounter in the region of a black hole is

small compared to the gravitational one, so in a sense we can ignore the magnetic contributions. If one wishes to include this coupling between the gravitational and magnetic field, he will have to solve Einstein field equations. The calculation is too painstaking and can only be achieved by the use of computational arithmetic procedures. Again, knowing that the “magnetic contribution” to the structure of spacetime is so little, we can ignore it.

- we assume that no radiation of electromagnetic or gravitational nature is emitted from the charged particle. Any of these mechanisms would “absorb” energy from the particle.
- the mechanism that provides us with the magnetic field is not studied here. Generally speaking this mechanism arise from currents inside the accretion disk. The magnetic fields we have studied have a relatively simple structure compared to the realistic ones that are generated in the disk. In order to deduce a realistic-like magnetic field one has to solve the GRMHD equations describing the plasma fluid in the accretion disk. A uniform-like test-magnetic field could correspond to a galactic magnetic field, or be used to approximate the magnetic dipole field near the black hole and for a distance  $r < r_o$ , where  $r_o$  the situation of the accretion disk.
- particle do not affect the spacetime metric. The motion of the black hole or the magnetic fields. Its mass compared to the black hole is too small to be considered. Its charge can only produce electromagnetic fields of very low magnitude. Therefore we regard the charged particle as a classical test particle with charge which in no way alters the topology of the system.

### 3.1.2 Integral of Motions

We have discussed in §2.3 that the motion of a charged particle has at least three integrals of motion. In particular, energy  $E$ , angular momentum  $L$  and the rest mass are constants of motion in any stationary and axisymmetric spacetime.

$$-E = p_t + \frac{q}{m}A_t = -\left(1 - \frac{2Mr}{\Sigma}\right)\dot{t} - a\sin^2\theta\left(\frac{2Mr}{\Sigma}\right)\dot{\phi} + \frac{q}{m}A_t \quad (3.1.2)$$

$$L_z = p_\phi + \frac{q}{m}A_\phi = -a\sin^2\theta\left(\frac{2Mr}{\Sigma}\right)\dot{t} + \frac{B}{\Sigma}\dot{\phi} + \frac{q}{m}A_\phi \quad (3.1.3)$$

$$p^\alpha p_\alpha = -\left(E + \frac{q}{m}A_t\right)^2 \frac{B - Q^2 a^2 \sin^2\theta}{\Sigma(\Delta + Q^2)} + \frac{2a(2Mr - Q^2)}{\Sigma(\Delta + Q^2)} \left(E + \frac{q}{m}A_t\right) \left(L_z - \frac{q}{m}A_\phi\right) \quad (3.1.4)$$

$$+ \left(L_z - \frac{q}{m}A_\phi\right)^2 \left(1 - \frac{2Mr - Q^2}{\Sigma}\right) \frac{1}{\sin^2\theta} + \Sigma\dot{\theta}^2 + \frac{\Sigma}{\Delta + Q^2}\dot{r}^2 = -1 \quad (3.1.5)$$

The three quantities above will help us check of the correctness of our code. The conservation of these quantities is a sign that our code is up and running and yields the desired results.

## 3.2 Trajectories in the Equatorial Plane

This sections refers to equatorial motions, namely motions with initial conditions  $\theta = \pi/2$  and  $u_\theta = 0$ . The motion of a particle in the field of a dipole or uniform magnetic in a Kerr background geometry will remain on the equatorial plane forever, unless the trajectory crosses the outer event horizon. The reason why this happens is that axisymmetric magnetic fields acting upon a particle are pointing towards the z direction. This means that locally the magnetic force they exert on a charged particle is parallel to the z direction. As we know from classical electrodynamics, a particle moving on  $r - \phi$  plane will feel a force that forces it to remain in that  $r - \phi$  plane. Eq.

$mdv/dt = q/m v \times \mathbf{B}/c$  forbids any motion on  $\theta$ -direction. Consequently a particle initially placed on the equatorial plane, with  $u_\theta = 0$  will remain on the equatorial plane.

The reaction of particle's motion to the gravitational and magnetic field is essential because it provides us with information about the interplay of electromagnetism and the curvature of spacetime due to strong gravitational fields. Equatorial plane motions give us only a taste of this interaction. Prasanna and Varma [27]; Sengupta [33]; Prasanna and Vishveshwara [28]; Prasanna and Sengupta [26] have found that the presence of a magnetic field, in different geometries, increases the range of stable orbits. What we expect to see is a Larmor-like motion, modified by any effects of gravity for specific values of energy, momentum and location of the particle. We will exhibit the differences between motions in a Kerr background geometry with and without a magnetic field acting upon the particle.

### 3.2.1 Uniform Magnetic Field

This section refers to the uniform magnetic field case. In this case no particle escapes from the black hole. Of course the realistic magnetic fields observed near a black hole are far from uniform, this is a good approximation in the vicinity of the black hole. Fig. 3.1-3.5 illustrate the motion of a charged particle with different initial conditions. By placing  $\theta = \pi/2$ ,  $Q = 0$  and  $A_t$ ,  $A_\phi$  from eq. (2.1.8), (2.1.9) in (2.3.12) and (2.3.13) we deduce a relation for the effective potential of the black hole with and without a superimposed magnetic ( $A_t$ ,  $A_\phi=0$ ) field. We observe that most of the trajectories depicted could not have been observed in the absence of the uniform magnetic field.

It is evident that increasing the magnetic field strength  $B_o$  the Larmor radius of the particle's motion is decreased (fig.3.1). Concerning the angular momentum of the particle, increasing its value we observe the widening of the potential well. Finally, the greater the particle's energy is the bigger the radius of particle's Larmor motion. The potential well for the motion of an electron is different than that of a proton. This means that there will be places where charge concentration would be allowed. For negative angular momentum the potential well appears in longer distances from the black hole something presumable, because in the vicinity of the black hole the dragging of inertial frames is significant (fig.3.4).

### 3.2.2 Dipole Magnetic Field

This section refers to the dipole magnetic field case. Concerning particles for which  $r < r_o$  the internal solution for the magnetic field has to be used when replacing  $A_t$ ,  $A_\phi$  in (2.3.12) and (2.3.13) to deduce a relation for the effective potential of the black hole with and without a superimposed magnetic ( $A_t$ ,  $A_\phi=0$ ) field. Conversely, for particles that move only for  $r > r_o$  the external solution of the magnetic dipole field has to be used. The internal solution can be approximated by the uniform magnetic field in the vicinity of the black hole, so we expect a similar behavior to that of motions in uniform magnetic fields. The only difference is that the value of a dipole magnetic field varies from place to place. In other words, the value of the dipole magnetic field is greater near the horizon than away from it. This implies that the radius of Larmor motion has to vary too. In the cases examined here this is not obvious because the difference is small. Later on, when we examine lateral motion this will become more clear. The existence of bound orbits in the presence of a dipole magnetic field (external solution) depending on the structure of the potential well is similar to the cases of the internal solution of the magnetic field and the uniform magnetic field ([28]). The curvature of the magnetic field lines of the external solution is not important here. The motion will be affected by this curvature when we include lateral motion.

A particle residing in the region  $r < r_o$  can only escape if it has energy greater than the value of the effective potential at the limit  $r = r_o$  (3.6). The discontinuity at  $r = r_o$  of the effective potential is due to the discontinuity of the magnetic field where the ring current is placed.

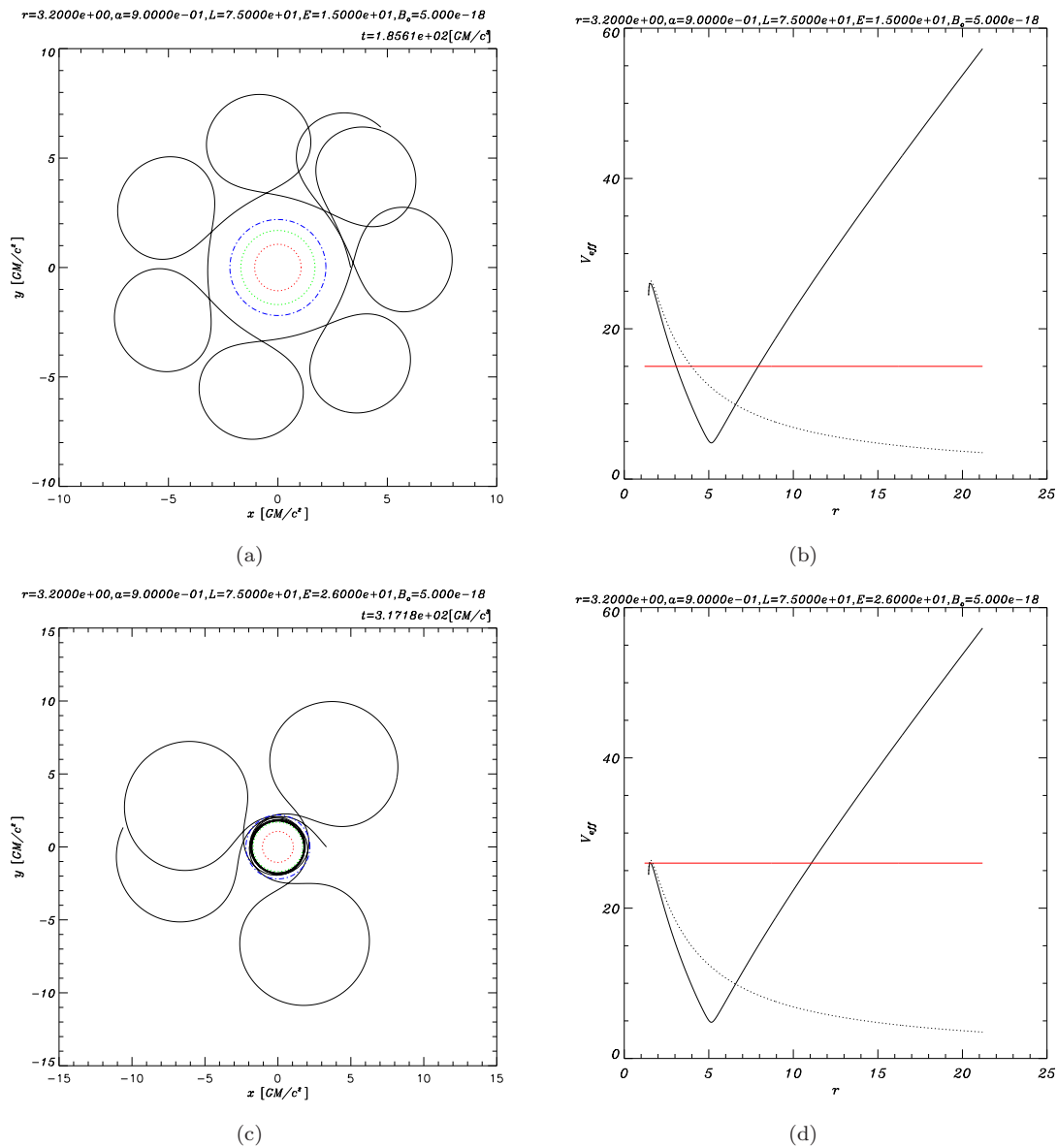


**Figure 3.1:** (a,c) The motion of a proton in the field of Kerr black hole endowed in a uniform magnetic field is depicted for different initial conditions. (b,d) The effective potential is illustrated for this case (black solid line). The effective potential for the case without a magnetic field is shown is represented with the dotted line. Finally the red line corresponds to the particle's energy  $E$ .

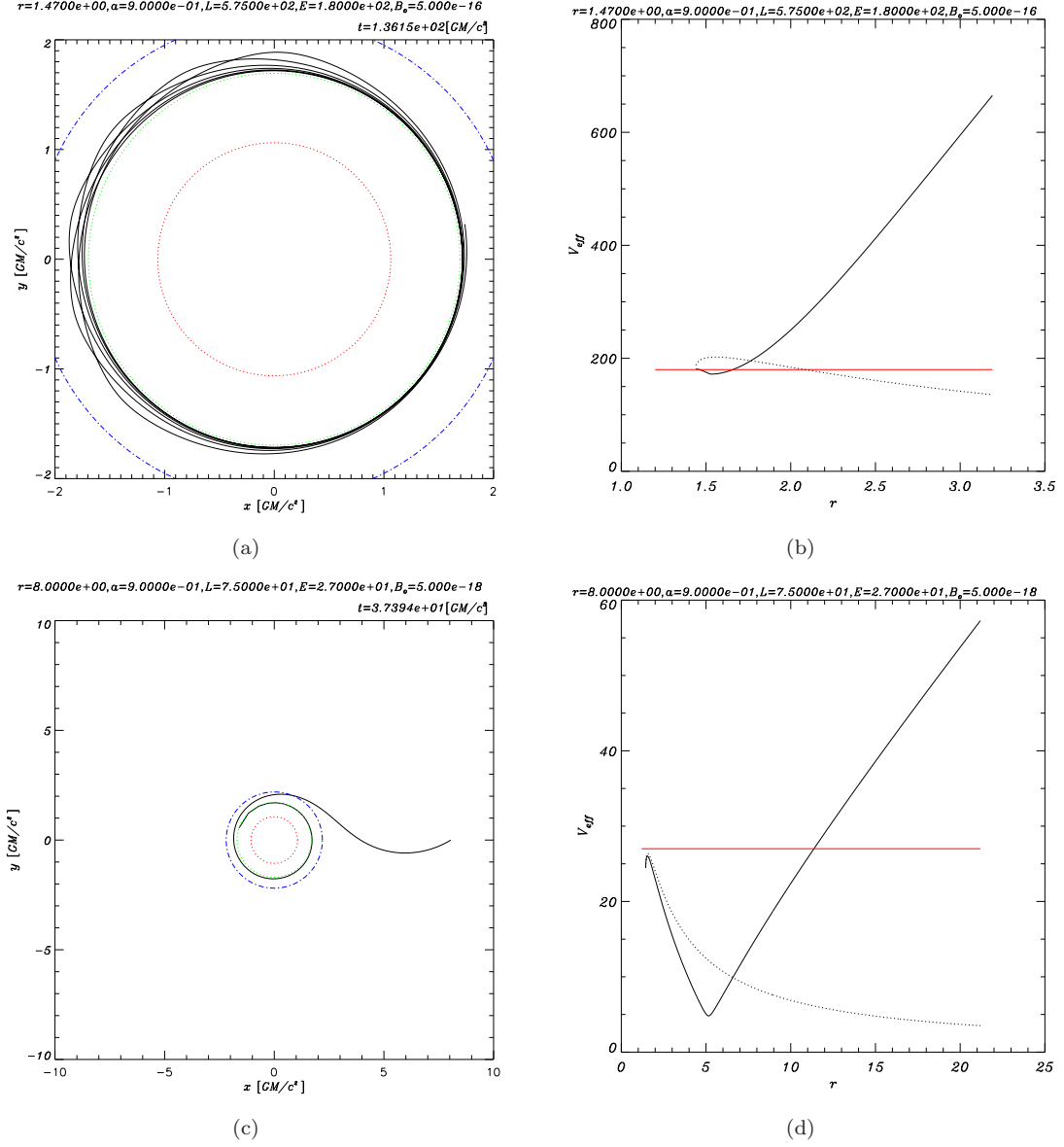


**Figure 3.2:** (a,c) The motion of a proton in the field of Kerr black hole endowed in a uniform magnetic field is depicted for different initial conditions. In fig.(a) the particle performs a nearly-circular energetically bound orbit almost touching the horizon. In fig.(c) the particle “hits” the event horizon. (b,d) The effective potential is illustrated for this case (black solid line). The effective potential for the case without a magnetic field is shown is represented with the dotted line. Finally the red line corresponds to the particle’s energy  $E$ .

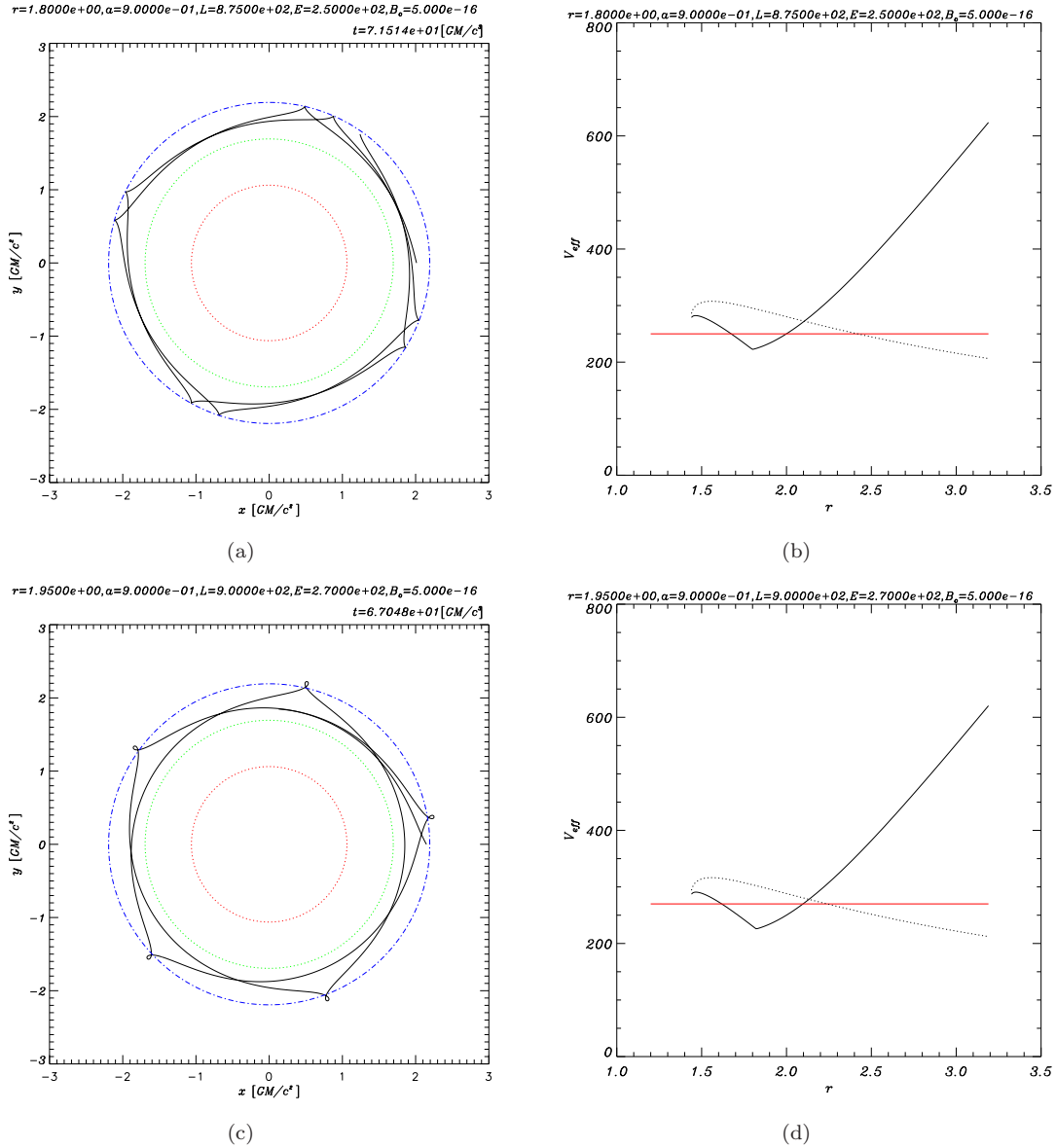


**Figure 3.3:** (a,c) The motion of a proton in the field of Kerr black hole endowed in a uniform magnetic field is depicted for different initial conditions. We observe that outside ergosphere the particle is allowed to gyrate, will inside circular motions are forbidden. (b,d) The effective potential is illustrated for this case (black solid line). The effective potential for the case without a magnetic field is shown is represented with the dotted line. Finally the red line corresponds to the particle's energy  $E$ .

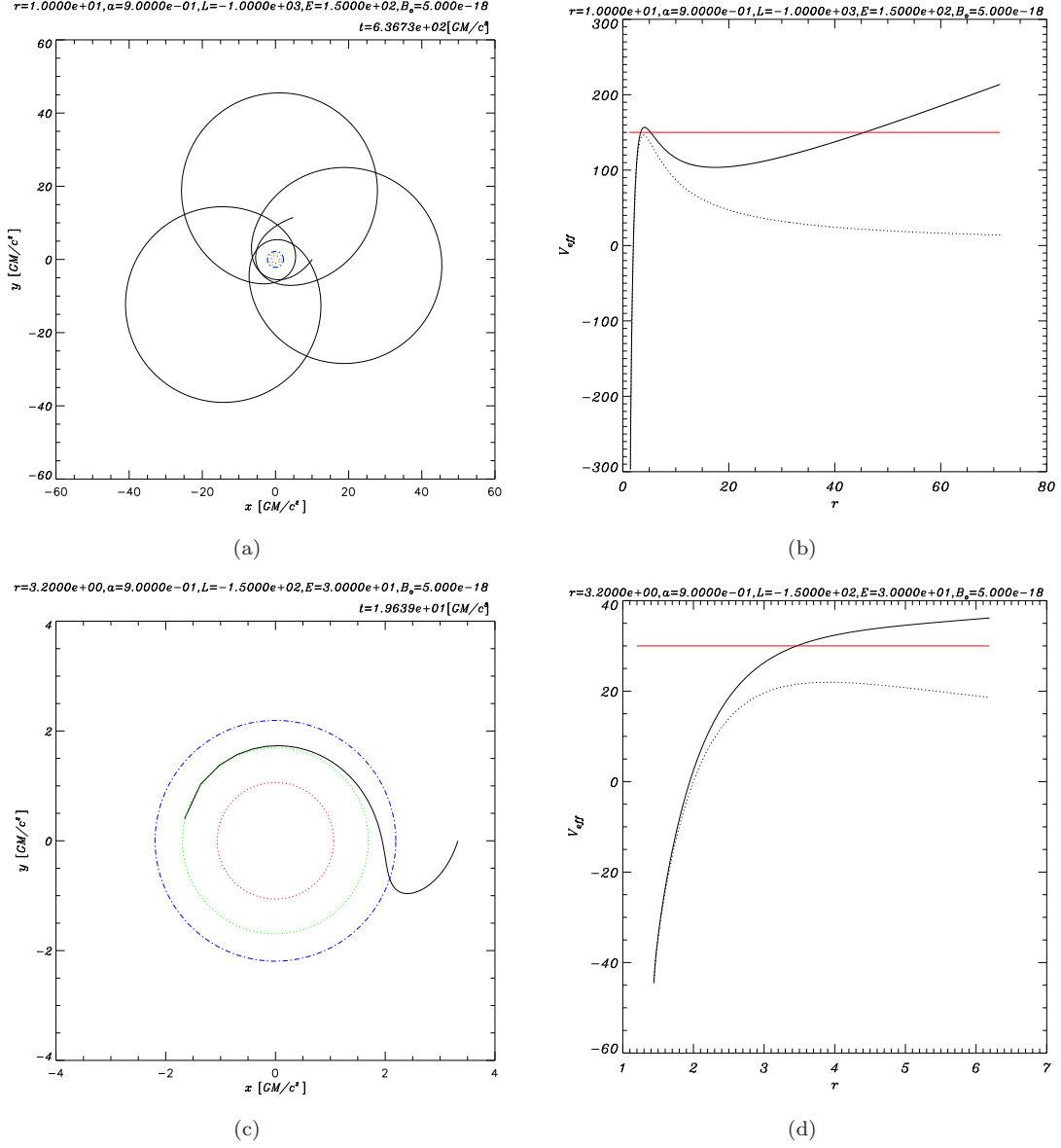


**Figure 3.4:** (a,c) The motion of a proton in the field of Kerr black hole endowed in a uniform magnetic field is depicted for different initial conditions. (b,d) The effective potential is illustrated for this case (black solid line). The effective potential for the case without a magnetic field is shown with the dotted line. Finally the red line corresponds to the particle's energy  $E$ . For negative angular momentum the potential well appears in longer distances from the black hole something which is presumable.

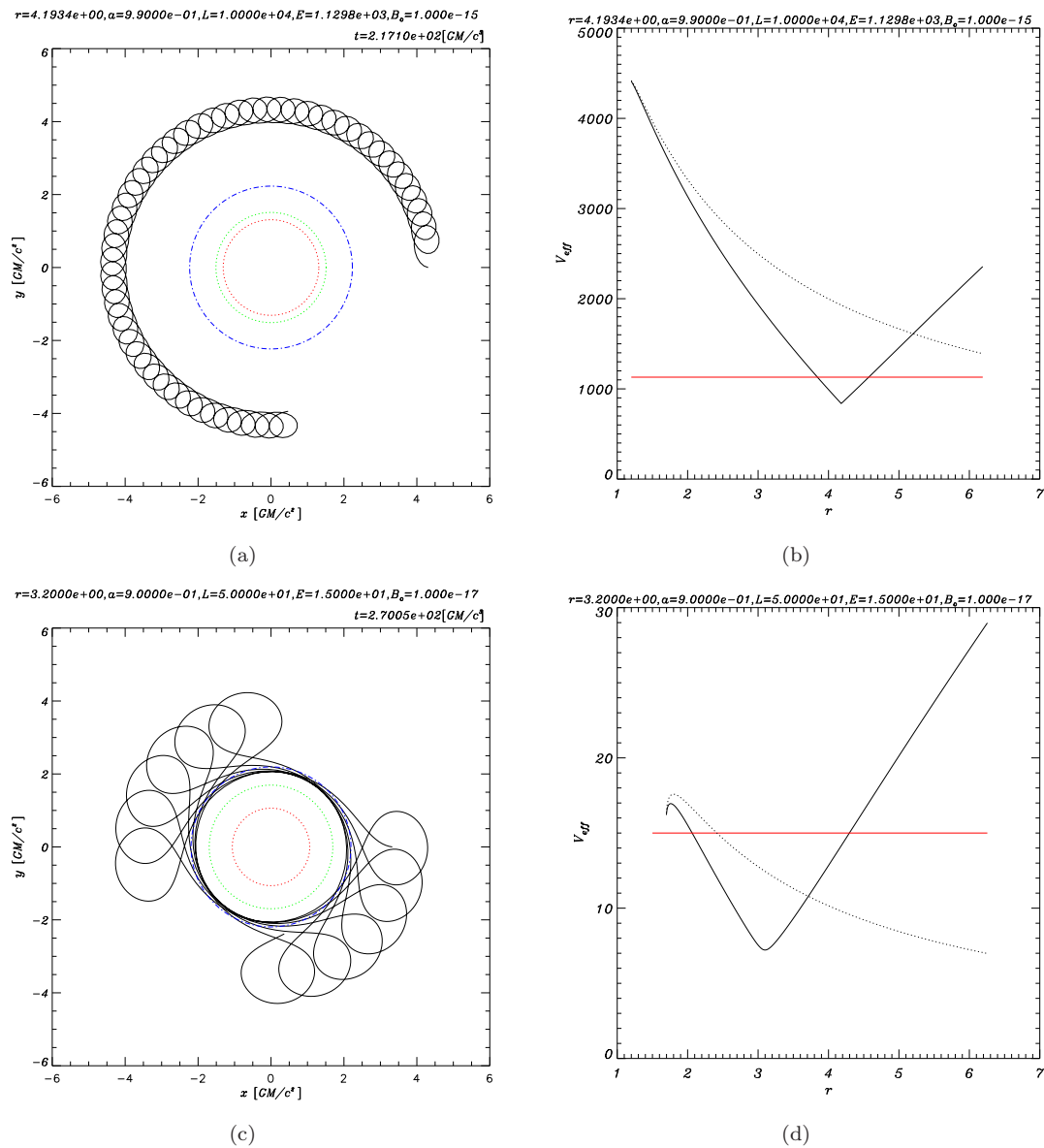


**Figure 3.5:** (a,c) The motion of a proton in the field of Kerr black hole endowed in a uniform magnetic field is depicted for different initial conditions. (b,d) The effective potential is illustrated for this case (black solid line). The effective potential for the case without a magnetic field is shown is represented with the dotted line. Finally the red line corresponds to the particle's energy  $E$ .

## Internal Solution

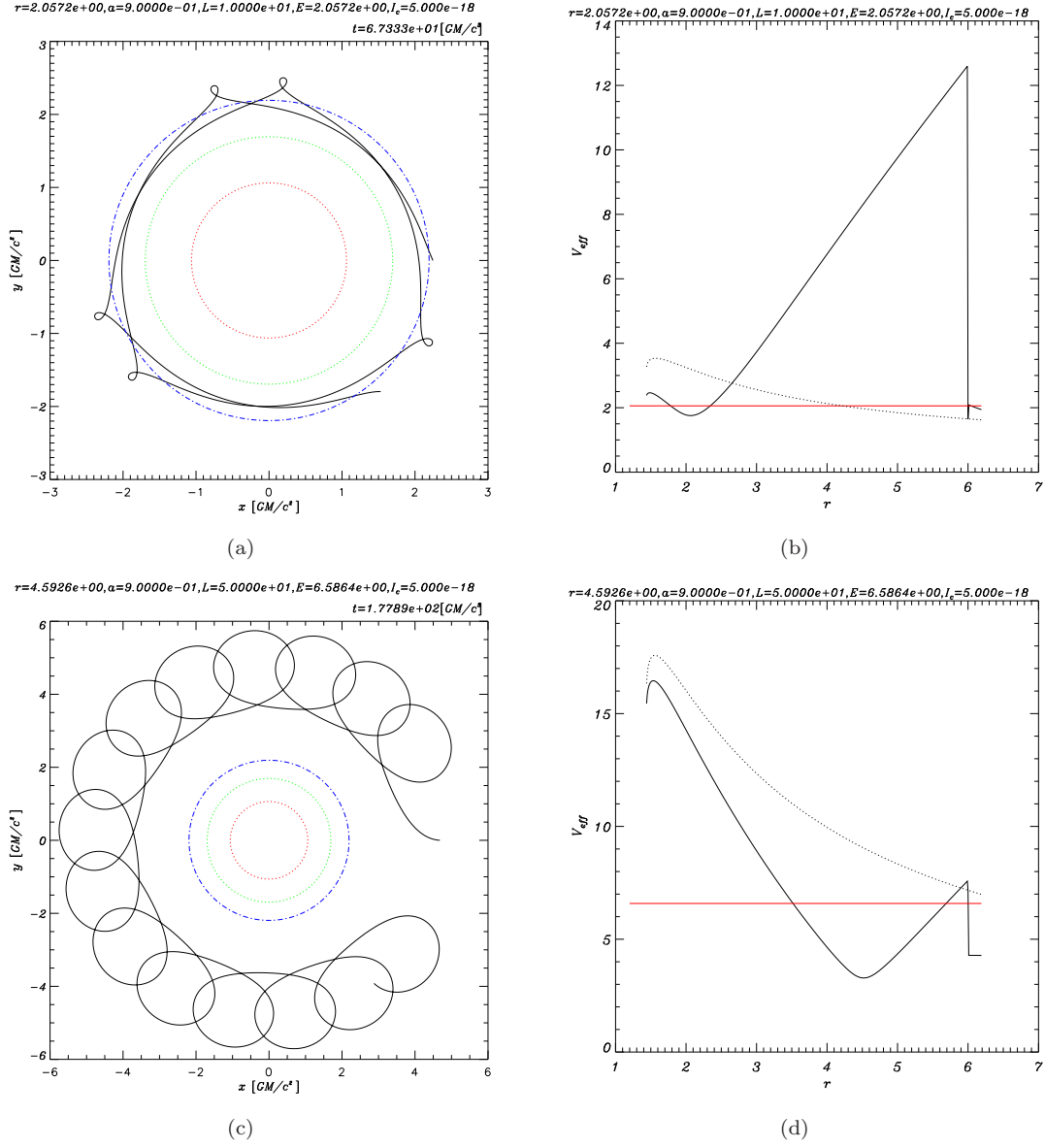


**Figure 3.6:** (a,c) The motion of a proton in the field of Kerr black hole endowed in a dipole magnetic field (internal solution) is depicted for different initial conditions. (b,d) The effective potential is illustrated for this case (black solid line). The effective potential for the case without a magnetic field is shown is represented with the dotted line. We observe that a particle residing in the region  $r < r_o$  can only escape if it has energy greater than the value of the effective potential at the limit  $r = r_o$ .

## External Solution

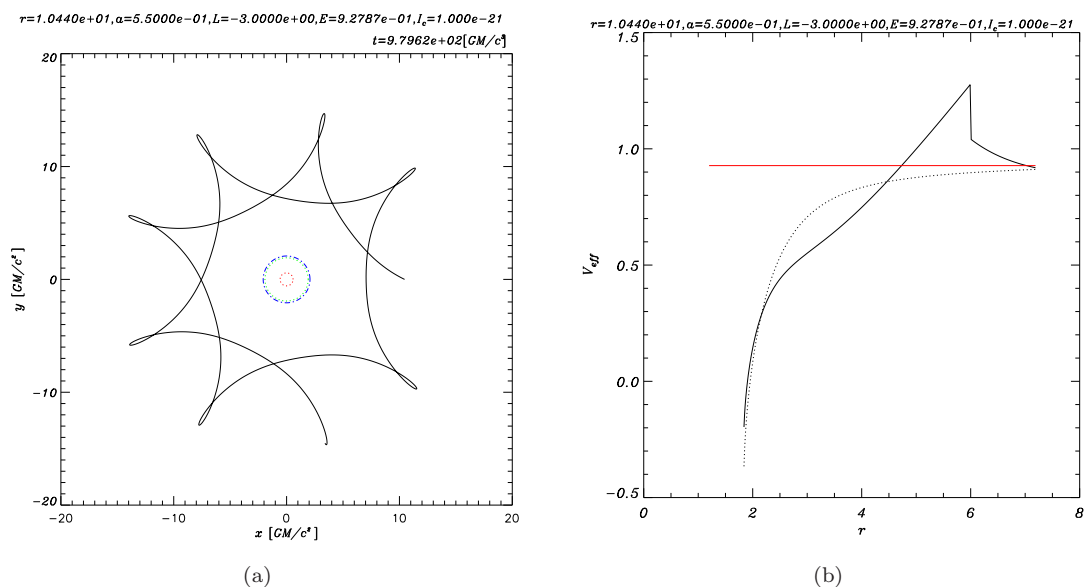


**Figure 3.7:** (a,c) The motion of an electron is depicted in the field of Kerr black hole endowed in a dipole magnetic field (external solution) is depicted. The Larmor motion of the particle has the opposite direction because of the negative charge of the electron. (b,d) The effective potential is illustrated for this case (black solid line). The effective potential for the case without a magnetic field is shown is represented with the dotted line. Finally the red line corresponds to the particle's energy  $E$ . For negative angular momentum the potential well appears in longer distances from the black hole something which is presumable.

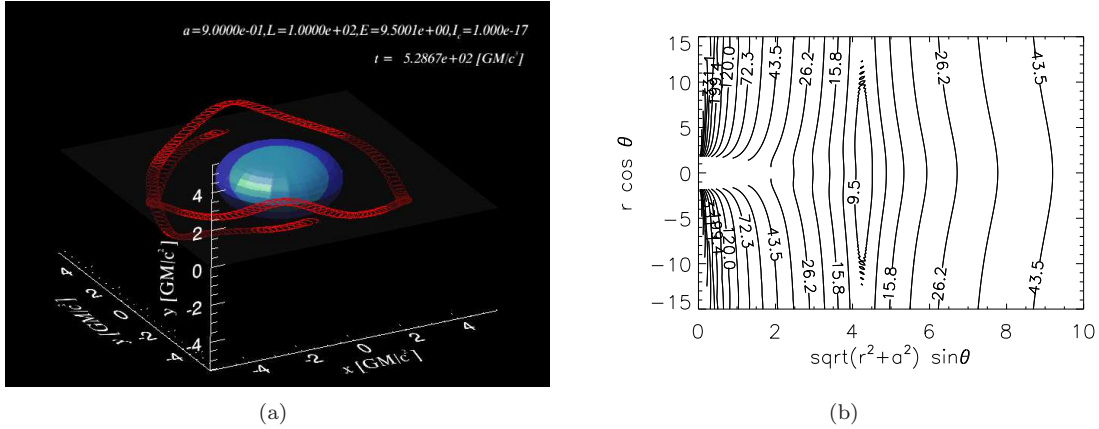
### 3.3 Trajectories including Lateral Motion

Now that we have an idea of charged particle interaction with the combined gravitational and magnetic field of the magnetized black hole we are ready to examine off-equatorial plane trajectories. Only the cases of energetically bound orbits are of significant importance. We consider that the particle has a non-zero velocity component  $v^\theta$ .

Bearing in mind the analysis in §2.4 we would expect that charged particles would gyrate around the magnetic lines but also drift. We clearly see that positive particles have a toroidal drift velocity which originates from eq. (2.4.5). Because of the straight magnetic field lines corresponding to a uniform magnetic field outside the ergoregion, the radius of Larmor motion is constant. On the other hand, it is evident from 3.9 that the divergence of the magnetic dipole field (internal solution) is responsible for the variable radius of the Larmor motion performed by the guiding center. Moreover, due to the fact that the magnetic lines of the internal solution for the dipole magnetic field are almost straight lines we don't observe any bending of the magnetic field lines in this region. We observe another drift for both the uniform and dipole magnetic fields. The drift is in  $\theta$  direction and appears because of the gravitational force. The structure of the effective potential confirms the results following. We see that for a uniform magnetic field the closed line is narrow and stretched vertically. In the dipole magnetic field however there is a wider range of values for quantity  $\sqrt{r^2 + a^2} \sin \theta$  implying a variable Larmor radius.

The existence of trapped orbits with reflection points at different "altitudes" for different initial conditions highlight the possibility of thick accretion disk formation in the region.

#### 3.3.1 Uniform Magnetic Field



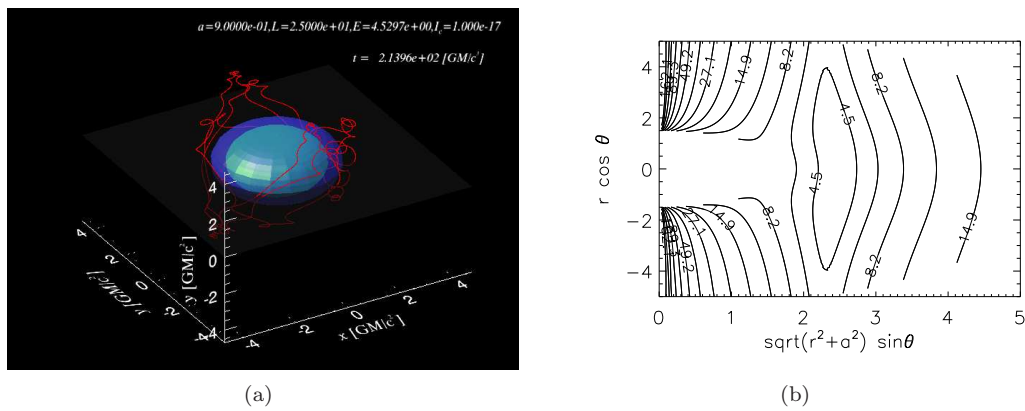


**Figure 3.9:** (a) The motion of a proton is depicted for the magnetic dipole field case (internal solution). (b) The effective potential is illustrated for this case. The closed line corresponds to the bound orbit.

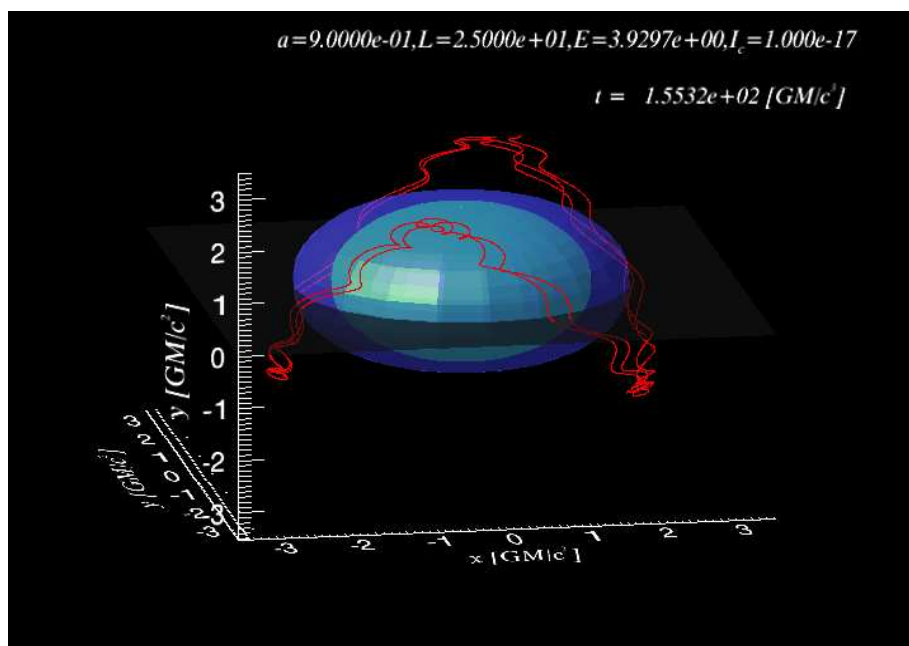


**Figure 3.10:** The motion of a proton is depicted for the magnetic dipole field case (internal solution)

### External Solution

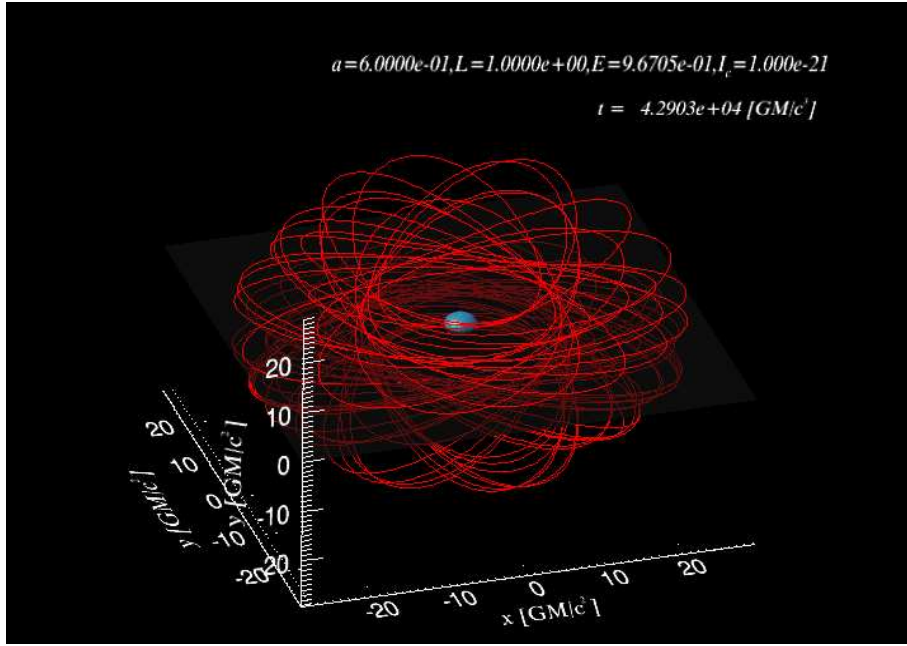


Figure 3.11: The motion of an electron is depicted.

## 3.4 Motion of a Group of Particles

Our intention for this section is to demonstrate some of the capabilities of the code we have created. Following the steps described in [1] we deduce a function describing the distribution of an accretion disk around a Kerr black hole with no external magnetic fields,

$$\rho = \left\{ \frac{\Gamma - 1}{k\Gamma} \left[ \frac{u^t}{u_{\text{out}}^t} \left( \frac{1 - l_o\Omega}{1 - l_o\Omega_{\text{out}}} \right) - 1 \right] \right\}^{\frac{1}{\Gamma-1}} \quad (3.4.1)$$

where  $u_{\text{out}}^t$  is the time velocity component of the outer boundary of the disk and  $\Omega_{\text{out}}$  the angular velocity of the outer boundary of the disk. In addition, throughout our analysis we take  $k = 1$ ,  $\Gamma = 4/3$  and  $l_o = 3.9$ .

We know that eq. (2.2.1)-(2.2.4) are valid only outside the disk, where gas pressure is considered small enough that can be ignored. Finally for particles traveling in the region outside the disk, their motion reduces to that described in equations (2.2.1)-(2.2.4). Finding the locus of points for which  $\rho = 0$  we have determined the shape of the accretion disk. We have achieved that by implementing the bisection root finding method given in [29]. The reason we do this is because we want to obtain a more "realistic" shape for the accretion disk and a more "realistic" velocity distribution for the particles comprising the accretion disk. Particle's velocity distribution refers only to the case where no external magnetic fields are imposed to the Kerr background geometry. Supposing that at  $\tau = 0$  we switch on an external magnetic field source and rearranging particles' velocities a little bit so they are consistent with the external magnetic field we acquire a new velocity distribution for the particles. This of course, is not the right approach for finding the velocity distribution of particles at the edge of the accretion disk when external magnetic fields are present nearby (usually generated by the accretion disk itself). By perturbing a little bit the new

velocity distribution for particles exactly at the edge of the accretion disk, that is by increasing the  $\theta$ -component, we derive the final velocity distribution of particles residing at the edge of the "hypothetical" accretion disk with velocities slightly larger than those permitted by the effective potential. At this point a better manipulation for the velocity distribution would be to add a thermal velocity component (hot disk) to the already acquired values, but due to lack of time we limit ourselves to the previous approach. We present our code in App. 5. One of the questions which remains to be answered is whether the accretion disk with the given velocities distribution would maintain its bound orbit in the absence of magnetic fields. We expect the accretion disk to be dissipated, because we have neglected the gas pressure terms in the calculation of the charged particles motion. The accretion disk described by Abramowicz et al. [1] is maintained because of hydrodynamic stability. Will the presence of external magnetic fields allow bound orbits to exist for the given velocities? The answer is yes. Moreover, for different values of energy we observe that electrons react differently than protons to the presence of magnetic fields. This implies that for the study of an accretion disk using an MHD approach it is suggestive that we regard a two component plasma in operation.

### 3.4.1 No magnetic field

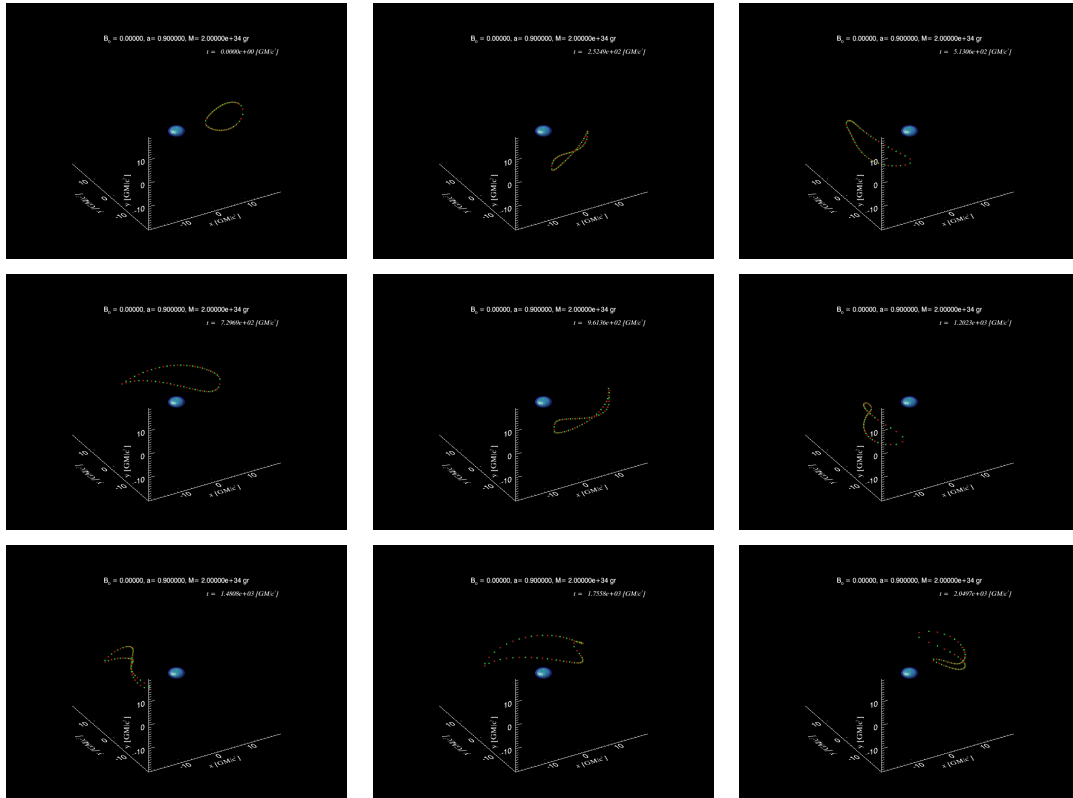
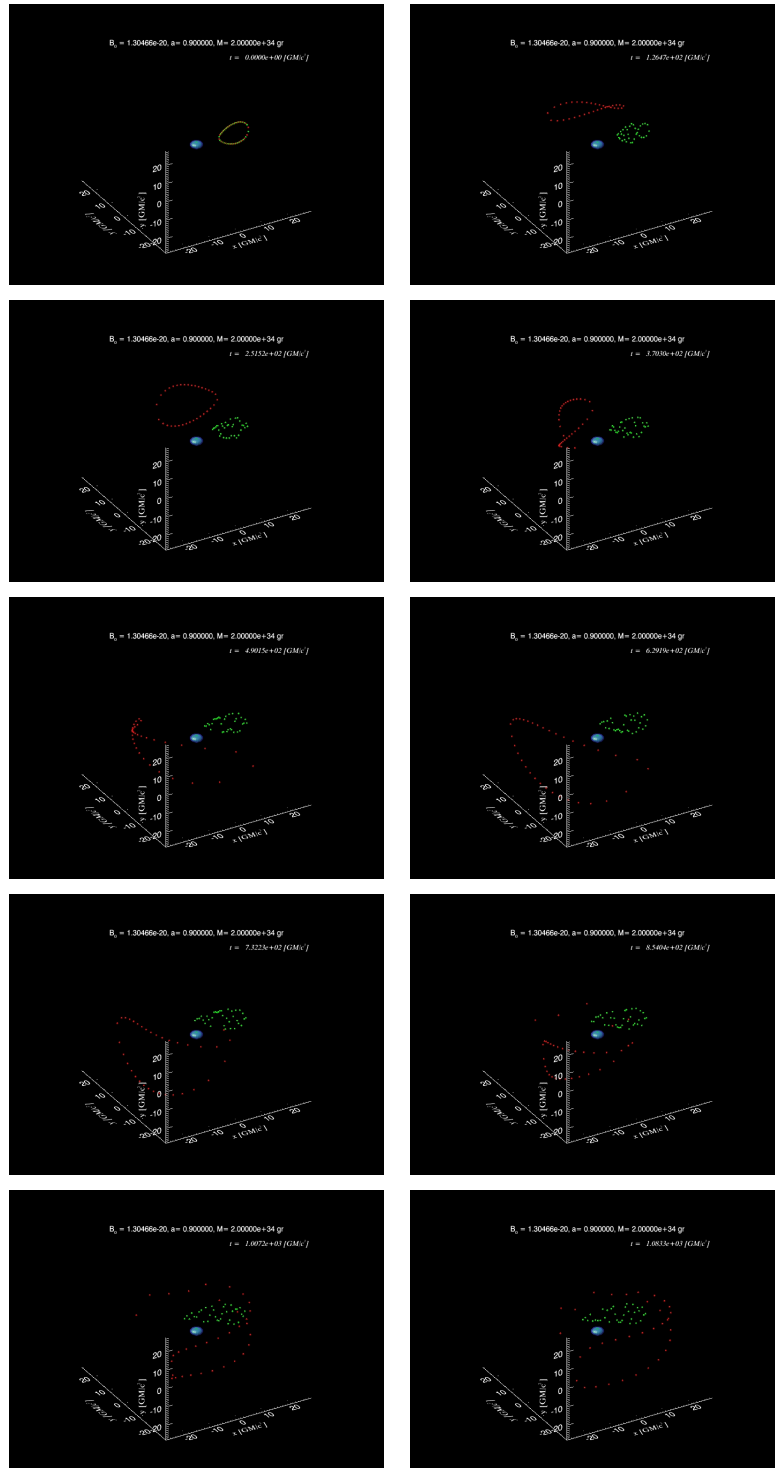


Figure 3.12: The trajectories of protons (red dots) and electrons (green dots) are depicted.

3.4.2 Uniform magnetic field



**Figure 3.13:** The trajectories of protons (red dots) and electrons (green dots) are depicted for the uniform magnetic field case.

## 3.4.3 Dipole magnetic field

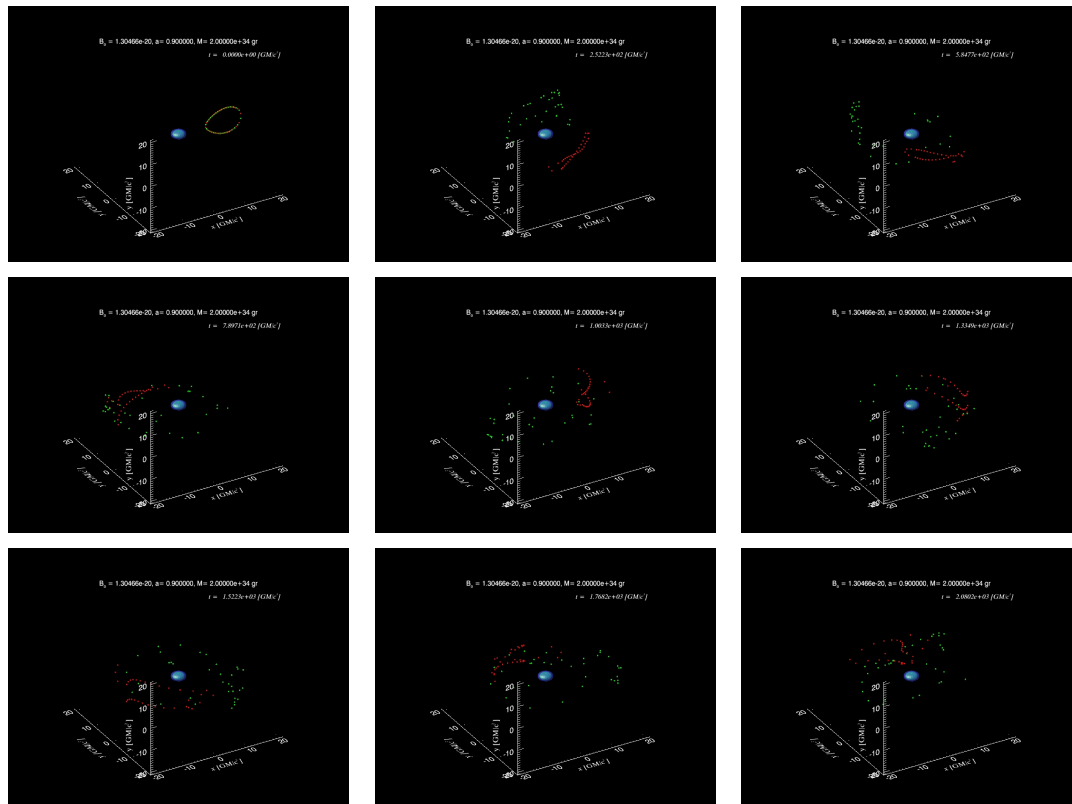


**Figure 3.14:** The trajectories of protons (red dots) and electrons (green dots) are depicted for the dipole magnetic field case.

For the dipole magnetic field we have placed the ring current at  $r_c = 9.44$  (approximately where the maximum density occurs) and  $\theta_c = \pi/2$ .

## Chapter 4

# Halo Orbits

In our experience astrophysical phenomena occurring near compact objects, such as black holes, are governed by the laws of gravity and electrodynamics. Some of these phenomena, jets, formation and maintenance of accretion disks and gamma ray bursts for example, include motions of charged and neutral particles around a magnetized massive “star”.

Stars and astronomical objects in general are observed through the radiation they emit in different wavelengths. A good percentage of this radiation is related to the magnetic fields produced by the internal currents of stars, or by plasma surrounding these objects. The magnetic fields are responsible for the synchrotron radiation that is observed in pulsars, black holes, etc.

Synchrotron radiation is emitted whenever a charged particle moves inside a strong magnetic field. Its motion is hugely affected by the magnitude and type of the magnetic field (toroidal, poloidal, uniform etc.). As a consequence magnetic fields have a definite impact on the dynamics of charged particles.

It is well known that an electrically neutral black hole cannot have intrinsic magnetic field. However, plenty of observations confirm that magnetic fields reside near black holes. Generally speaking, magnetic fields show up when nearby magnetized objects, such as magnetars, neutron stars and accretion discs are present. The latter object is of significant importance in the context of astrophysics. Accretion matter indicates the formation of a plasma disc with a super strong magnetic field. The magnitude of the magnetic field can rise up to  $B_M = 1/M \simeq 1 \times 10^{10} (M/10^9 M_\odot)^{-1} G$  around a supermassive black hole. The upper boundary of the magnetic field strength is derived when one equates the magnetic pressure with the gravitational pressure. Keeping in mind that spacetime becomes distorted in the presence of gravitational sources such as mass or energy, we realize that the spacetime around a supermassive black holes immersed in a superstrong magnetic field is significantly distorted. However, when  $B \ll B_M$  there is a region near the black hole where the distortion of spacetime due to the magnetic energy density is neglected. In this case we consider the magnetic field as a perturbation. The energy contribution from the magnetic field to the energy-momentum tensor is therefore treated as zero. Though we accept that the magnetic field does not alter the spacetime metric, we take into account that the backreaction of the curved spacetime to the magnetic field change its pattern. The field is now found by magnetizing the metric [36].

We know that neutral particles follow the worldline geodesics, so there is “nothing” interesting there. However, charged particles deviate from the geodesics and follow a different path. Their trajectory is affected not only by the strong gravitational field of the star but also by electromagnetic forces. The electromagnetic forces near a star are either generated by currents inside the object, or by currents further away.

In the current chapter we will analyze the motion of charged particles, residing near the accretion disk, in the gravitomagnetic potential of the hole. Our study is focused on the existence of some peculiar off-equatorial orbits of charged particles, similar to the Störmer halo orbits [35].

## 4.1 Introduction

The current chapter is dedicated to charged particle motion near magnetized Kerr black holes in 3D-space. Moreover we examine the possibility of the occurrence of halo orbits in Kerr spacetimes. The interplay between the gravitational and magnetic fields is not yet fully understood.

As previously mentioned, magnetic fields influence the dynamics of a charged particle. One way to examine the magnetic fields near strongly gravitating sources is by perturbing the Maxwell equations (Teukolsky [36]). It is suggestive that any effects of the magnetic fields, upon the metric describing the spacetime in the neighborhood of the black hole, are neglected. Adopting this approach regarding the magnetic field, we have to limit our cases to phenomena that involve weak magnetic field compared to the gravitational one. In principle, gravitational effects, due to the presence of a compact object in nearby spacetime, are becoming weaker and weaker as we move away from the gravitating object. For this reason this approach requires particular attention when one employs it. For example, in a Kerr spacetime endowed in an asymptotically uniform magnetic field, the effects of gravity are neglected as we move to  $r \rightarrow \infty$ , while the magnetic effects are still appreciable. However, the magnetic fields we encounter, near black holes, are not strictly asymptotically uniform neither of such great magnitude that this approach is of no use.

An the equatorial current can replace in a way the more complicated pattern of an accretion disk. But before we investigate the astrophysically relevant models with a viscous disc, we need to understand the motion of an individual charged particle that doesn't affect the spacetime around the hole neither alters the electromagnetic fields of the accretion disc or the toroidal current.

The motion of charged particles in the gravitomagnetic field of the black hole may give us critical information about the properties of the black hole. Hence, we will study the existence of potential traps for highly relativistic particles in the neighborhood a hole immersed in an external magnetic field. The motion of relativistic particles in a magnetic field could give us valuable clues for the black hole's charge, mass and rotation through their spectra. We already know that these kind of traps cannot exist close to a black hole environment ([15],[22]) without an external magnetic field acting upon it.

There are lots of papers in the literature in search of the existence or not of potential traps at the equatorial plane and off the equatorial plane for charged particles and for various cases. The cases investigated are the following:

1. the pure Kerr black hole [15]
2. a Schwarzschild black hole immersed in a dipole magnetic field (equatorial potential traps [30], off equatorial potential traps [22]). These works employ the solution acquired by the perturbation of the Maxwell equations.
3. a Schwarzschild black hole immersed in a magnetic field (equatorial potential traps [38]), off equatorial potential traps [22]). These works employ the full solution for the magnetic field by considering its influence to the spacetime metric.
4. a Kerr black hole in an asymptotically uniform magnetic field (only equatorial potential traps considered [16])
5. a pure Kerr-Newman black hole (equatorial potential traps [3], non-existence of off equatorial potential traps [22])

We would like to point out that the question of whether off-equatorial potential traps occur in a background geometry of Kerr and Kerr-Newman black holes still remains open. We will contribute some results that point to a positive answer.

But anyone could just think "What happens if we add a little rotation to the hole and an external magnetic field?". Is it possible to observe off-equatorial orbits if we employ a different formula for the magnetic field? The following section answers to all of the questions above.

We examine the stable energetically bound off-equatorial orbits of charged particles near magnetized black holes. Two cases of black holes are of special interest. The cases of Kerr and Kerr-Newman black holes immersed in either a uniform (galactic) magnetic field or a dipole magnetic field- produced by a current ring at distance  $r_o$  from the black holes. For the vector potential we will use two different solutions. The first one is obtained by Wald [39] and the second one is derived by Petterson [25] and corrected by Znajek [40]. These solutions refer only to the case of pure Kerr black holes. The first part of this chapter will be dedicated to the study of the dynamics of a Kerr magnetized black hole, while the second part will deal with a Kerr-Newman magnetized black hole.

Throughout our discussion we will deal with uniform and dipole magnetic fields. Keeping in mind the limitations that arise due to the perturbation theory, especially for the uniform magnetic field, we will only consider motion of charged particles rather close to the black hole. The dipole magnetic field is generated by an ideal equatorial current loop, located at  $r_o = 6 M$ . In our calculations we will keep only the first order multipoles of the solution.

On the score of the vector potentials [25] and [40] being calculated only for Kerr black holes, it would be wrong to employ this magnetic field to study halo orbits in Kerr-Newman spacetimes. Hence, the second part is just a toy model. The aim of this second part is just to show that under certain conditions the existence of such off-equatorial orbits is possible.

In addition, extra care has been taken in order to choose a physically coherent magnetic field for the case of the magnetic dipole. The solution for the vector potential of a magnetic dipole as given by Znajek [40] implies that there are two solutions. One for the inner region where  $r < r_o$  and one for the outer region ( $r > r_o$ )<sup>1</sup>. Some of the previous work on this subject, carried out by different authors, was based only on the external solution, except for Preti [30] and Li [23]. Their assumption was that the ring current was placed exactly at the event horizon. However, this is not completely true from a physical point of view. The ring current consists of charged and neutral particles. Geodesics near a black hole dictate that the inner most stable corrotating circular orbit for a Schwarzschild black hole occurs at  $r = 6 M$ , while for an extreme Kerr black hole ( $a = M$ ) at  $r = M$ . As a consequence, there are some limitations introduced for the position of the circular current. In order to be physically consistent, the minimum distance for the ring current will have to be between the values  $M < r_o < 6 M$  depending on the rotation of the hole.

An interesting result of our analysis is the existence of such energetically bound off-equatorial orbits in Kerr and Kerr-Newman black holes. Each off-equatorial orbit correspond to a potential trap. Their existence is of significant importance because inside the traps might be sources of synchrotron radiation, namely relativistic charged particles.

The structure of the chapter will be as follows. In section 2 a general calculation for the effective potential will be given. In section 3 we will investigate the off-equatorial potential traps for the uniform and magnetic dipole field in a Kerr background geometry. The dependence of the location of the off-equatorial circular orbits to free parameters will be studied. Orbits in a Kerr-Newman background geometry endowed in a magnetic field will be the subject of section 4. The analysis in this section will not be mathematically strict. We will use the magnetic dipole solution of Znajek [40], even though they are meant to be used only in a Kerr background geometry.

Throughout the current chapter the sign conventions of Misner, Thorne, and Wheeler [24] will be adopted.

## 4.2 Halo Orbits

Halo orbits are the off-equatorial energetically bound orbits that are stable to small perturbations with respect to each of the coordinates. Charged particles who follow these orbits limit their motion to the  $z > 0$ -space or  $z < 0$ -space. They never cross the surface  $z = 0$  and they are confined. The

---

<sup>1</sup>where  $r_o$  is the distance of the ring current from the black hole

condition for a halo orbit to occur is

$$\partial_r V_{\text{eff}} = 0, \quad \partial_\theta V_{\text{eff}} = 0$$

This condition corresponds to the local minima of the effective potential. Each local minimum answers to a circular orbit for which  $z > 0$  or  $z < 0$ . To define the local minima we implemented the Powell method developed in [29].

### 4.2.1 Kerr Black hole

For a Kerr black hole the constants in eq. (2.3.13) reduce to

$$\alpha = B \tag{4.2.1a}$$

$$\beta = -\frac{qB}{m} A_t + 2Mra \left( L_z - \frac{q}{m} A_\phi \right) \tag{4.2.1b}$$

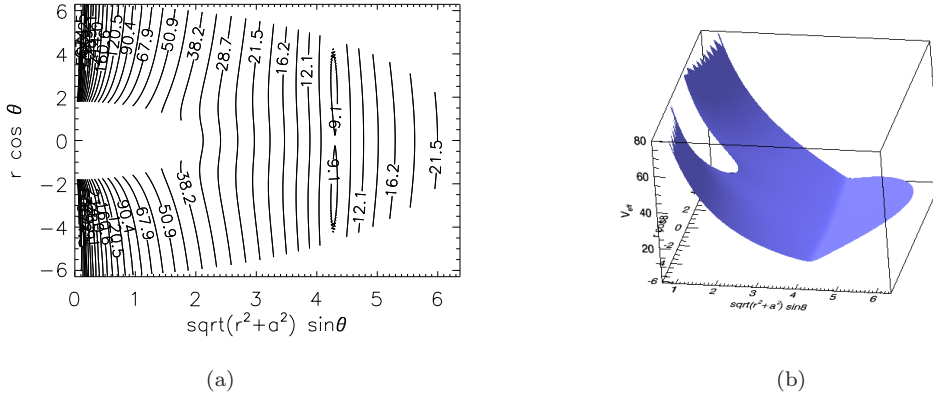
$$\gamma = \frac{q^2 B}{m^2} A_t^2 - \frac{4Mraq}{m} A_t \left( L_z - \frac{q}{m} A_\phi \right) - \frac{\Sigma}{\sin^2 \theta} \left( L_z - \frac{q}{m} A_\phi \right)^2 \left( 1 - \frac{2Mr}{\Sigma} \right) - \Delta \Sigma \tag{4.2.1c}$$

#### Uniform Magnetic Field

The asymptotically uniform covariant components of the vector potential in a Kerr background geometry are given by eq. (2.1.8), (2.1.9). Replacing eq. (2.1.8), (2.1.9) and (4.2.1) into eq. (2.3.13), we acquire the form of the effective potential for an uncharged rotating black hole in a uniform magnetic field.

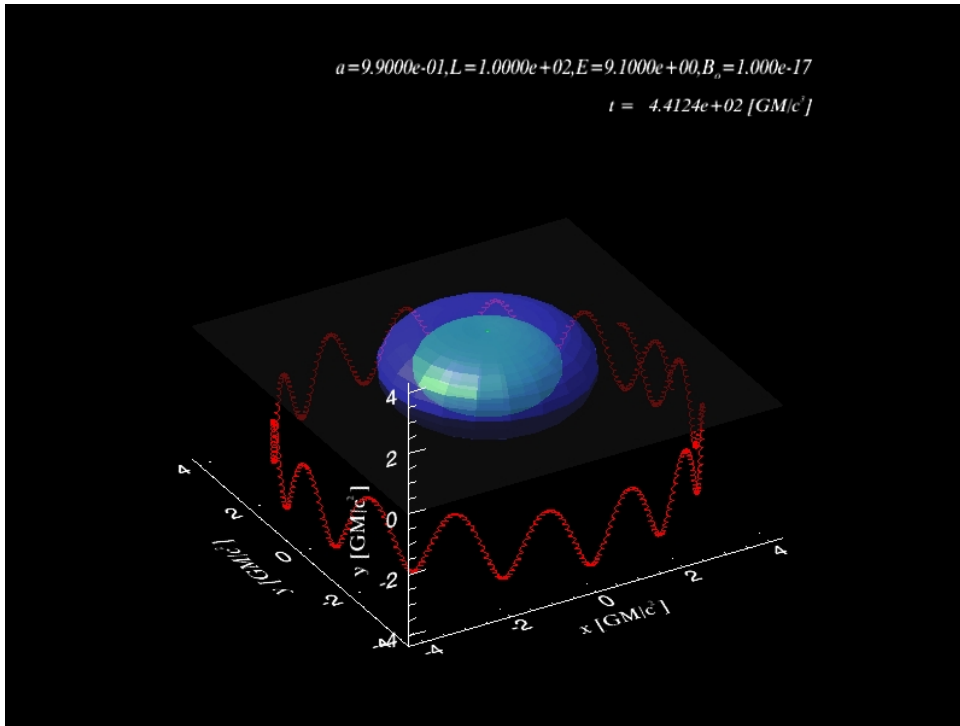
Throughout the numerical calculation we have used the dimensionless coordinates  $t/M \rightarrow t$ ,  $r/M \rightarrow r$ .

Figure 4.1 shows the behavior of the effective potential for the uniform magnetic field. The two closed lines suggest the existence of halo orbits for a specific value of energy.



**Figure 4.1:** Effective potential  $V_{\text{eff}}$  and its contours for motion of a charged particle in an extreme  $a = 0.9$  Kerr black hole and an external uniform magnetic field. The axis of the magnetic field is parallel to the angular momentum of the black hole. The constants of motion are  $L = 100$ ,  $E = 9.0999971$  and the magnetic field strength  $B_o = 10^{-17}$ . The particle is a proton.

In figure 4.2 the trajectory of a proton is depicted. The halo orbit is clearly visible. The particle is confined between two turning points for  $z > 0$ . The location of the local minima of the effective potential depends on five factors. The first one is the magnitude of the magnetic field, the second is the angular momentum  $a$  of the black hole, the third the specific angular momentum of the



**Figure 4.2:** The motion of a proton is depicted. The magnetic field forces the particle to execute Larmor motion of constant radius. The particle doesn't cross the equatorial plane.

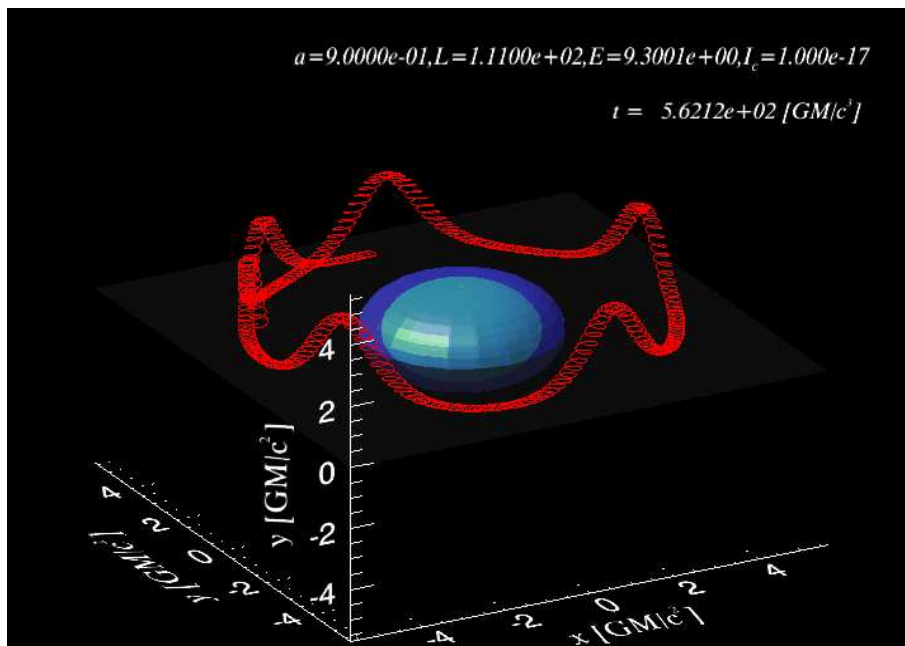


**Figure 4.3:** The motion of an electron is depicted. This motion is an intermediate step between the trajectories depicted in 3.8(a) and 4.2

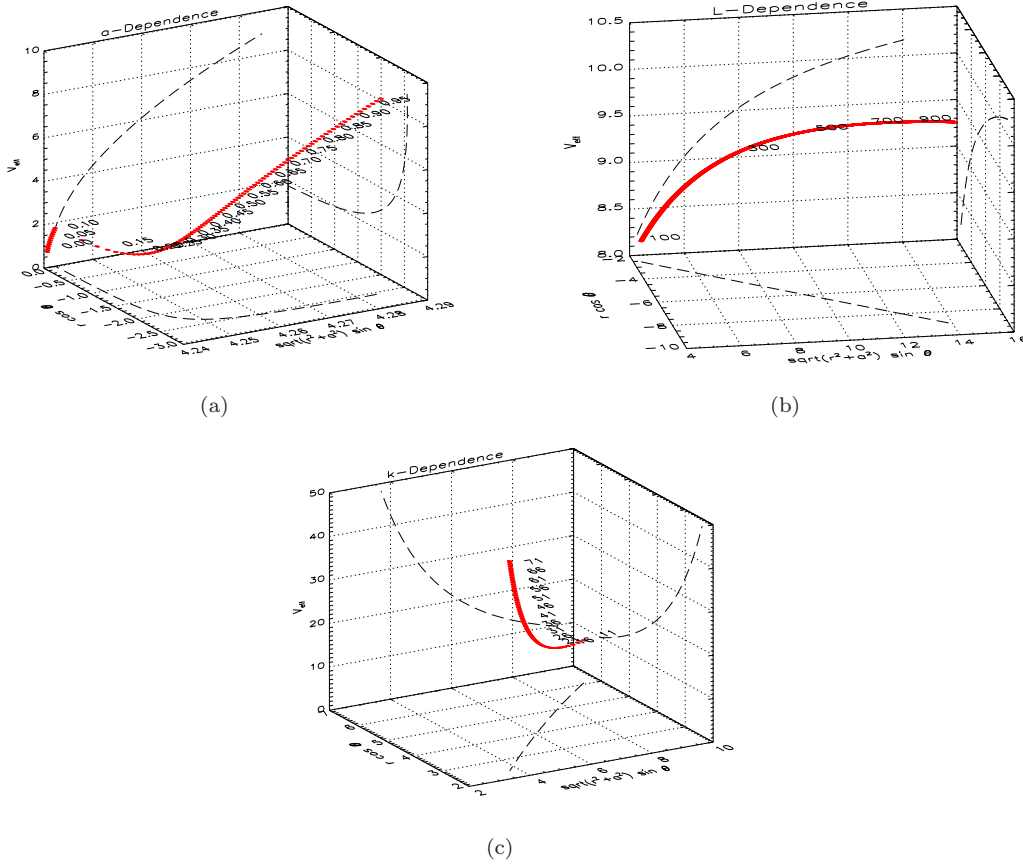


**Figure 4.4:** The dependence of  $V_{\text{eff}}$  is shown in the pictures above. Roughly, increasing the angular momentum of the black hole, the lowest energy for a particle to participate in an off-equatorial circular motion is increased. Coinstantaneously the local minimum moves to a greater distance. As the angular momentum  $L$  of the particle grows bigger, both the lowest energy and the distance of the local minimum from the black hole take greater values. Lastly, increasing the factor  $k = qB_o/m_{\text{part}}$ , the lowest energy increases too, while the position of the local minimum moves towards  $z = 0$ .

particle and lastly the particle's mass and charge. The strength of the magnetic field multiplied by the particle's charge to mass ratio can be combined in one factor  $k = qB_o/m_{\text{part}}$ . The relation between all of these factors and the effective potential is illustrated in 4.4.

## Dipole Magnetic Field

For the dipole magnetic field there are two solutions [40] in a Kerr background geometry. The internal solution, regarding the magnetic field that the particle feels when its distance from the hole is smaller than  $r_o^2$  and the external solution, regarding the magnetic field for distances greater than  $r_o$ .

### Internal Solution

The internal solution, though not investigated in other papers ([22; 28; 11; 26]), is very substantial. Halo orbits can exist very close to the black hole, in the area between the accretion disc and the outer event horizon. In the previously described region, electromagnetic energy can be extracted from the black hole [7; 30].

The magnetic fields threading the accretion disc are responsible for the voltage drop between the accretion disc and the black hole. But what supplies the magnetic field and how can energy be transferred to the inner area of the black hole even though there are no wires connecting the two regions? The answer is that the currents in an accretion disc power the magnetic fields, and the black hole manages to make its own wires to connect the accretion disc region with the inner region of the magnetosphere of the hole. Were there no conducting wires between the accretion disc and the hole, there would still be a voltage drop of the order

$$V \sim \Omega_H B \pi r_H^2 \sim (10^{20} \text{Volts} (\Omega_H M)) \left( \frac{M}{10^9 M_\odot} \right) \left( \frac{B}{10^4 \text{ Gauss}} \right)$$

where  $\Omega_H$  and  $r_H$  are the angular velocity and the distance of the outer horizon.

This huge amount of energy difference and the accompanying field would quickly accelerate any stray electrons to relativistic velocities. The electron would radiate photons, which in turn would split into a pair. Then the two constituents are accelerated again and produce more photons. This phenomenon continues and quickly the cascade fills up the nearby space with plasma and electric fields. This is the electrically conducting link between the inner region of the black hole and the accretion disc. Now, the charged particles that reside in this region would be of relativistic velocities. The question is how this power is turned into radio jets.

In our opinion, the presence of toroidal magnetic fields near a black hole induce an electric field due to the rotation of the black hole. The induced electric field in conjunction with the toroidal component of the magnetic field are efficient to provide a kick for the charged particles and expel them away from the black hole. The toroidal component of the magnetic field, according to Prasanna and Sengupta [26], acts like an electric field and it becomes stronger in the vicinity of the black hole. The problem is how can a charged particle approach the axis of the black hole. The off-equatorial orbits limit the motion of the particles in the  $z_{\geq 0}$ -space. It is evident from fig. 4.2 that the particles in the off-equatorial orbits tend to approach the axis of black hole. They become vulnerable by the toroidal magnetic forces and the electric field, they gain a kick of energy and are radiated away from the hole producing a jet like formation. The rotation axis provides a natural axis for the jets. One of our future plans it to test if this scenario is possible and if the off-equatorial orbits play a critical role for the formation of jets.

However, the internal solution can be approximated with a uniform magnetic field close to the black hole. In other words, for small  $r$  the two solutions coincide. Therefore we expect a similar behavior to that of fig. 4.1, 4.4, 4.2.

The example in fig. 4.5 depicts the similarities between the two formulas. The off-equatorial motion is very important because it extends in the region between the accretion disc and the black hole, where the Blandford-Znajek mechanism is dominant.

---

<sup>2</sup>Where  $r_o$  is the distance of the ring current from the hole.

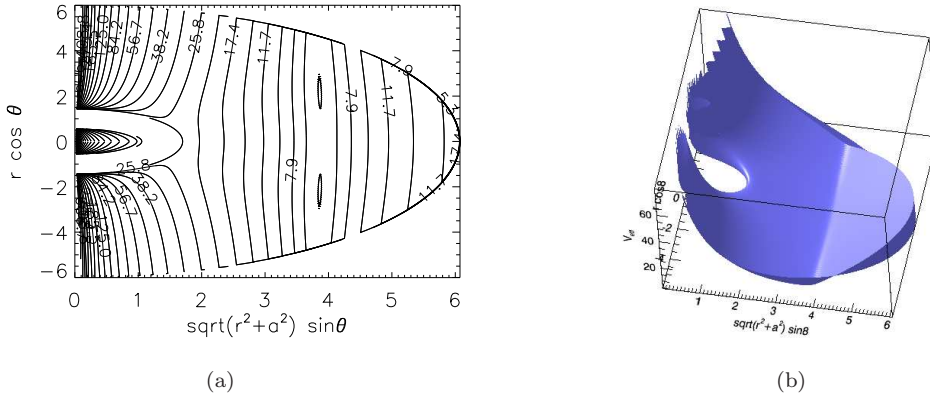
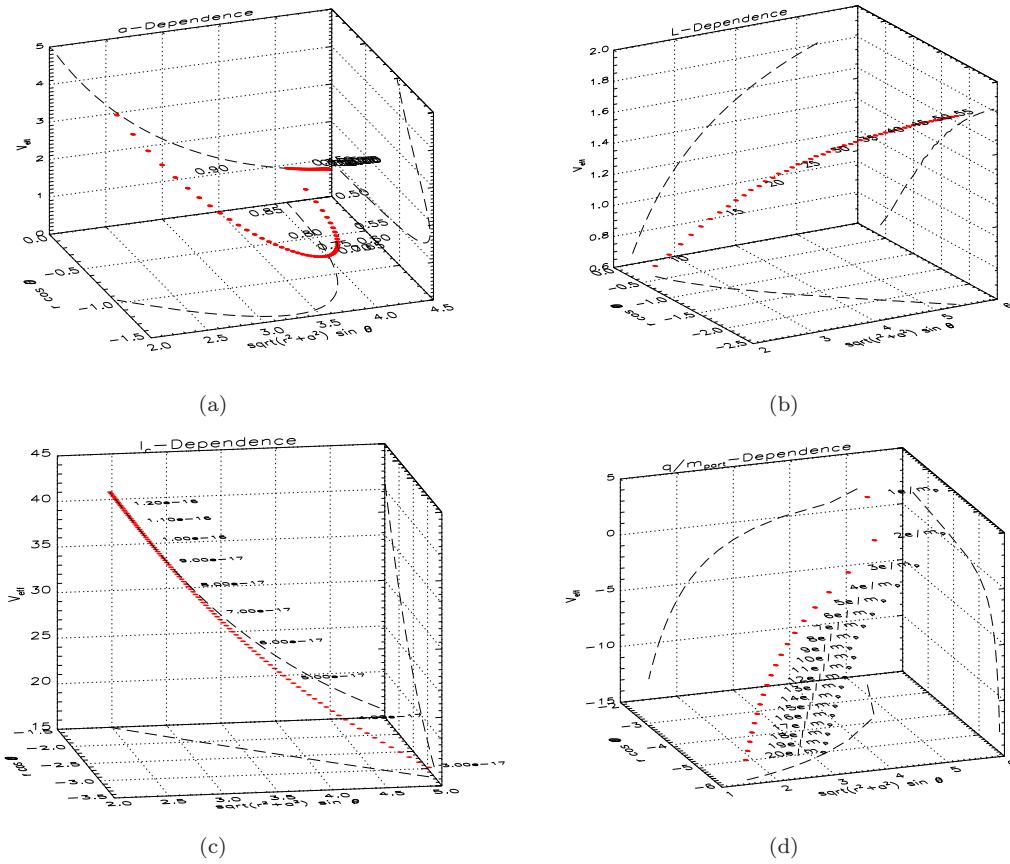


**Figure 4.5:** Effective potential  $V_{\text{eff}}$  and its contours for motion of a charged particle in a  $a = 0.9$  Kerr black hole and an external dipole magnetic field. The internal solution of the magnetic dipole is considered. The axis of the magnetic field is parallel to the angular momentum of the black hole. The constants of motion are  $L = 70$ ,  $E = 5.3059152$  and the ring current that generates the magnetic field is  $I_c = 10^{-17}$ . The particle is a proton.

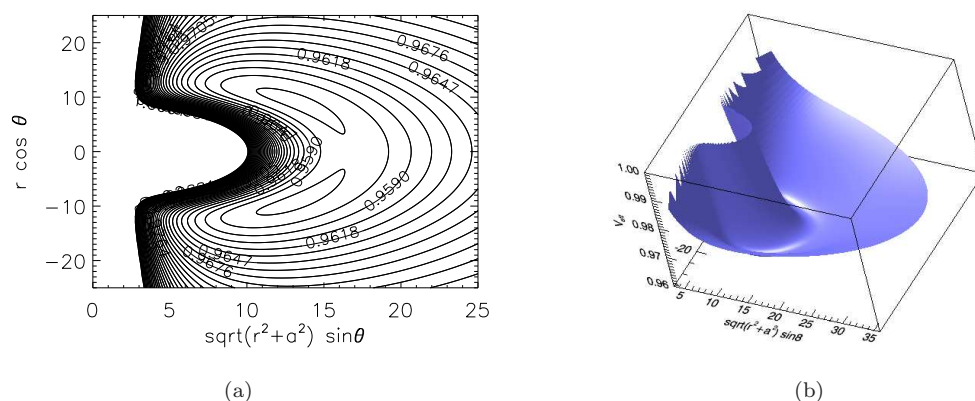
### External Solution

Figure 4.7 shows the behavior of the effective potential in the case of the dipole magnetic field (external solution). The two closed lines suggest the existence of halo orbits for that specific energy. This behavior of the effective potential, namely the existence of halo orbits, is due to the presence of the external magnetic field. A magnetic field with only poloidal components confines the charged particles. On the other hand, a toroidal component is responsible for jet-like orbits.

In figure 4.8 the trajectory of an electron is depicted. It is evident that halo orbits exist for the case we are currently studying. Again the particle is confined between two turning points with  $z > 0$ . The location of the local minima depends once more on the value of the ring current, the angular momentum  $a$  of the black hole, the specific angular momentum of the particle and lastly the particle's mass and charge. The relation of some of the factors to the effective potential is illustrated in fig. 4.9.



**Figure 4.6:** The dependence of  $V_{\text{eff}}$  is shown in the pictures above. (a) Roughly, increasing the angular momentum of the black hole, the lowest energy for a particle to participate in an off-equatorial circular motion is increased. Coinstantaneously the local minimum moves to a greater distance until it reaches a maximum and then moves towards the black hole. (b) As the angular momentum  $L$  of the particle grows bigger, both the lowest energy and the distance of the local minimum from the black hole take greater values. (c),(d) Lastly, increasing the current  $I_c$  and the factor  $q/m_{\text{part}}$ , the minimum energy increases too. The position of the local minimum moves away from the black hole in both graphs (c,d).



**Figure 4.7:** Effective potential  $V_{\text{eff}}$  and its contours for motion of charged particle in a  $a = 0.55$  Kerr black hole and an external dipole magnetic field. The external solution of the dipole magnetic field is considered. The axis of the magnetic field is parallel to the angular momentum of the black hole. The constants of motion are  $L = 1$ ,  $E = 0.95608159$  and the ring current that generates the magnetic field is  $I_c = 10^{-21}$ . The particle is an electron.

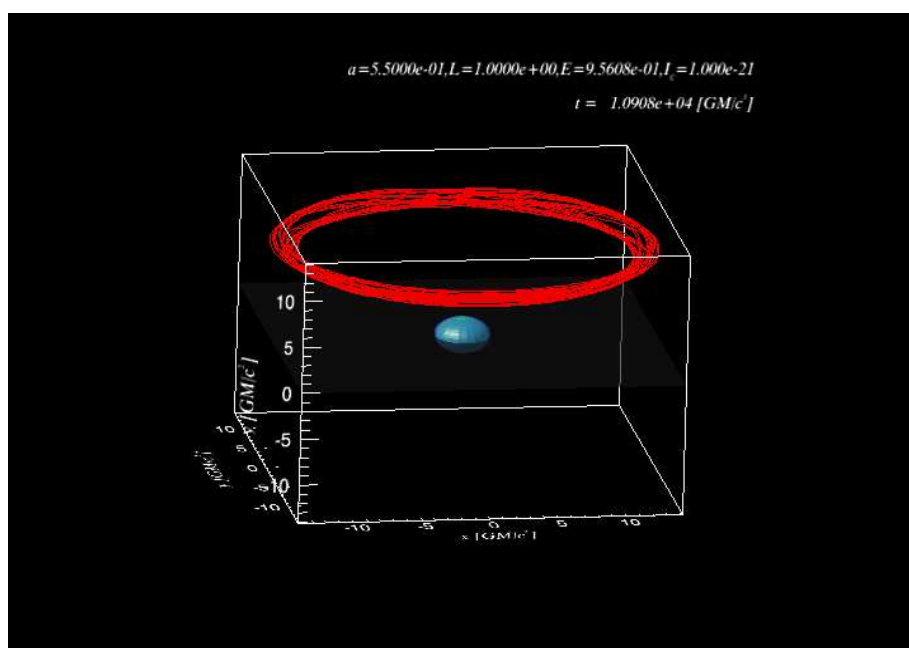


**Figure 4.8:** The motion of an electron is depicted. The magnetic field forces the particle to execute Larmor motion of variable radius. The particle doesn't cross the equatorial plane.

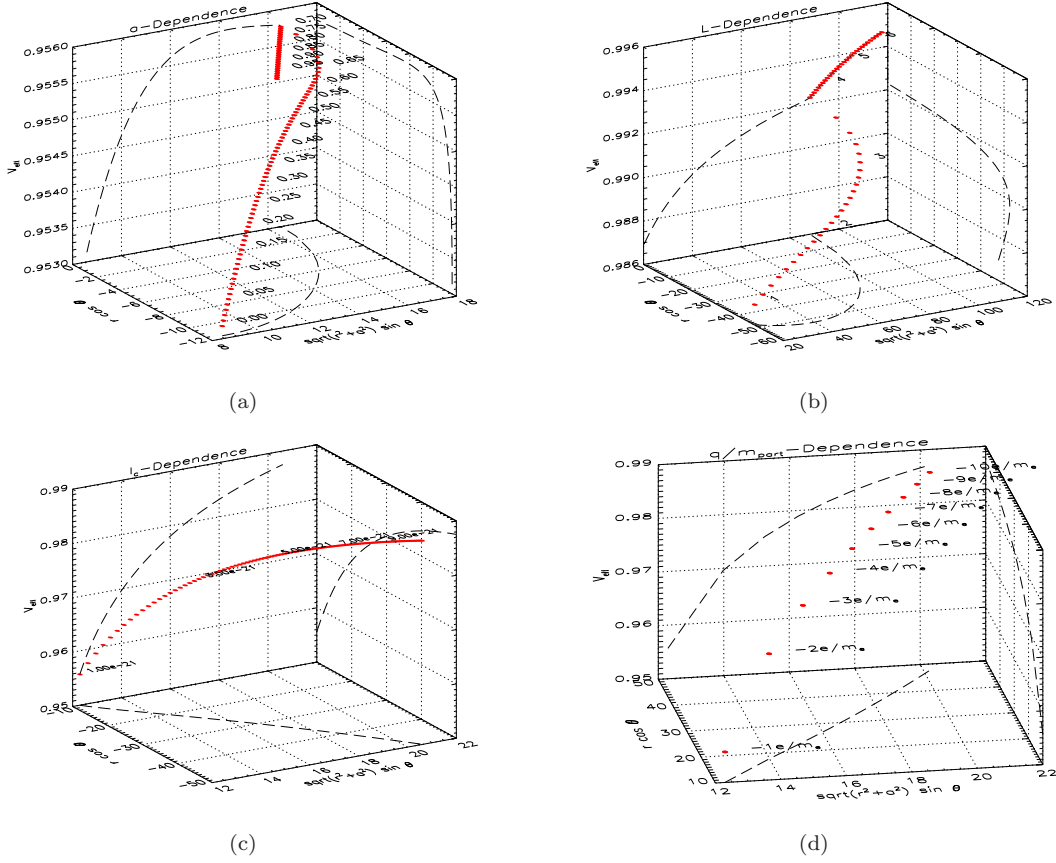


**Figure 4.9:** The dependence of  $V_{\text{eff}}$  is shown in the pictures above. Roughly, increasing the angular momentum of the black hole, the minimum energy for a particle to participate in an off-equatorial circular motion is decreased. Coinstantaneously the local minimum moves to a greater distance from the black hole. As the angular momentum  $L$  of the particle grows bigger, the minimum energy increases while the local minimum approaches  $z = 0$ . For  $L = 3.5 - 6.0$  there are no halo orbits. The local minimum, for these values of  $L$ , corresponds to circular orbits exactly at the equatorial plane. Increasing  $I_c$  and  $q/m$  the local minima occur for greater values of energy. In addition, they move away from the black hole.

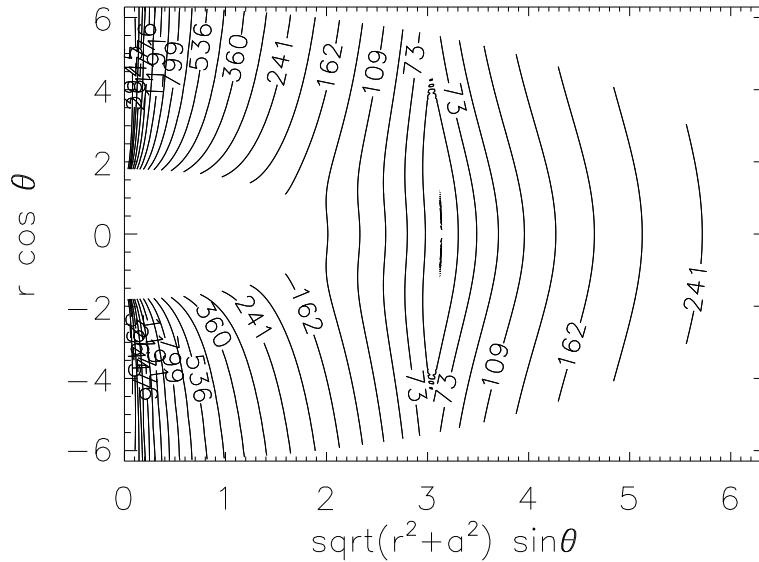
### 4.2.2 Kerr-Newman black hole

We will follow the same steps as before, this time for the Kerr-Newman black hole. As pointed out by Kovář et al. [22], there happen to be no off-equatorial orbits for the Kerr-Newman black hole outside the outer horizon. In their paper they conclude that either these orbits are hidden under the inner horizon, or they require the presence of a hidden singularity.

We will show that the appearance of such off-equatorial orbits is plausible in a Kerr-Newman spacetime requires an external magnetized source. We have regarded the external magnetic field not to be influenced by the charge  $Q$  of the black hole as in [40]. Therefore we can use eq. (2.3.1) to describe the spacetime near the compact object. Our analysis is limited only for small values of the net charge  $Q$ .

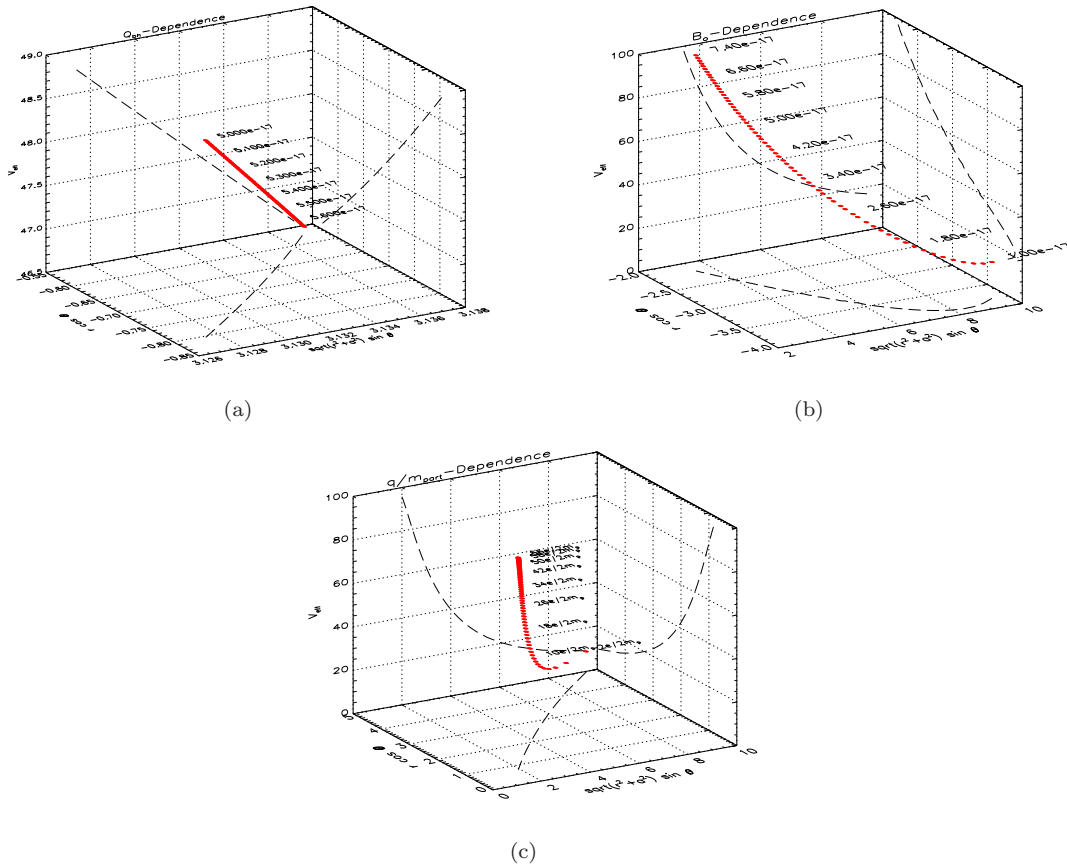
#### Uniform Magnetic Field

Figure 4.10 shows the behavior of the effective potential for the uniform magnetic field.



**Figure 4.10:** The contours of the effective potential for motion of charged particle in a  $a = 0.9$ ,  $Q = 5 \times 10^{-17}$  Kerr-Newman black hole and an external uniform magnetic field. The axis of the magnetic field is parallel to the angular momentum of the black hole. The constants of motion are  $L = 500$ ,  $E = 48.866846$  and the magnetic field  $B_o = 1.0 \times 10^{-16}$ . The particle is a proton.

The location of the local minima depending on the magnitude of the magnetic field and the particle's charge to mass ratio  $q/m$  is depicted in 4.11.



**Figure 4.11:** The dependence of  $V_{\text{eff}}$  is shown in the pictures above. Roughly, increasing the net charge of the black hole, the minimum energy for a particle to participate in an off-equatorial circular motion is decreased. Coinstantaneously the position of the local minimum moves to larger  $z$ . As the magnetic field strength  $B_o$  grows bigger, the minimum energy takes greater values. The particle now moves towards the black hole. Lastly, increasing the factor  $q/m$ , the lowest energy increases too, while the particle moves towards  $z = 0$ .

### Dipole Magnetic Field

Figure 4.12 shows the behavior of the effective potential for the external (a) and the internal (b) dipole magnetic field cases. The two closed lines suggest the existence of halo orbits in Kerr-Newman spacetimes.

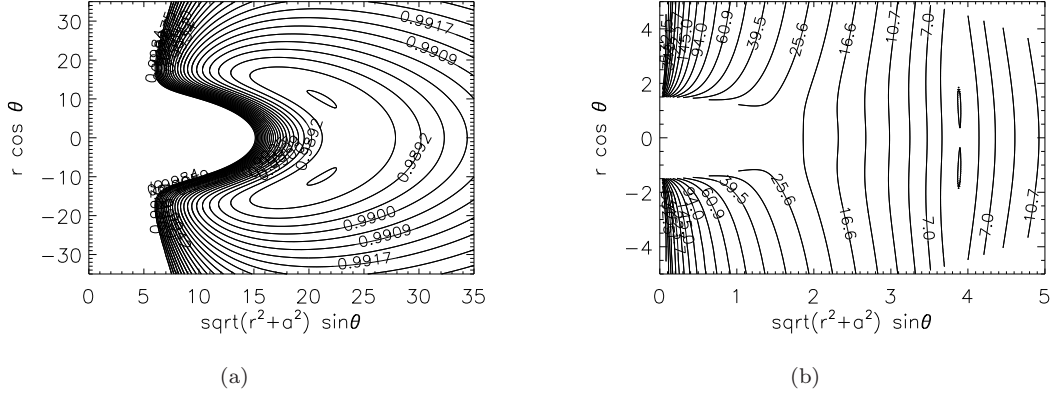


**Figure 4.12:** (a) Contour plots of the effective potential  $V_{\text{eff}}$  for motion of charged particle in a  $a = 0.25$ ,  $Q = 3 \times 10^{-22}$  Kerr-Newman black hole and an external dipole magnetic field (external solution). The constants of motion are  $L = 1$ ,  $E = 0.98837041$  and the value of the ring current is  $I_c = 1.0 \times 10^{-21}$ . The particle is an electron. (b) Contour plots of the effective potential  $V_{\text{eff}}$  for motion of a proton in a  $a = 0.9$ ,  $Q = 3 \times 10^{-18}$  Kerr-Newman black hole and an external dipole magnetic field (internal solution). The constants of motion are  $L = 70$ ,  $E = 4.513327310$  and the value of the ring current is  $I_c = 1.0 \times 10^{-17}$ .

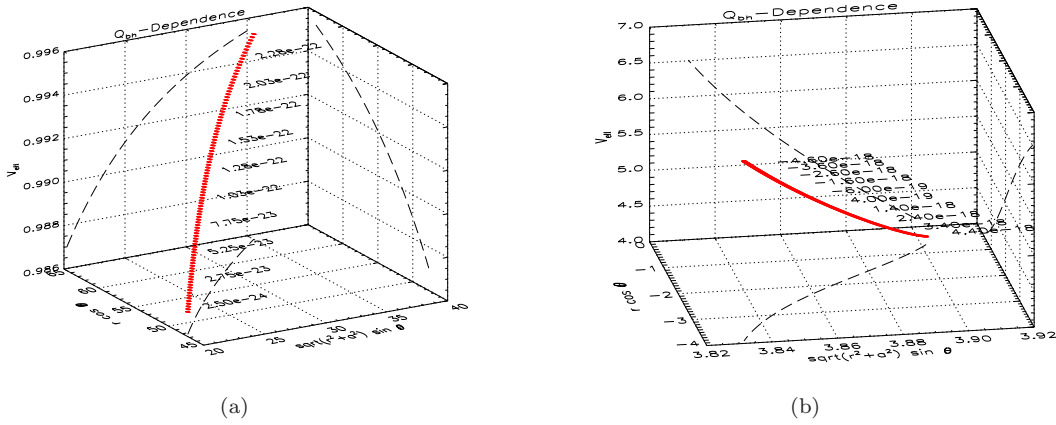


**Figure 4.13:** The dependence of  $V_{\text{eff}}$  is shown in the pictures above. (a) Increasing the net charge of the black hole, the minimum energy for a particle to participate in an off-equatorial circular motion is increased. Coinstantaneously the position of local minimum moves to a greater distance (external solution). (b) The local minima occur for lower values of energy while the net charge of the hole increases. In addition it moves towards  $z = 0$  (internal solution).

The dependence of the effective potential with respect to the net charge of the black hole is illustrated in 4.13.

## Chapter 5

# Conclusions

The presence of external magnetic fields in the neighborhood of rotating black holes forces charged particles to follow non-geodesics orbits. External magnetic fields are responsible for the stability of particle's orbits near the black hole. Charged particles can reside very close to the event horizon without falling into the hole. After theoretical and numerical calculations we have concluded that charged particles can get trapped by the potential of the magnetized gravitating object and follow periodic orbits around the black hole. There two kind of orbits, the equatorial ones and the off-equatorial. Of greatest importance are the off-equatorial orbits which can be divided into two categories, those that cross the equatorial plane and those that do not. The latter orbits are off-equatorial energetically bound orbits that are confined above or below the equatorial plane. These orbits may be accountable for the violent variations in the optical spectra of black holes, though this subject has to be investigate further. Generally speaking, off-equatorial orbits could probably give us valuable information about the properties of the magnetized black hole and its surroundings. Lastly, the study of a group of particles that escape the surface of a simple model of an accretion disk shows that the magnetohydrodynamic approach is not a suitable description for plasma surrounding the black hole. In conclusion, the best approach would be to employ a two-fluid plasma description.



# APPENDIX



# The Numerical Code

The purpose of this chapter is to explain and contribute our code to the public, so that anyone can access it. We have chosen to give only the most basic routines.

As expected, our code has been through many stages. At first, we were only concerned of a single-particle's motion around a magnetized Kerr-black hole with a uniform magnetic field. Therefore, there was no need to create a separate routine which would calculate the magnetic field outside the main routine at that time. The numerical scheme we used to integrate the equations of motion was an adaptive stepsize 4<sup>th</sup>-order Runge-Kutta algorithm. After several tests, our code yielded the expected results and we had to move on to more realistic magnetic fields.

The second stage was to create two separate subroutines which would calculate a uniform and a dipole magnetic field respectively. Inputting a certain logical variable would correspond to either the uniform or the dipolar magnetic field. This was achieved by the insertion of the dummy subroutine `magnetic`. Whenever `magnetic` was set to `magnetize`, through the `dipole=.true.` option, the results would correspond to a magnetized black hole with a dipolar magnetic field, otherwise, the `magnetic` subroutine would point to subroutine `uniformB`. The dummy subroutine (`magnetic`) enabled us to easily compare and draw conclusions for different forms of magnetic fields, simply by altering an input logical parameter (`dipole`).

After testing/running our code for different initial conditions and magnetic fields we observed the existence of some peculiar off-equatorial halo orbits for both the uniform and dipolar magnetic field cases. As mentioned in the main body of this project, similar orbits were found by Kovář et al. [22] for a magnetized non-rotating black hole. This led us to believe that particles ejected from an accretion-disk like distribution, with low energies, might interpret this kind of orbits and form a low-density-torus-like structure above and below the equatorial plane. In addition, we had observed that electrons and protons of the same energy, angular momentum and position sometimes followed very different trajectories and tended to be separated (charge separation). Thus we had to create a new program (`findroot.x`) that would calculate an accretion-disk distribution. We would only need to specify the outer boundaries of this structure in order to find out where low-density plasma would be located.

Theory states that away from an accretion disk plasma particles behave like single-non-interacting-particles. This is the region where the results of our code would be generally valid. We finally employed the mass-density distribution of [1]. Solving for  $\rho = 0$  we would find the limits of the accretion-disk. Abramowicz et al. [1] have not taken into account the magnetic field of the accretion disk, so the density distribution derived would only correspond to an unmagnetized rotating black hole. In order to apply this solution to our problem, we assumed the presence of a magnetic field, either uniform or dipolar. We assumed that the charged-particle distribution would generate the dipolar magnetic field <sup>1</sup>. Because the solution of Abramowicz et al. [1] is not self-consistent with the presence of a dipolar magnetic field, we have rearranged the energies of the outer particles of the accretion disk so that they correspond to the minimum required energy for particles to be located in the specific region, with the specific angular momentum (defined by the plasma distribution) in the presence of magnetic fields. This was not the most suitable manner of treating this

---

<sup>1</sup>We approximate the charged-particles' distribution by a ring current.

problem, but could be considered a rough approximation. To achieve all of the above, we had to modify our code to calculate the orbits of more than one particles. The initial conditions for these particles were defined by solving the equation  $\rho = 0$ , bearing in mind any effects of the present magnetic fields.

Basically we have organized our code in the following manner. Any files with an extension `.txt`, `.dat`, `.f90` are located under the folder `code`. The same goes for any bash-script files with an extension of `.sh`. All IDL files and scripts with the extension `.pro` and `.sh` are placed under the `code/idl` folder. Images are stored inside the `code/idl` folder in separate subfolders. In the subfolder named `code/idl/dipole`, there are only images and plots regarding the dipole magnetic field case. Plots and images concerning the uniform and no magnetic field cases are stored under subfolder `code/idl/uniform` and `code/idl/no_magnetic_field`, respectively. 3-D plots that are utilized in the production of movie files are saved under subfolder `code/idl/jpg`, unless stated otherwise.

## A.1 Equations of Motion

### A.1.1 Fortran

#### Finding accretion-disk-particle distribution

In order to solve the equations of motion for a charged particle around a magnetized black hole we have to specify the initial conditions for its motion, namely its initial position and velocity, or its initial position, angular momentum and energy. Providing the values of the initial conditions, and the parameters of the problem (such as black hole's mass, rotation etc.) in file `inirel.txt` we are ready to solve the system of equations described in Sec. 2.2.

```

***** Initial Conditions

***      h1          hmin          eps          numdt
***      1.0d-11     1.d-90         1.d-14         300
***      tau(1)      tau(end)
***      0.d0        1.d3
***      a          mb (in gr)   Bo (in Gauss)/void   Ic      ro
***      0.9d0      2.0d34      1.30466d-26         6.0d0

***      lo          rext
***      3.9d0      20.d0

*** Trajectory Inwards?      Dipole?      complete?
***      .true.              .false.      .false.

*** STEPSIZE DEFINITIONS

*** h1: Initial Guess
*** hmin: Minimum Stepsize
*** eps: Allowable error for the adaptive size method
*** numdt: Defines every how many steps it prints the results

*** tau(1): Initial tau
*** tau(end): Final tau

*** a: The rotation of the black hole in dimensionless units
*** mb: The mass of the black hole in cgs units
*** Bo/Ic: Define the magnetic field of a uniform or dipole magnetic
           field in dimensionless units
*** ro: the location of the ring current at the equatorial plane

*** lo: the angular momentum of an accretion-like distribution of
           particles
*** rext: the outer boundary of the disk-like distribution

*** Trajectory Inwards?: A logical unit which corresponds to .true. if
                           the particle is moving towards the black hole
                           and .false. when it moves away from the hole.

```

```

*** Dipole?: Set this to .true. if you need to study the dipole
magnetic field and .false in order to study the uniform
magnetic field.

*** complete?: Set this to .true. if you need to study the full
solution of the dipole magnetic field, or only the
external solution.

```

Program `findroot.x` finds the root of equation 3.4.1 written in `funcd.f90`. Then it finds the particles' velocity distribution and position and outputs the result in `iniparticles.dat`. The total number of particles is written in file `numofparticles.dat`.

```

program findroot
implicit none
double precision::r1,r2,rho,gamma,k,k1,S1,Del1,B1,ro,thetao,gtt1,gff1,&
&gthetatheta1,gtf1,grr1,omega1,utin,uphi1
double precision::thetaacc,theta,r,dr,funcd,rtbis,kappa,ik,q,qe,&
&mparte,mparti,mb
double precision::gtt,gff,gthetatheta,grr,gtf,omega,ut,lo,B,S,&
&Del,M,a,ur,utheta,L,en,delta,uphi
double precision::Gcgs,t,phi,mpart,charge,t2,qi,pi,&
&gammaconst,alphaeff,betaeff,gammaeff
double precision::theta1,theta2,At,Af,mu,rect,tini,&
&tend,h1,hmin,eps,numdt,Ic,alpha,beta,BoIc,Bo
parameter(thetaacc=1.d-100,M=1.0d0,k=1.0d0,pi=3.14159265359d0)
parameter(Gcgs=6.6726d-8)
integer::it,numofparts,i3,i4,i2,i1
CHARACTER(256)::file="iniparticles.dat",file2="numofparticles.dat"
logical::inwards,dipole,complete
external rtbis,funcd,cstrip,open

READ(i1,*)h1,hmin,eps,numdt
READ(i1,*)tini,tend
READ(i1,*)a,mb,BoIc,ro
read(i1,*)lo,rect
read(i1,*)inwards,dipole,complete

if (dipole) then
  Ic=BoIc
else
  Bo=BoIc
endif
theta1=0.d0
theta2=3.141592653589793d0

qe=4.803204d-10
mparte=9.10938188d-28
mparti=1.67262158d-24
r1=6.0d0
r2=23.0d0
numofparts=25
dr=abs(r2-r1)/numofparts
ur=0.d0
utheta=0.d0
gammaconst=4.0d0/3.0d0
it=-1
ik=0
t2=0.d0
mparte=mparte/mb
mparti=mparti/mb
charge=sqrt(Gcgs)*mb
qe=qe/charge
qi=qi/charge
ur=0.d0
utheta=0.d0
t=0.d0

gamma=sqrt(M**2-a**2)

call open(i3,file,1,'unknown')
do

```

```

r=r1+ik*dr

if (r.eq.r2) goto 2

theta=rtbis(a,lo,rest,r,funcd,theta1,theta2,thetaacc)
S = r**2 + a**2*cos(theta)**2
Del = r**2 + a**2 - 2.d0*M*r
B = (r**2 + a**2)**2 - Del*a**2*sin(theta)**2

gtt= -(1.d0 - 2.d0*M*r/S)
gtf= -2.d0* a *M* r *sin(theta)**2/S
gff= B*sin(theta)**2/S
grr= S/Del
gthetatheta= S

omega=-(gtf+ lo*gtt)/(gff+lo*gtf)

phi=0.d0

ut=1.d0/sqrt(-gtt- 2.d0*omega*gtf-omega**2*gff)
uphi = omega*ut

rho=((gammaconst-1.d0)/k/gammaconst*funcd(a,lo,rest,r,theta))**3

if (abs(rho).lt.1.d-40) then
  it=it+1
  q=(-1.d0)**(it)*qe
  if(q.gt.0.d0) then
    mpart=mparti
  else
    mpart=mparte
  endif
  if (dipole) then
    if (complete) then
      if (r.gt.ro) then
        beta=-3.d0*Ic/8.d0/(gamma**2)/ro*(ro*(ro**2+a**2)-2.d0*a**2*M)

        At=2.d0*a*beta/S*((r*(r-M)&
          &+(a**2-M*r)*cos(theta)**2)/2.d0/gamma*dlog((r-M+&
          &gamma)/(r-M-gamma))-(r-M*cos(theta)**2))

        Af=(beta*sin(theta)**2/S)*((r - M)*a**2*cos(theta)**2 +&
          &r*(r**2 + M*r +2.d0*a**2) - (r*(r**3 - 2.d0*M*a**2 + a**2*r))&
          &+Del*a**2*cos(theta)**2)/2.d0/gamma*dlog((r - M + gamma)/&
          &(r - M - gamma)))
      else
        alpha= 3.d0*Ic/8.d0/ro/gamma*((ro*(ro+M)+2.d0*a**2)-&
          &1.d0/2.d0/gamma*log((ro-m+gamma)/(ro-M-gamma))*(ro*&
          &(ro**2+a**2)-2.d0*M*a**2))

        At=2.d0*a*alpha/S/gamma*(r**2-M*r*M*r*cos(theta)**2+&
          &a**2*cos(theta)**2)+a*Ic/ro
        Af=alpha*sin(theta)**2/S/gamma*(Del*(-2.d0*a**2*cos(theta)**2&
          &+S)-2.d0*r*(r**2+a**2)*(r-M))
      endif
    else
      beta=-3.d0*Ic/8.d0/(gamma**2)/ro*(ro*(ro**2+a**2)-2.d0*a**2*M)

      At=2.d0*a*beta/S*((r*(r-M)&
        &+(a**2-M*r)*cos(theta)**2)/2.d0/gamma*dlog((r-M+&
        &gamma)/(r-M-gamma))-(r-M*cos(theta)**2))

      Af=(beta*sin(theta)**2/S)*((r - M)*a**2*cos(theta)**2 +&
        &r*(r**2 + M*r +2.d0*a**2) - (r*(r**3 - 2.d0*M*a**2 + a**2*r))&
        &+Del*a**2*cos(theta)**2)/2.d0/gamma*dlog((r - M + gamma)/&
        &(r - M - gamma)))
    endif
  else
    At=-a*Bo*(1.d0-M*r/S*(2.d0-sin(theta)**2))
    Af=Bo*sin(theta)**2/2.d0/S*(B-4.d0*M*a**2*r)
  endif
endif

L = B/S*sin(theta)**2*uphi - 2.d0*M*a*r/S*sin(theta)**2*ut+&
  & q/mpart*Af

```

```

alphaeff=B
betaeff=-q/mpart*At*B+2.d0*M*r*a*(L-q/mpart*Af)
gammaeff=q**2/mpart**2*At**2*B-4.d0*M*r*a*q/mpart*At*&
&(L-q/mpart*Af)-Del*S-S/sin(theta)**2*(L-&
&q/mpart*Af)**2*(1.d0-2.d0*M*r/S)

en = (betaeff+sqrt(betaeff**2-alphaeff*gammaeff))/alphaeff

ut=1.d0/Del/S*(-2.d0*M*r*a*(L-q/mpart*Af)+(B*(en+q/mpart*At)))
uphi=((1.d0-2.d0*M*r/S)*(L-q/mpart*Af))/Del/sin(theta)**2&
&+2.d0*M*r*a*(en+q/mpart*At)/Del/S

delta=-(en+q/mpart*At)*ut + (L-q/mpart*Af)*uphi + &
&S*ur**2/Del + S*utheta**2

print '(I,3d18.10)',it+1,ur,ut,delta
write(i3,'(I,2d45.29)')it+1,q,mpart
write(i3,'(2d45.29)') t,r
write(i3,'(2d45.29)') theta,phi
write(i3,'(4d45.29)') ut,ur,utheta,uphi

endif
ik=ik+1
enddo
2 theta1=3.141592653589793d0
theta2=3.141592653589793d0*2.d0
ik=0
ur=0.d0
do
r=r1+ik*dr
if (r.eq.r2) goto 3

theta=rtbis(a,lo,rest,r,funcd,theta1,theta2,thetaacc)
theta=-theta
S = r**2 + a**2*cos(theta)**2
Del = r**2 + a**2 - 2.d0*M*r
B = (r**2 + a**2)**2 - Del*a**2*sin(theta)**2

gtt= -(1.d0 - 2.d0*M*r/S)
gtf= -2.d0* a *M* r *sin(theta)**2/S
gff= B*sin(theta)**2/S
grr= S/Del
gthetatheta= S

omega=-(gtf+ lo*gtt)/(gff+lo*gtf)

phi=0.d0

rho=((gammaconst-1.d0)/k/gammaconst*funcd(a,lo,rest,r,theta))**3
if (abs(rho).lt.1.d-40) then
it=it+1
q=-(-1.d0)**(it)*qe
if(q.gt.0.d0) then
mpart=mparti
else
mpart=mparte
endif

if (dipole) then
if(complete) then
if (r.gt.ro) then
beta=-3.d0*Ic*2.d0*pi/8.d0/(gamma**2)/ro*(ro*(ro**2+a**2)-&
&2.d0*a**2*M)

At=2.d0*a*beta/S*((r*(r-M)&
&+(a**2-M*r)*cos(theta)**2)/2.d0/gamma*dlog((r-M*&
&gamma)/(r-M-gamma)-(r-M*cos(theta)**2))

Af=(beta*sin(theta)**2/S)*((r - M)*a**2*cos(theta)**2 +&
&r*(r**2 + M*r + 2.d0*a**2) - (r*(r**3 - 2.d0*M*a**2 + a**2*r)&

```

```

&+Del*a**2*cos(theta)**2)/2.d0/gamma*dlog((r - M + gamma)/&
&(r - M - gamma))

else
alpha= 3.d0*Ic/8.d0/ro/gamma*((2.d0*(ro**2+a**2)-(ro-M)*ro)+&
&1.d0/2.d0/gamma*log((ro-M+gamma)/(ro-M-gamma))*(ro**2*&
&(ro-2.d0*M)-2.d0*(ro-M)*(ro**2+a**2)))

At=2.d0*a*alpha/S/gamma*(r**2-M*r-M*r*cos(theta)**2&
&a**2*cos(theta)**2)+a*Ic/ro
Af=alpha*sin(theta)**2/S/gamma*(Del*(-2.d0*a**2*cos(theta)**2&
&+S)-2.d0*r*(r**2+a**2)*(r-M))
endif
else
beta=-3.d0*Ic*2.d0*pi/8.d0/(gamma**2)/ro*(ro*(ro**2+a**2)-&
&2.d0*a**2*M)

At=2.d0*a*beta/S*((r*(r-M)&
&+(a**2-M*r)*cos(theta)**2)/2.d0/gamma*dlog((r-M+&
&gamma)/(r-M-gamma))-(r-M*cos(theta)**2))

Af=(beta*sin(theta)**2/S)*((r - M)*a**2*cos(theta)**2 +&
&r*(r**2 + M*r +2.d0*a**2) - (r*(r**3 - 2.d0*M*a**2 + a**2*r)&
&+Del*a**2*cos(theta)**2)/2.d0/gamma*dlog((r - M + gamma)/&
&(r - M - gamma)))
endif
else
At=-a*Bo*(1.d0-M*r/S*(2.d0-sin(theta)**2))
Af=Bo*sin(theta)**2/2.d0/S*(B-4.d0*M*a**2*r)
endif

ut=1.d0/sqrt(-gtt- 2.d0*omega*gtf-omega**2*gff)
uphi = omega*ut
L = B/S*sin(theta)**2*uphi - 2.d0*M*a*r/S*sin(theta)**2&
&*ut+q/mpart*Af

alphaeff=B
betaeff=-q/mpart*At*B+2.d0*M*r*a*(L-q/mpart*Af)
gammaeff=q**2/mpart**2*At**2*B-4.d0*M*r*a*q/mpart*At&
&*(L-q/mpart*Af)-&
&Del*S-S/sin(theta)**2*(L-q/mpart*Af)**2*(1.d0-2.d0*M*r/S)

en = (betaeff+sqrt(betaeff**2-alphaeff*gammaeff))/alphaeff

ut=1.d0/Del/S*(-2.d0*M*r*a*(L-q/mpart*Af)+(B*(en+q/mpart*At)))
uphi=((1.d0-2.d0*M*r/S)*(L-q/mpart*Af))/Del/sin(theta)**2&
&+2.d0*M*r*a*(en+q/mpart*At)/Del/S

delta=-((en+q/mpart*At)*ut + (L-q/mpart*Af)*uphi + S*ur**2/Del+&
&S*utheta**2

print '(I,3d18.10)',it+1,ur,ut,delta
write(i3,'(I,2d45.29)')it+1,q,mpart
write(i3,'(2d45.29)') t,r
write(i3,'(2d45.29)') theta,phi
write(i3,'(4d45.29)') ut,ur,utheta,uphi

endif

ik=ik+1
enddo
3 close(i3)

call open(i4,file2,1,'unknown')
write(i4,'(I)') it+1
close(i4)

print*, "info: program completed"
!enddo
end program

```

```

function funcd(a,lo,r1,r,theta)
implicit none
double precision::r,a,theta,theta1,r1,S,B,Del,Del1,S1,B1,gtt
double precision:: gtt1,gtf,gff1,grr,gthetatheta,grr1,gthetatheta1
double precision:: omega,omega1,M,lo,ut,utin,gff,gff1,funcd
Parameter (M=1.d0,theta1=1.5707963267948966d0)

S = r**2 + a**2*cos(theta)**2
Del = r**2 + a**2 - 2.d0*M*r
B = (r**2 + a**2)**2 - Del*a**2*sin(theta)**2

S1 = r1**2 + a**2*cos(theta1)**2
Del1 = r1**2 + a**2 - 2.d0*M*r1
B1 = (r1**2 + a**2)**2 - Del1*a**2*sin(theta1)**2

gtt= -(1.d0 - 2.d0*M*r/S)
gtf= -2.d0*a*M*r*sin(theta)**2/S
gff= B*sin(theta)**2/S
grr= S/Del
gthetatheta= S

gtt1= -(1.d0 - 2.d0*M*r1/S1)
gtf1= -2.d0*a*M*r1*sin(theta1)**2/S1
gff1= B1*sin(theta1)**2/S1
grr1= S1/Del1
gthetatheta1= S1

omega=-(gtf+ lo*gtt)/(gff+lo*gtf)
omega1=-(gtf1+ lo*gtt1)/(gff1+lo*gtf1)

ut=1.d0/sqrt(-gtt- 2.d0*omega*gtf-omega**2*gff)
utin=1.d0/sqrt(-gtt1- 2.d0*omega1*gtf1-omega1**2*gff1)
funcd=(ut*(1.d0 - lo*omega)/utin/(1.d0 - lo*omega1))-1.d0
end function

```

## Solving equations of Motion

After the definition of the parameters and initial conditions of the problem (in `inirel.txt`) we are ready to run program `bh.x`, which solves the equations of motion. The differential equations of motion are written in file `ode.f90`. To integrate the differential equations we have implemented a 4<sup>th</sup> order adaptive stepsize Runge-Kutta scheme. The particles' initial conditions (`iniparticles.dat`) are read in by subroutine `particleini.f90`. The output is written in `rtheta.dat`.

```

!      Last change:  DD 13 Aug 2007   2:53 pm
program bh
implicit none

integer:: nvar,nok,nbad,kmax,nmax
parameter (nvar=8,kmax=200,nmax=8)
double precision:: t,Ic,ro
double precision:: B1,S1,At1,Af1,D1
double precision:: B,S,At,Af,D,mu
double precision:: Afr1,Aftheta1,Atr1,Attheta1,Afr,Aftheta,Atr,Attheta
double precision:: eps,h1,hmin,tp(kmax)
double precision:: tini,tend,t1,t2,dt12
double precision,dimension(nvar)::rr,uu,uustart,rrstart,dydt
integer:: i,k,w,nstp,numdt,numpart
double precision,allocatable,dimension(:,:,:)::yp,yy
double precision,allocatable,dimension(:,:)::rstart,uustart,yustart
double precision,allocatable,dimension(:,:)::r,u,y
double precision,allocatable,dimension(:)::L,e,q,mpart,delta
double precision,allocatable,dimension(:)::L1,e1,delta1
double precision::L2,e2,delta2,B2,S2,D2
double precision::Veffect,alphaeff,betaeff,gammaeff

INTEGER:: i3,i4,ierr1,ierr2,ierr3,i1

double precision::mb,a,Bo

double precision,PARAMETER::Gcgs=6.6726d-8,pi=3.14159265359d0,&
&cgs=2.99792458d10, c=1.0d0,G=1.0d0,m=1.0d0

```

```

LOGICAL::cgsl,cgso,le=.true.,inwards,dipole,complete
CHARACTER(132)::FILE='rtheta.dat',scratch='scratch2.txt'

external rkqs,ode,magnetize,uniformB

call open(i3,file,1,'unknown')

! Integration boundaries and initial values:
call open(i1,'numofparticles.dat',1,'unknown')
read(i1,*) ,numpart
close(i1)
print*,"info:_file_(numofparticles.dat)_was_read_successfully"

!Deallocate (rrstart,ustart,LL,ee,Lend,eend,stat=ierr)
Allocate(q(numpart),mpart(numpart),L(numpart),e(numpart),delta&
&(numpart),delta1(numpart),L1(numpart),e1(numpart),Carter1&
&(numpart),Carter(numpart),stat=ierr1)
Allocate(rstart(numpart,nvar/2),ustart(numpart,nvar/2),ystart&
&(numpart,nvar),yp(numpart,nmax,kmax),stat=ierr2)
Allocate(r(numpart,nvar/2),u(numpart,nvar/2),&
&y(numpart,nvar),stat=ierr3)

if ((ierr1 .eq. 0).and.(ierr2 .eq. 0).and.(ierr3 .eq. 0)) &
&print*,"info:_arrays_have_been_allocated_successfully"
if ((ierr1 .ne. 0).or.(ierr2 .ne. 0).or.(ierr3 .ne. 0)) &
&stop "err:_cannot_allocate_memory"

call rdstrt(nvar,h1,hmin,eps,numdt,tini,tend,mb,a,&
&inwards,Bo,dipole,Ic,ro,complete)
print*,"info:rdstrt_file_was_read_successfully"

call particleini(numpart,q,mpart,rstart,ustart,L,e,Ic,ro,Bo,a,&
&dipole,complete)
print*,"info:particleini_file_was_read_successfully"

dt12=abs(tend-tini)/numdt

t1=tini
t2=tini

do k=1,numpart
do i=1,nvar/2
ystart(k,i)=ustart(k,i)
enddo
!Inwards L-E
if (inwards) then
ystart(k,2)=-ystart(k,2)
endif

do i=1+nvar/2,nvar
ystart(k,i)=rstart(k,i-nvar/2)
enddo

do i=1,nvar
y(k,i) = ystart(k,i)
enddo
enddo
print*,"info:_init.f90_read_successfully"

do w=0,numdt
t1=t2
t2=w*dt12

do k=1,numpart

if (dipole) then
call odeint(nstp,y,tp,yp,nvar,&
&numpart,k,t1,t2,eps,h1,hmin,nok,nbad,ode,rkqs,&
&a,q,mpart,At,Af,Bo,magnetize,Ic,ro,complete)
else
call odeint(nstp,y,tp,yp,nvar,numpart,k,t1,t2,&
&eps,h1,hmin,nok,nbad,ode,rkqs,&
&a,q,mpart,At,Af,Bo,uniformB,Ic,ro,complete)

```

```

endif

do i=1,nvar/2
  rr(i)=y(k,i+nvar/2)
  uu(i)=y(k,i)
enddo
D=rr(2)**2+a**2-2.d0*m*rr(2)
S=rr(2)**2+a**2*cos(rr(3))**2
B=(rr(2)**2+a**2)**2-D*a**2*sin(rr(3))**2
if (dipole) then
  call magnetize(Ic,ro,rr,uu,Bo,a,D,S,B,At,Af,Afr,Aftheta,Atr,&
    &Attheta,complete)
else
  call uniformB(Ic,ro,rr,uu,Bo,a,D,S,B,At,Af,Afr,Aftheta,Atr,&
    &Attheta,complete)
endif

do i=1,nvar/2
  u(k,i)=y(k,i)
enddo

do i=1+nvar/2, nvar
  r(k,i-nvar/2)=y(k,i)
enddo

print '(10d15.7)',t2,y(k,6),y(k,7),y(k,8),L2+q(k)/mpart(k)*Af,&
  &e2-q(k)/mpart(k)*At,delta2
write(i3,'(13d23.15)')q(k),mpart(k),t2,y(k,5),y(k,6),y(k,7),&
  &y(k,8),y(k,1),y(k,2),y(k,3),y(k,4),L(k),e(k)

do i=1,nvar/2
  u(k,i)=y(k,i)
enddo

do i=1+nvar/2, nvar
  r(k,i-nvar/2)=y(k,i)

enddo

enddo
enddo

close(i3)
call open(i4,scratch,1, 'unknown')
write(i4,*) numdt
close(i4)

print*, "info: program finished"
print*, '*** Info'
print*, '#####k', '#####e#####', &
  &'#####Delta'
do k=1,numpart

D1=rstart(k,2)**2+a**2-2.d0*m*rstart(k,2)
S1=rstart(k,2)**2+a**2*cos(rstart(k,3))**2
B1=(rstart(k,2)**2+a**2)**2-D1*a**2*sin(rstart(k,3))**2

do i=1,nvar/2
  rrstart(i)=rstart(k,i)
  ustart(i)=ustart(k,i)
enddo

if (dipole) then
  call magnetize(Ic,ro,rrstart,ustart,Bo,a,D1,S1,B1,At1,Af1,&
    &Afr1,Aftheta1,Atr1,Attheta1,complete)
else
  call uniformB(Ic,ro,rrstart,ustart,Bo,a,D1,S1,B1,&
    &At1,Af1,Afr1,Aftheta1,Atr1,Attheta1,complete)
endif

L1(k)=B1/S1*sin(rstart(k,3))**2*ustart(k,4) - 2.d0*m*a*rstart(k,2)&
  &/S1* sin(rstart(k,3))**2*ustart(k,1)
e1(k)=(1.d0- 2.d0*m*rstart(k,2)/S1)*ustart(k,1) + 2.d0*a*m*&
  &rstart(k,2)/S1*sin(rstart(k,3))**2*ustart(k,4)

delta1(k)=- (e1(k))*ustart(k,1)+(L1(k))*ustart(k,4)+&
  &S1*ustart(k,2)**2/D1+S1*ustart(k,3)**2

```

```

L1(k)=L1(k)+q(k)/mpart(k)*Af1
e1(k)=e1(k)-q(k)/mpart(k)*At1

D=r(k,2)**2+a**2-2.d0*m*r(k,2)
S=r(k,2)**2+a**2*cos(r(k,3))**2
B=(r(k,2)**2+a**2)**2-D*a**2*sin(r(k,3))**2

do i=1,nvar/2
  rr(i)=r(k,i)
  uu(i)=u(k,i)
enddo

if (dipole) then
  call magnetize(Ic,ro,rr,uu,Bo,a,D,S,B,At,Af,Afr,Aftheta,&
    &Atr,Attheta,complete)
else
  call uniformB(Ic,ro,rr,uu,Bo,a,D,S,B,At,Af,Afr,&
    &Aftheta,Atr,Attheta,complete)
endif

L(k)=B/S*sin(r(k,3))**2*u(k,4) - 2.d0*m*a*r(k,2)/&
  &S*sin(r(k,3))**2*u(k,1)!+q(k)/mpart(k)*Af

e(k)=(1.d0-2.d0*m*r(k,2)/S)*u(k,1)+2.d0*a*m*r(k,2)/&
  &S*sin(r(k,3))**2*u(k,4)!-q(k)/mpart(k)*At
delta(k)=-(e(k))*u(k,1)+(L(k))*u(k,4)+S*u(k,2)**2/D+S*u(k,3)**2

L(k)=L(k) + q(k)/mpart(k)*Af
e(k)=e(k) - q(k)/mpart(k)*At

print '(I,2e22.14,f22.14,e22.14)',k,e1(k),L1(k),delta1(k)
print '(A,2e22.14,f22.14,e22.14)', ' ',e(k),L(k),delta(k)

enddo

Deallocate(L,e,L1,e1,delta,delta1,stat=ierr1)
Deallocate(yp,ystart,rstart,ustart,stat=ierr2)
Deallocate(y,r,u,q,mpart,stat=ierr3)
if ((ierr1 .eq. 0).and.(ierr2 .eq. 0).and.(ierr3 .eq. 0)) &
  &print*, "info: memory deallocated"
if ((ierr1 .ne. 0).or.(ierr2 .ne. 0).or.(ierr3 .ne. 0)) &
  &stop "err: cannot deallocate memory"

stop
end

```

The following subroutine is responsible for the inputting of the initial conditions and parameters. It also defines the initial velocity components when initial angular momentum and energy is given.

```

subroutine particleini(numpart,q,mpart,rrstart,ustart,LL,ee,Ic,ro,&
  &Bo,a,dipole,complete)
implicit none
INTEGER::i1,i2,i
integer::numdt,numpart

double precision,intent(out),DIMENSION(numpart,4)::rrstart,ustart
double precision,intent(out),dimension(numpart)::LL,ee,q,mpart
double precision,intent(in)::Ic,ro,Bo,a
double precision::L,E,At,Af,Afr,Aftheta,Atr,Attheta,D,S,B,m,delta
double precision,dimension(4)::r,u
integer::j
parameter(m=1.d0)
logical::dipole,complete
external magnetize,uniformB

call open(i2,'iniparticles.dat',1,'unknown')

do i=1,numpart
  READ(i2,*) numpart,q(i),mpart(i)
  READ(i2,*) rrstart(i,1),rrstart(i,2)
  READ(i2,*) rrstart(i,3),rrstart(i,4)
  !Read(i2,*) e(i),ustart(i,3),L(i)
  Read(i2,*) ustart(i,1),ustart(i,2),ustart(i,3),ustart(i,4)

```

```

!      Read(i2,*) E,uustart(i,3),L
!      L(i)=0.d0
!      e(i)=0.d0
!Read(i2,*) uustart(i,3),uustart(i,4)

      do j=1,4
         r(j)=rrstart(i,j)
         u(j)=uustart(i,j)
      enddo

      D=r(2)**2+a**2-2.d0*m*r(2)
      S=r(2)**2+a**2*cos(r(3))**2
      B=(r(2)**2+a**2)**2-D*a**2*sin(r(3))**2

      if (dipole) then
         call magnetize(Ic,ro,r,u,Bo,a,D,S,B,At,Af,Afr,Aftheta,Atr,&
                       &Attheta,complete)
      else
         call uniformB(Ic,ro,r,u,Bo,a,D,S,B,At,Af,Afr,Aftheta,Atr,&
                       &Attheta,complete)
      endif

      LL(i)=0.d0
      ee(i)=0.d0
    enddo
    print '(4d22.14)',uustart(1,1),uustart(1,2),uustart(1,3),uustart(1,4)
    close(i2)
  end subroutine

```

Subroutine `ode.f90` contains all the differential equations of motion. The numerical integration of these equations yields the equations of motion for charged particles.

```

subroutine ode(x,y,dydx,a,q,mpart,At,Af,Bo,magnetic,Ic,ro,complete)
!use iface
!use magneticfield
implicit NONE

double precision,INTENT(IN)::x
double precision,DIMENSION(8),INTENT(IN)::y
double precision,DIMENSION(8),intent(OUT)::dydx
double precision,DIMENSION(4)::r,u
double precision:: G,m,r2,rtheta,f2,ft,t2,theta2,e,L,D,S,B
double precision,intent(inout):: At,Af,Ic,ro
double precision:: Afr,Aftheta,Atr,Attheta,part
double precision,intent(in):: a,q,mpart,Bo
double precision::tr,ttheta,fr,thetaf
parameter (G=1.0d0,m=1.0d0)
integer::i
logical::complete
external magnetic

do i=1,4
  u(i)=y(i)
end do

do i=5,8
  r(i-4)=y(i)
end do

D=r(2)**2+a**2-2.d0*m*r(2)
S=r(2)**2+a**2*cos(r(3))**2
B=(r(2)**2+a**2)**2-D*a**2*sin(r(3))**2

call magnetic(Ic,ro,r,u,Bo,a,D,S,B,At,Af,Afr,Aftheta,Atr,Attheta,complete)

tr=-2.d0*m*(r(2)**2-a**2*cos(r(3))**2)*(r(2)**2+a**2)/S**2/D
fr=-2.d0*a*m*sin(r(3))**2*((a**2-r(2)**2)/S/D-2.d0*r(2)**2*(r(2)**2+&
&a**2)/S**2/D)
ttheta=4.d0*m*r(2)*a**2*sin(r(3))*cos(r(3))/S**2
thetaf=-4.d0*m*a**3*r(2)*sin(r(3))**3*cos(r(3))/S**2

dydx(1)=tr*u(1)*u(2)+fr*u(4)*u(2)+ttheta*u(1)*u(3)+thetaf*u(3)*u(4)&
&+q/mpart*(2.d0*m*r(2)*a/S/D*(Afr*u(2)+Aftheta*u(3))&

```

```

&+B/S/D*(Atr*u(2)+Attheta*u(3))

r2=(m*(r(2)**2 -a**2 *cos(r(3))**2)-r(2)*a**2 *sin(r(3))**2)/D/S
rtheta=2.d0*a**2 *sin(r(3))*cos(r(3))/S
theta2=r(2)*D/S
t2=-m*D/S**3 *(r(2)**2 -a**2 *cos(r(3))**2)
f2=D*sin(r(3))**2 /S**3*(r(2)**5 +2.d0*r(2)**3 *a**2 *cos(r(3))**2&
&-m*r(2)**2 *a**2 *sin(r(3))**2+&
&(m-r(2))*a**4 *sin(r(3))**2 *cos(r(3))**2 +r(2)*a**4 *cos(r(3))**2)
ft=2.d0*D*a*m*sin(r(3))**2 *(r(2)**2 -a**2 *cos(r(3))**2)/S**3

!r derivatives
dydx(2)=r2*u(2)**2+rtheta*u(2)*u(3)+theta2*u(3)**2+t2*u(1)**2+&
&f2*u(4)**2+ft*u(4)*u(1)+&
&q/mpart*D/S*(Afr*u(4)+Atr*u(1))

r2=-a**2 *sin(r(3))*cos(r(3))/S/D
rtheta=-2.d0*r(2)/S
theta2=a**2 *sin(r(3))*cos(r(3))/S
ft=-4.d0*m*r(2)*a*(r(2)**2 +a**2)*sin(r(3))*cos(r(3))/S**3
t2=2.d0*m*r(2)*a**2 /S**3 *sin(r(3))*cos(r(3))
f2=sin(r(3))*cos(r(3))/S**3 *((r(2)**2+a**2)**3 -&
&(r(2)**2 +a**2 +S)*D*a**2 *sin(r(3))**2)

!theta derivatives
dydx(3)=r2*u(2)**2+rtheta*u(2)*u(3)+theta2*u(3)**2+&
&ft*u(4)*u(1)+t2*u(1)**2+f2*u(4)**2&
&+q/mpart/S*(Aftheta*u(4)+Attheta*u(1))

tr=(2.d0*a*m*(-r(2)**2 + a**2 *cos(r(3))**2))/(D*S**2)
ttheta=(4.d0*a*m*r(2)*cos(r(3))/sin(r(3)))/S**2
fr=-2.d0*(r(2)/S-a**2*sin(r(3))**2*(r(2)/D/S+m*(r(2)**2&
&-a**2*cos(r(3))**2)/D/S**2)
thetaf=-2.d0*cos(r(3))*(1.d0/sin(r(3))+2.d0*a**2*m*r(2)*sin(r(3))/S**2)
dydx(4)=tr*u(1)*u(2)+ttheta*u(1)*u(3)+fr*u(2)*u(4)+thetaf*u(3)*u(4)+&
&q/mpart*(2.d0*m*r(2)*a/S/D*(Atr*u(2)+Attheta*u(3))-&
&(1.d0-2.d0*m*r(2)/S)/sin(r(3))**2/D*(Afr*u(2)+Aftheta*u(3))

! t
dydx(5)=u(1)
! r
dydx(6)=u(2)
! theta
dydx(7)=u(3)
! phi
dydx(8)=u(4)
return
end subroutine

```

The uniform and dipolar magnetic fields are defined in files `uniformB.f90` and `magnetize.f90` respectively. The input variables are the ring current  $I_c$  (only for the dipole magnetic field), the distance of the ring current from the black hole  $r_o$  (only for the dipole magnetic field), the particle's position  $r$  and velocity  $u$ , the magnetic field strength  $B_o$  (only for the uniform magnetic field), the black hole's rotation  $a$  and the quantities  $\Delta$ ,  $\Sigma$ ,  $B$ . These subroutines return the components of the vector potential and its derivatives  $A_t$ ,  $A_\phi$ ,  $A_{t,r}$ ,  $A_{t,\theta}$ ,  $A_{\phi,r}$ ,  $A_{\phi,\theta}$ .

```

subroutine uniformB(Ic,ro,r,u,Bo,a,D,S,B,At,Af,Afr,Aftheta,Atr,Attheta)
implicit none
double precision,DIMENSION(4),intent(in)::r,u
double precision,intent(in)::D,S,B,Ic,ro
double precision,intent(out)::At,Af
double precision,intent(out)::Afr,Aftheta,Atr,Attheta
double precision,intent(in)::a,Bo
double precision::m,part
parameter(m=1.0d0)

At=-a*Bo*(1.d0-m*r(2)/S*(2.d0-sin(r(3))**2))
Atr=-a*Bo*(-m*(2.d0-sin(r(3))**2)/S+2.d0*m*r(2)**2*(2.d0-&
&sin(r(3))**2)/S**2)
Attheta=-a*Bo*(-4.d0*m*r(2)*a**2*cos(r(3))*sin(r(3))/S**2&
&+2.d0*sin(r(3))*cos(r(3))*m*r(2)/S+&
&2.d0*m*r(2)*sin(r(3))**3*a**2*cos(r(3))/S**2)

```

```

Af=Bo*sin(r(3))**2/2.d0/S*(B-4.d0*m*a**2*r(2))
Afr=-Bo*sin(r(3))**2*r(2)/S**2*(B-4.d0*m*a**2*r(2))+&
&Bo*sin(r(3))**2/S*(2.d0*r(2)*(r(2)**2+a**2)-(-m+&
&r(2))*a**2*sin(r(3))**2-2.d0*m*a**2)

part=(B-4.d0*m*a**2*r(2))
Atheta=Bo*sin(r(3))*cos(r(3))/S*part+Bo*sin(r(3))**3*&
&a**2*cos(r(3))/S**2*part&
&-Bo*sin(r(3))**3*D*a**2*cos(r(3))/S

return
end subroutine

```

```

subroutine magnetize(Ic,ro,r,u,Bo,a,D,S,B,At,Af,Afr,Atheta,Atr,&
&Atheta,complete)
implicit none
double precision,DIMENSION(4),intent(in)::r,u
double precision,intent(in)::D,S,B
double precision,intent(out)::At,Af
double precision,intent(out)::Afr,Atheta,Atr,Atheta
double precision,intent(in)::a,Bo,Ic,ro
double precision::gamma,beta,alpha,pi
double precision::m
parameter(m=1.0d0,pi=3.14159265359d0)
logical::complete

gamma=dsqrt(m**2-a**2)

if(complete)then
if(r(2).gt.ro)then
beta=-3.d0*Ic/8.d0/(gamma**2)/ro*(ro*(ro**2+a**2)-2.d0*a**2*m)

At=2.d0*a*beta/S*((r(2)*(r(2)-m)&
&+(a**2-m*r(2))*cos(r(3))**2)/2.d0/gamma*dlog((r(2)-m+&
&gamma)/(r(2)-m-gamma))-r(2)-m*cos(r(3))**2)

Af=(beta*sin(r(3))**2/S)*((r(2)-m)*a**2*cos(r(3))**2+&
&r(2)*(r(2)**2+m*r(2)+2.d0*a**2)-r(2)*(r(2)**3-&
&2.d0*m*a**2+a**2*r(2))&
&+D*a**2*cos(r(3))**2)/2.d0/gamma*dlog((r(2)-m+gamma)/&
&r(2)-m-gamma))

Atr=1.d0/(r(2)**2+a**2*cos(r(3))**2)*2.d0*a*beta*(-1.d0+&
&((-gamma-m+r(2))*(1.d0/(-gamma-m+r(2))-(gamma-m+&
&r(2))/(-gamma-m+r(2))**2)*(r(2)*(-m+r(2))+(a**2-m*r(2))*&
&cos(r(3))**2))/(2.d0*gamma*(gamma-m+r(2)))+((-m+2.d0*r(2)-&
&m*cos(r(3))**2)*log((gamma-&
&m+r(2))/(-gamma-m+r(2)))/(2.d0*gamma))-4.d0*a*beta*r(2)*(-r(2)+&
&m*cos(r(3))**2+((r(2)*(-m+r(2))+(a**2-m*r(2))*cos(r(3))**2)*&
&log((gamma-m+r(2))/(-gamma-m+r(2)))/(2.d0*gamma)))/(r(2)**2+&
&a**2*cos(r(3))**2)**2

Atheta=(4.d0*a**3*beta*cos(r(3))*(-r(2)+m*cos(r(3))**2+((r(2)*&
&(-m+r(2))+(a**2-m*r(2))*cos(r(3))**2)*log((gamma-m+&
&r(2))/(-gamma-m+r(2)))/&
&(2.d0*gamma))*sin(r(3)))/(r(2)**2+a**2*cos(r(3))**2)**2+&
&1.d0/(r(2)**2+a**2*cos(r(3))**2)*2.d0*a*beta*(-2.d0*m*&
&cos(r(3))*sin(r(3))-((a**2-m*r(2))*cos(r(3)))*log((gamma-m+&
&r(2))/(-gamma-m+r(2)))*sin(r(3)))/gamma)

Afr=1.d0/(r(2)**2+a**2*cos(r(3))**2)*beta*(2.d0*a**2+m*r(2)+r(2)**2&
&+r(2)*(m+2.d0*r(2))+a**2*cos(r(3))**2+((-gamma-m+r(2))*(1.d0/&
&(-gamma-m+r(2))-(gamma-m+r(2))/(-gamma-m+r(2))**2)*(-r(2)*(-2.d0*&
&a**2*m+a**2*r(2)+r(2)**3)+&
&a**2*(-a**2+2.d0*m*r(2)-r(2)**2)*cos(r(3))**2)/(2.d0*gamma*(gamma-m+&
&r(2)))+(2.d0*a**2*m-a**2*r(2)-r(2)**3-r(2)*(a**2+3.d0*r(2)**2)+&
&a**2*(2.d0*m-2.d0*r(2))*cos(r(3))**2)*log((gamma-m+r(2))/&
&(-gamma-m+r(2)))/(2.d0*gamma))*sin(r(3))**2-(2.d0*beta*r(2)*&
&r(2)*(2.d0*a**2+m*r(2)+r(2)**2)+&
&a**2*(-m+r(2))*cos(r(3))**2+1.d0/(2.d0*gamma)*(-r(2)*(-2.d0*a**2*m+&
&a**2*r(2)+r(2)**3)+&
&a**2*(-a**2+2.d0*m*r(2)-r(2)**2)*cos(r(3))**2)*log((gamma-m+r(2))/&

```

```

&(-gamma-&
&m+r(2))) *sin(r(3)) **2 / (r(2) **2 + a **2 * cos(r(3)) **2) **2

Atheta=1.d0/S*2.d0*beta*cos(r(3))*(r(2)*(2.d0*a**2+m*r(2)+r(2)**2)+&
&a**2*(-m+r(2))*cos(r(3))**2+((-r(2)*(-2.d0*a**2*m+a**2*r(2)+r(2)**3)+&
&a**2*(-a**2+2.d0*m*r(2)-r(2)**2)*cos(r(3))**2)*log((gamma-m+r(2))/&
&(-gamma-m+r(2))))/(2.d0*gamma))*sin(r(3))+(2.d0*a**2*beta*cos(r(3))&
&*(r(2)*(2.d0*a**2+&
&m*r(2)+r(2)**2)+a**2*(-m+r(2))*cos(r(3))**2+1.d0/&
&(2.d0*gamma))*(-r(2)*(-2.d0*a**2*m+a**2*r(2)+r(2)**3)+a**2*(-a**2+&
&2.d0*m*r(2)-r(2)**2)*cos(r(3))**2)*log((gamma-m+r(2))/(-gamma-m+&
&r(2))))*sin(r(3))**3)/&
&(r(2)**2+a**2*cos(r(3))**2)**2+1.d0/(r(2)**2+a**2*cos(r(3))**2)*beta*&
&sin(r(3))**2*(-2.d0*a**2*(-m+r(2))*cos(r(3))*sin(r(3))-(a**2*(-a**2+&
&2.d0*m*r(2)-r(2)**2)*cos(r(3))*log((gamma-m+r(2))/(-gamma-m+r(2))))*&
&sin(r(3)))/gamma

else if (r(2) .lt. ro) then
alpha=3.d0*Ic/8.d0/ro/gamma*((ro*(ro+m)+2.d0*a**2)-&
&1.d0/2.d0/gamma*log((ro-m+gamma)/(ro-m-gamma))*&
&(ro*(ro**2+a**2)-2.d0*m*a**2))
At=2.d0*a*alpha/S/gamma*(r(2)**2-m*r(2)-m*r(2)*cos(r(3))**2+&
&a**2*cos(r(3))**2)+a*Ic/ro

Af=alpha*sin(r(3))**2/S/gamma*(D*(-2.d0*a**2*cos(r(3))**2+S)-&
&2.d0*r(2)*(r(2)**2+a**2)*(r(2)-m))

Atr=(2.d0*a*alpha*(2.d0*r(2)-m*(1.d0+cos(r(3))**2)))/&
&(gamma*(r(2)**2+a**2*cos(r(3))**2))-(4.d0*a*alpha*r(2)*&
&(r(2)**2+a**2*cos(r(3))**2-m*r(2)*(1.d0+cos(r(3))**2)))/&
&(gamma*(r(2)**2+a**2*cos(r(3))**2)**2)

Atheta=(4.d0*a**3*alpha*cos(r(3))*&
&(r(2)**2+a**2*cos(r(3))**2-m*r(2)*(1.d0+cos(r(3))**2))*&
&sin(r(3)))/(gamma*(r(2)**2+a**2*cos(r(3))**2)**2)+&
&(2.d0*a*alpha*(-2.d0*a**2*cos(r(3))*sin(r(3)))+&
&2.d0*m*r(2)*cos(r(3))*sin(r(3)))/(gamma*(r(2)**2+&
&a**2*cos(r(3))**2))

Afr=(alpha*(-4.d0*r(2)**2*(-m+r(2))-2.d0*r(2)*(a**2+r(2)**2)-&
&2.d0*(-m+r(2))*(a**2+r(2)**2)+2.d0*r(2)*(a**2-2.d0*m*r(2)+&
&r(2)**2)+(-2.d0*m+2.d0*r(2))*(r(2)**2-a**2*cos(r(3))**2))*&
&sin(r(3))**2)/(gamma*(r(2)**2+a**2*cos(r(3))**2))-(2.d0*alpha*&
&r(2)*(-2.d0*r(2)*(-m+r(2))*(a**2+r(2)**2)+(a**2-2.d0*m*r(2)+&
&r(2)**2)*(r(2)**2-a**2*cos(r(3))**2))*sin(r(3))**2)/(gamma*&
&(r(2)**2+a**2*cos(r(3))**2)**2)

Atheta=(2.d0*alpha*cos(r(3))*(-2.d0*r(2)*(-m+r(2))*&
&(a**2+r(2)**2)+(a**2-2.d0*m*r(2)+r(2)**2)*(r(2)**2-&
&a**2*cos(r(3))**2))*sin(r(3)))/(gamma*(r(2)**2+&
&a**2*cos(r(3))**2))+(2.d0*a**2*alpha*(a**2-2.d0*m*r(2)+&
&r(2)**2)*cos(r(3))*sin(r(3))**3)/(gamma*(r(2)**2+&
&a**2*cos(r(3))**2))+(2.d0*a**2*alpha*cos(r(3))*(-2.d0*r(2)*(-m+&
&r(2))*(a**2+r(2)**2)+(a**2-2.d0*m*r(2)+r(2)**2)*(r(2)**2-&
&a**2*cos(r(3))**2))*sin(r(3))**3)/(gamma*(r(2)**2+&
&a**2*cos(r(3))**2)**2)
endif
else
beta=-3.d0*Ic/8.d0/(gamma**2)/ro*(ro*(ro**2+a**2)-2.d0*a**2*m)

At=2.d0*a*beta/S*((r(2)*(r(2)-m)&
&+(a**2-m*r(2))*cos(r(3))**2)/2.d0/gamma*dlog((r(2)-m+&
&gamma)/(r(2)-m-gamma))-(r(2)-m*cos(r(3))**2))

Af=(beta*sin(r(3))**2/S)*((r(2)-m)*a**2*cos(r(3))**2 +&
&(r(2)*(r(2)**2 + m*r(2) + 2.d0*a**2) - (r(2)*(r(2)**3 -&
&2.d0*m*a**2 + a**2*r(2))+D*a**2*cos(r(3))**2)/2.d0/gamma*&
&dlog((r(2)-m+gamma)/(r(2)-m-gamma)))

Atr=1.d0/(r(2)**2+a**2*cos(r(3))**2)*2.d0*a*beta*(-1.d0+&
&((-gamma-m+r(2))*(1.d0/(-gamma-m+r(2))-(gamma-m+&
&r(2))/(-gamma-m+r(2))**2)*(r(2)*(-m+r(2))+(a**2-m*r(2))*&

```

```

&cos(r(3)**2))/(2.d0*gamma*(gamma-m+r(2)))+((-m+2.d0*r(2)-&
&m*cos(r(3)**2)*log((gamma-m+r(2))/(-gamma-m+r(2))))/(2.d0*&
&gamma))-4.d0*a*beta*r(2)*(-r(2)+m*cos(r(3)**2)+((r(2)*(-m+&
&r(2))+(a**2-m*r(2))*cos(r(3)**2)*&
&log((gamma-m+r(2))/(-gamma-m+r(2))))/(2.d0*gamma)))/(r(2)**2+&
&a**2*cos(r(3)**2)**2

Attheta=(4.d0*a**3*beta*cos(r(3))*(-r(2)+m*cos(r(3)**2)+((r(2)*&
&(-m+r(2))+(a**2-m*r(2))*cos(r(3)**2)*log((gamma-m+&
&r(2))/(-gamma-m+r(2))))/(2.d0*gamma))*sin(r(3)))/(r(2)**2+&
&a**2*cos(r(3)**2)**2+1.d0/(r(2)**2+a**2*cos(r(3)**2)*2.d0&
&a*beta*(-2.d0*m*cos(r(3))*sin(r(3))-&
&((a**2-m*r(2))*cos(r(3))*log((gamma-m+r(2))/(-gamma-m+&
&r(2)))*sin(r(3)))/gamma)

Afr=1.d0/(r(2)**2+a**2*cos(r(3)**2)*beta*(2.d0*a**2+m*r(2)+r(2)**2&
&r(2)*(m+2.d0*r(2))+&
&a**2*cos(r(3)**2+((-gamma-m+r(2))*(1.d0/(-gamma-m+r(2))-&
&(gamma-m+r(2))/(-gamma-m+r(2)**2)*(-r(2)*(-2.d0*a**2*m+a**2*r(2)&
&r(2)**3)+&
&a**2*(-a**2+2.d0*m*r(2)-r(2)**2)*cos(r(3)**2)))/(2.d0*gamma*&
&(gamma-m+&
&r(2)))+(2.d0*a**2*m-a**2*r(2)-r(2)**3-r(2)*(a**2+3.d0*r(2)**2)+&
&a**2*(2.d0*m-2.d0*r(2))*cos(r(3)**2)*log((gamma-m+r(2))/&
&(-gamma-m+r(2))))/(2.d0*gamma))*sin(r(3)**2-(2.d0*beta*r(2)*&
&(r(2)*(2.d0*a**2+m*r(2)+r(2)**2)+&
&a**2*(-m+r(2))*cos(r(3)**2+1.d0/(2.d0*gamma))*(-r(2)*(-2.d0*a**2*m&
&+a**2*r(2)+r(2)**3)+&
&a**2*(-a**2+2.d0*m*r(2)-r(2)**2)*cos(r(3)**2)*log((gamma-m+r(2))/&
&(-gamma-&
&m+r(2))))*sin(r(3)**2)/(r(2)**2+a**2*cos(r(3)**2)**2

Afttheta=1.d0/S*2.d0*beta*cos(r(3))*(r(2)*(2.d0*a**2+m*r(2)+r(2)**2)+&
&a**2*(-m+r(2))*cos(r(3)**2+((-r(2)*(-2.d0*a**2*m+a**2*r(2)+r(2)**3)+&
&a**2*(-a**2+2.d0*m*r(2)-r(2)**2)*cos(r(3)**2)*&
&log((gamma-m+r(2))/(-gamma-&
&m+r(2))))/(2.d0*gamma))*sin(r(3))+(2.d0*a**2*beta*cos(r(3))*&
&(r(2)*(2.d0*a**2+m*r(2)+r(2)**2)+a**2*(-m+r(2))*cos(r(3)**2+1.d0/&
&(2.d0*gamma))*(-r(2)*(-2.d0*a**2*m+a**2*r(2)+r(2)**3)+a**2*(-a**2+&
&2.d0*m*r(2)-r(2)**2)*cos(r(3)**2)*log((gamma-m+r(2))/(-gamma-m+&
&r(2))))*sin(r(3)**3)/(r(2)**2+a**2*cos(r(3)**2)**2+1.d0/(r(2)**2+&
&a**2*cos(r(3)**2)*beta*sin(r(3)**2*(-2.d0*a**2*(-m+r(2))*cos(r(3))&
&+sin(r(3))-(a**2*(-a**2+&
&2.d0*m*r(2)-r(2)**2)*cos(r(3))*log((gamma-m+r(2))/(-gamma-m+r(2)))*&
&sin(r(3)))/gamma)

endif
return
end subroutine

```

We also provide some useful routines which are used to perform simple actions, such as:

- Remove comments containing triple stars in the file `inirel.txt`.

```

!Removes lines beginning with a * in 'files'=iunit and save
!values in file ldums.
subroutine cstrip(iunit,files,ldums)
CHARACTER *180::text
CHARACTER*(*)::files
LOGICAL::yn
INTEGER::i,iunit,ldums

REWIND ldums
call open (iunit,files,1,'old')
do
  read (iunit,'(a)',END=900) text
  if (text(1:1).ne.'*') then
    write (ldums,'(a)') text
  END if
END do

900 rewind(ldums)
CLOSE(iunit)
end subroutine

```

- Open files and assign them a logical unit number.

```

!This subroutine opens a file.
subroutine open(iunit,FILE,irecw,stat)
!irecw=0 unformatted sequential file
!irecw=1 formatted sequential file
!irecw>1 direct access file. irecw is record length in words
!status ('old','new',unknown')

INTEGER::i,iunit,irecw,maxlu=30 !maxlu=the maximum number of
!logical units to be examined
LOGICAL::yn
CHARACTER*(*)::FILE,stat

do i=1,maxlu
  inquire (i,OPENED=yn)
  if (.not.yn) exit !If this logical unit is not assigned
!to a file then exit the loop
end do
iunit=i !Give iunit the value of i.
if(irecw.eq.0) then
  open(iunit,file=file,form='unformatted',status=stat)
else if(irecw.eq.1) then
  open(iunit,file=file,form='formatted',status=stat)
else if(irecw.gt.1) then
  open(iunit,file=file,access='direct',recl=irecw,&
form='unformatted',status=stat)
else
  stop
endif
end subroutine

```

### A.1.2 IDL

**Creating Plots.** The routine `plotrel.pro` reads data from files `scratch.txt`, `scratch2.txt`, `numofparticles.dat` and `rtheta.dat`. Moreover, it plots a single-particle trajectory in 2-D space and the effective potential of the magnetized and non-magnetized black hole. File `scratch.txt` is the same as `inirel.txt` with the comments removed. File `scratch2.txt` contains the number of steps/points of the orbits. Data are equally spaced in a given time interval. File `numofparticles.dat` includes the number of particles orbits we would like to examine each time. Routine `plotrel.pro` provides us with the 2-D single-particle orbits plots and effective potential plots illustrated in Section 3.2.

```

pro plotrel,x,y,z;t,r,phi,theta,file=file

  get_lun,ldum
  openr,ldum,'scratch.txt'
  readf,ldum,h1,hmin,eps,numdt
  readf,ldum,t1,t2
  readf,ldum,a,mb,Ic,ro
  close,ldum
  free_lun,ldum
  print,"info: scratch.txt file was read"
  get_lun,ldum
  openr,ldum,'scratch2.txt'
  readf,ldum,n
  close,ldum
  free_lun,ldum
  print,"info: scratch2.txt file was read"

  get_lun,ldum
  openr,ldum,'numofparticles.dat'
  readf,ldum,numpart
  close,ldum
  free_lun,ldum
  print,"info: numofparticles.dat file was read"

  n=long(n)+1l ; array size in the dummy
  ;numpart=long(numpart)

```

```

print,'3-Dprojectiveplots'
file='rtheta.dat'

q=dblarr(numpart)
L=q
E=q
mpart=dindgen(numpart)
tau=dblarr(n,numpart)
t=dblarr(n,numpart)
r=dblarr(n,numpart)
phi=dblarr(n,numpart)
theta=dblarr(n,numpart)
vt=dblarr(n,numpart)
vr=dblarr(n,numpart)
vphi=dblarr(n,numpart)
vtheta=dblarr(n,numpart)

get_lun,ldum
openr,ldum,file
for i=0L,n-1L do begin
  for k=0,numpart-1 do begin
    readf,ldum,qi,mparti,taui,ti,ri,thetai,phii,vti,vri,$
      vthetai,vphii,Li,Ei
    q[k]=qi
    mpart[k]=mparti
    tau[i,k]=taui
    t[i,k]=ti
    r[i,k]=ri
    phi[i,k]=phii
    theta[i,k]=thetai
    vt[i,k]=vti
    vr[i,k]=vri
    vphi[i,k]=vphii
    vtheta[i,k]=vthetai
    L[k]=Li
    E[k]=Ei

  endfor
endfor
close,ldum
free_lun,ldum

x=dblarr(n,numpart)
y=dblarr(n,numpart)

x=sqrt(r^2+a^2)*cos(phi)
y=sqrt(r^2+a^2)*sin(phi)

rs1=1.d0-sqrt(1.d0^2-a^2)
rs2=1.d0+sqrt(1.d0^2-a^2)

DEVICE,RETAIN=2
ni=180
phiangle=(2.d0 * !dpi / double(ni-1)) * DINDGEN(ni)

xin=dblarr(ni)
yin=dblarr(ni)

rin=dblarr(ni)

xrs1=dblarr(ni)
yrs1=dblarr(ni)
xrs2=dblarr(ni)
yrs2=dblarr(ni)

for i=0,ni-1 do begin
  xrs1[i]=sqrt(rs1^2+a^2)*cos(phiangle[i])
  yrs1[i]=sqrt(rs1^2+a^2)*sin(phiangle[i])
endfor

for i=0,ni-1 do begin
  xrs2[i]=sqrt(rs2^2+a^2)*cos(phiangle[i])

```

```

        yrs2[i]=sqrt(rs2^2+a^2)*sin(phiangle[i])
    endfor

    rerg=2.d0
    for i=0,ni-1 do begin
        xin[i]=sqrt((rerg)^2+a^2)*cos(phiangle[i])
        yin[i]=sqrt((rerg)^2+a^2)*sin(phiangle[i])
    endfor

window, xs=500, ys=500
range1=max(x,/absolute,/NAN)
range2=max(y,/absolute,/NAN)
range=[range1, range2]
ranges=abs(max(range,/absolute,/NAN))
;xr=[-ranges, ranges]
;yr=xr
;zr=xr

    timestring='t_␣'+string(t[long(n-1),0],format='(e12.4)')

    close, ldum
    free_lun, ldum

    timestring=strcompress('!8t_␣'+string(t[n-11,0],
        format='(e12.4)')+ '!8[GM/c!S!E3!R_␣]',/remove_all)

    titlestring=strcompress('!8r='+string(r[0,0],format='(e12.4)')+
        '!8,␣a='+string(a,format='(e12.4)')+
        '!8,␣L='+string(L[0],format='(e12.4)')+ '!8,␣$
    E='+string(E[0],format='(e12.4)')+ '!8,␣I!Dc!N='+
    string(Ic,format='(e21.3)') ,/remove_all);+ '!8, I!Dc!$
    N='+string(Ic,format='(e21.3)')

name_jpg_␣=strcompress(Ic,/remove_all)

    ␣␣␣xr=[-ranges, ranges]
    ␣␣␣yr=xr
    ␣set_plot,'ps'
    ␣name='./di_motion.ps'

    ␣DEVICE, XSIZE=8, ␣YSIZE=8, ␣/inches, BITS_PER_PIXEL=8, ␣$
    ␣␣␣␣␣␣COLOR=1, filename=name

    ␣TVLCT, ␣[0,255,0,0], ␣[0,0,255,0], ␣[0,0,0,255]
    ␣get_lun, ldum
    ␣openr, ldum, name
    ␣␣␣␣plot, x[* ,0: numpart-1], y[* ,0: numpart-1], xr=xr, yr=yr, $
    ␣␣␣␣␣␣/isotropic, xtitle='!8x [GM/c!S!E2!R ]', $
    ␣␣␣␣␣␣ytitle='!8y [GM/c!S!E2!R ]', charsize=1.2

    ␣␣␣␣oplot, xrs1, yrs1, color=1, linestyle=1
    ␣␣␣␣oplot, xrs2, yrs2, color=2, linestyle=1
    ␣␣␣␣oplot, xin, yin, color=3, linestyle=3
    ␣␣␣␣xyouts, 0.5, 0.97, titlestring, align=0.5, /normal, charsize=1.2
    ␣␣␣␣xyouts, 0.95, 0.93, timestring, align=1.0, /normal, charsize=1.2
    ␣close, ldum
    ␣free_lun, ldum
    ␣device, /close
    ␣set_plot, 'x'
    ␣␣␣␣plot, x[* ,0: numpart-1], y[* ,0: numpart-1], xr=xr, yr=yr, $
    ␣␣␣␣␣␣/isotropic, xtitle='!8x [GM/c!S!E2!R ]', $
    ␣␣␣␣␣␣ytitle='!8y [GM/c!S!E2!R ]', charsize=1.4

    ␣␣␣␣oplot, xrs1, yrs1, color=255, linestyle=1
    ␣␣␣␣oplot, xrs2, yrs2, color=255, linestyle=1
    ␣␣␣␣oplot, xin, yin, color=100, linestyle=3
    ␣␣␣␣xyouts, 0.5, 0.95, titlestring, align=0.5, /normal, charsize=1
    ␣␣␣␣xyouts, 0.95, 0.91, timestring, align=1.0, /normal, charsize=1

    ␣␣k=600
    ␣␣r=(dindgen(k)+1.2d0*100.d0)/100.d0
    ␣␣theta1=!dpi/2.d0

```

```

uutheta=theta1

uuq1=-0.92972282038001278947774046315D-40
uumpart1=0.455469094000000000000000000000D-61

uuL1=L[0]

uuq=q1
uumpart=mpart1
uuL=L1

uuS=dblarr(k)
uuD=dblarr(k)
uuB=dblarr(k)
uuNewmanAt=dblarr(k)
uuNewmanAf=dblarr(k)
uuAt=dblarr(k)
uuAf=dblarr(k)
uualpha=dblarr(k)
uubeta=dblarr(k)
uugamma0=dblarr(k)
uualpha1=dblarr(k)
uubeta1=dblarr(k)
uuVeffect=dblarr(k)
uuEn=dblarr(k)
uuxy=dblarr(k)
uuz=dblarr(k)
uualphano=dblarr(k)
uubetano=dblarr(k)
uugamma0no=dblarr(k)
uuVeffno=dblarr(k)

uum=1.d0
uuQbh=0.d0

uuS=r^2+a^2*cos(theta)^2
uuD=r^2+a^2-2.d0*m*r
uuB=(r^2+a^2)^2-D*a^2*sin(theta)^2

uuEn[*]=E[0]
uugamma=sqrt(m^2-a^2)

;uuuNewmanAt=Qbh*r/S

;uuuNewmanAf=-Qbh*a*r/S*sin(theta)^2

uforuj=0,k-1douubegin

uuS[j]=r[j]^2+a^2*cos(theta)^2
uuD[j]=r[j]^2+a^2-2.d0*m*r[j]
uuB[j]=(r[j]^2+a^2)^2-D[j]*a^2*sin(theta)^2

uuNewmanAt[j]=Qbh*r[j]/S[j]

uuNewmanAf[j]=-Qbh*a*r[j]/S[j]*sin(theta)^2
uuif(r[j]_gt_uro)thenuubegin
uubeta1=-3.d0*Ic/8.d0/(gamma^2)/ro*(ro*(ro^2+a^2)-2.d0*a^2*m)

uuAt[j]=2.d0*a*beta1/S[j]*((r[j]*(r[j]-m)$
uuuu+(a^2-m*r[j])*cos(theta)^2)/2.d0/gamma*log((r[j]-m+$
uuuuuugamma)/(r[j]-m-gamma))-(r[j]-m*cos(theta)^2));+NewmanAt[j]

uuAf[j]=(beta1*sin(theta)^2/S[j])*((r[j]_um)*a^2*cos(theta)^2+$
uuuuuuuurr[j]*(r[j]^2+um*r[j]+2.d0*a^2)_um(r[j]*(r[j]^3_um$
uuuuuuuu2.d0*m*a^2+um*a^2*r[j]))$
uuuuuuuu+D[j]*a^2*cos(theta)^2)/2.d0/gamma*$
uuuuuuuuuualog((r[j]_um+ugamma)/(r[j]_um_ugamma));+NewmanAf[j]

uuuENDIF_ELSE_IF(r[j]_lt_uro)thenuuBEGIN

uuualpha1=3.d0*Ic/8.d0/ro/gamma*((2.d0*(ro^2+a^2)-(ro-m)*ro)+$
uuuuuuuuuuuu1.d0/2.d0/gamma*log((ro-m+gamma)/(ro-m-gamma))*(ro^2*$
uuuuuuuuuuuu(ro-2.d0*m)$
uuuuuuuuuuuu-2.d0*(ro-m)*(ro^2+a^2)))

uuAt[j]=2.d0*a*alpha1/S[j]/gamma*(r[j]^2-m*r[j]-m*r[j]*cos(theta)^2+$

```

```

uuuuuuuuu a^2*cos(theta)^2)+$
uuuuuuuuu a*Ic/ro;+NewmanAt

uuAf[j]=alpha1*sin(theta)^2/S[j]/gamma*(D[j]*(-2.d0*a^2*cos(theta)^2+$
uuuuuuuuu S[j])-2.d0*r[j]*(r[j]^2+a^2)*(r[j]-m));+NewmanAf

uuuend

uualpha[j]=uB[j]-Qbh^2*a^2*sin(theta)^2
uubeta[j]=u(-q/mpart*At[j]*(B[j]-Qbh^2*a^2*sin(theta)^2)+$
uuuuuuuuuu (2.d0*m*r[j]-Qbh^2)*a*(L_u-q/mpart*Af[j]))
uu gamma0[j]=uq^2/mpart^2*At[j]^2*(B[j]-Qbh^2*a^2*sin(theta)^2)+$
uuuuuuuuuu (4.d0*m*r[j]-2.d0*Qbh^2)*a*q/mpart*At[j]*(L_u-$
uuuuuuuuuu q/mpart*Af[j])_u_u S[j]/sin(theta)^2*(L_u-q/mpart*Af[j])^2$
uuuuuuuuuu *(1.d0_u (2.d0*m*r[j]-Qbh^2)/S[j])_u_u (D[j]+Qbh^2)*S[j]

uuVeffect[j]=u(beta[j]+uSqrt(beta[j]^2_u_alpha[j]*gamma0[j]))/$
uuuuuuuuuu alpha[j]
uuxy[j]=r[j]
uuend

uuAt[*]=0
uuAf[*]=0
uualphano_u=B

uubetano_u=(-q/mpart*At*(B)$
uuuuuuuuu +(2.d0*m*r)*a*(L_u-q/mpart*Af))

uu gamma0no_u=q^2/mpart^2*At^2*(B)$
uuuuuuuuuu -(4.d0*m*r)*a*q/mpart*At*(L_u_u $
uuuuuuuuuu S/sin(theta)^2*(L_u)^2_u*(1.d0_u (2.d0*m*r)/S)_u_u (D)*S

uuVeffno=(betano_u+uSqrt(betano^2_u_alphano*gamma0no))/alphano

set_plot,'ps'
name='./di_potential.ps'
DEVICE,_BITS_PER_PIXEL=8,_COLOR=1,filename=name
uTWLCT,_[0,255,0,0],_u[0,0,255,0],_u[0,0,0,255]
uget_lun,ldum
uopenr,ldum,name

plot,xy[where(r_u_nu_ro)],Veffect[where(r_u_nu_ro)],xtitle='!8r',$
uuuuuuu ytitle='!8V!Deff!N',charsize=1.4

oplot,xy,En,color=1
oplot,xy[where(r_u_nu_ro)],Veffno[where(r_u_nu_ro)],linestyle=1
xyouts,0.5,0.96,titlestring,align=0.5,/normal,charsize=1.2
uclose,ldum
ufree_lun,ldum
udevice,/close
uset_plot,'x'

window,1,xs=500,ys=500
plot,xy[where(r_u_nu_ro)],Veffect[where(r_u_nu_ro)],xtitle='!8r',$
uuuuuuu ytitle='!8V!Deff!N',charsize=1.4
oplot,xy,En,color=255
oplot,xy,Veffno,linestyle=1
xyouts,0.5,0.96,titlestring,align=0.5,/normal,charsize=1.2
cursor,xp,yp
print,xp,yp

end

```

Routine `testrel.pro` reads data from files `scratch.txt`, `scratch2.txt`, `rtheta.dat` and `numofparticles.dat` and plots the trajectories of particles in 3-D space. Routine `plotrel.pro` provides us with the 2-D single-particle orbits plots and effective potential plots illustrated in Sect. 3.3 and Chap. 4 .

```

pro testrel,x,y,z,field;,t,r,phi,theta,file=file
get_lun,ldum
openr,ldum,'scratch.txt'
readf,ldum,h1,hmin,eps,numdt
readf,ldum,t1,t2
readf,ldum,a,mb,Ic

```

```

close,ldum
free_lun,ldum
print,"info: scratch.txt file was read"
get_lun,ldum
openr,ldum,'scratch2.txt'
readf,ldum,n
close,ldum
free_lun,ldum
print,"info: scratch2.txt file was read"

get_lun,ldum
openr,ldum,'numofparticles.dat'
readf,ldum,numpart
close,ldum
free_lun,ldum
print,"info: numofparticles.dat file was read"

n=long(n);+1l ; array size in the dummy
;numpart=long(numpart)
print,'3-D\projective\plots'
file='rtheta.dat'

q=dblarr(numpart)
L=q
E=q
mpart=dblarr(numpart)
tau=dblarr(n,numpart)
t=dblarr(n,numpart)
r=dblarr(n,numpart)
phi=dblarr(n,numpart)
theta=dblarr(n,numpart)
vt=dblarr(n,numpart)
vr=dblarr(n,numpart)
vphi=dblarr(n,numpart)
vtheta=dblarr(n,numpart)

get_lun,ldum
openr,ldum,file
for i=0L,n-1L do begin
  for k=0,numpart-1 do begin
    readf,ldum,qi,mparti,taui,ti,ri,thetai,phii,vti,vri,vthetai,$
      vphii,Li,Ei
    q[k]=qi
    mpart[k]=mparti
    tau[i,k]=taui
    t[i,k]=ti
    r[i,k]=ri
    phi[i,k]=phii
    theta[i,k]=thetai
    vt[i,k]=vti
    vr[i,k]=vri
    vphi[i,k]=vphii
    vtheta[i,k]=vthetai
    L[k]=Li
    E[k]=Ei
  endfor
endfor
close,ldum
free_lun,ldum

x=dblarr(n,numpart)
y=dblarr(n,numpart)
z=dblarr(n,numpart)

x=sqrt(r^2+a^2)*cos(phi)*sin(theta)
y=sqrt(r^2+a^2)*sin(phi)*sin(theta)
z=r*cos(theta)

a_dummy = fltarr(10,10) ; the dummy array to be used
x_dummy = findgen(10) ; the dummy axis vectors
y_dummy = findgen(10)
x_dummy = x_dummy;-x1 ; the axis starts at -n/2, not a 0
y_dummy = y_dummy;-y1
a_dummy=a_dummy

;x2=max(x_dummy)

```

```

;y2=max(y_dummy)

x2=max(x)           ; the upper limit of the plot
y2=max(y)
z2=max(z)
x1=min(x)          ; min. values of the axes
y1=min(y)
z1=min(z)

rs1=1.d0-sqrt(1.d0^2-a^2)
rs2=1.d0+sqrt(1.d0^2-a^2)

DEVICE,RETAIN=2

ni=21
thetaangle=findgen(ni)
rerg=findgen(ni)
phiangle=findgen(ni)
thetaangle=thetaangle*(180/(ni-1))
phiangle=phiangle*(180/(ni-1))
xin=dblarr(ni,ni)
yin=dblarr(ni,ni)
zin=dblarr(ni,ni)
rin=dblarr(ni,ni)
thetaangle=thetaangle*!dpi/(180.d0)
phiangle=2.d0*phiangle*!dpi/(180.d0)

xrs2=dblarr(ni,ni)
yrs2=dblarr(ni,ni)
zrs2=dblarr(ni,ni)

for j=0,ni-1 do begin
  for i=0,ni-1 do begin
    xrs2[i,j]=sqrt(rs2^2+a^2)*cos(phiangle[i])*sin(thetaangle[j])
    yrs2[i,j]=sqrt(rs2^2+a^2)*sin(phiangle[i])*sin(thetaangle[j])
    zrs2[i,j]=rs2*cos(thetaangle[j])
  endfor
endfor

for j=0,ni-1 do begin
  rerg[j]=1.d0+sqrt(1.d0-a^2*(cos(thetaangle[j]))^2)
  for i=0,ni-1 do begin
    xin[i,j]=sqrt((rerg[j])^2+a^2)*cos(phiangle[i])*sin(thetaangle[j])
    yin[i,j]=sqrt((rerg[j])^2+a^2)*sin(phiangle[i])*sin(thetaangle[j])
    zin[i,j]=rerg[j]*cos(thetaangle[j])
    rin[i,j]=sqrt(xin[i,j]^2+yin[i,j]^2)
  endfor
endfor

window, xs=500, ys=500

range1=max(x,/absolute,/NAN)
range2=max(y,/absolute,/NAN)
range3=max(z,/absolute,/NAN)
range=[range1,range2,range3]
ranges=abs(max(range,/absolute,/NAN))
;xr=[-ranges,ranges]
;yr=xr
;zr=xr

Surface,zin,xin,yin,/SAVE,$
  xstyle=1,ystyle=1,xrange=[-ranges,ranges],$
  yrange=[-ranges,ranges],$
  zrange=[-ranges,ranges],zst=1,$
  ax=30,az=30,$
  CHARSIZE=2.0,$
  xtitle='!3x_{G_{\mu}/c!S!E2!R_{\mu}}', $
  ytitle='!3y_{G_{\mu}/c!S!E2!R_{\mu}}', $
  ztitle='!3z_{G_{\mu}/c!S!E2!R_{\mu}}',/noerase

plotsym, 0, 1, /FILL,Color= 1

  for i=0,numpart-1 do begin

    plots,x[*],y[*],z[*],/T3D,/data,color=255,/continue

```

```

end
timestring='t_□'+string(t[long(n-1),0],format='(e12.4)')
xyouts,0.7,0.9,timestring,/normal

close,ldum
free_lun,ldum

sphereImg1 = obj_new('orb', POS=[0,0,0], $
    RADIUS=2.0,COLOR=[240,0,0])

sphereImg2= obj_new('orb', POS=[0,0,0], $
    RADIUS=2.0,COLOR=[0,240,0])

oModel1 = obj_new('IDLgrModel')
oModel1->Add, sphereImg1; Don't need [i,j] referencing in IDL

; Add directional light to the model to highlight the 3D shape of the
; spheres

oLight1 = obj_new('IDLgrLight', LOCATION=[799,499,12], TYPE=2)
oModel1->Add, oLight1

oModel2 = obj_new('IDLgrModel')
oModel2->Add, sphereImg2 ; Don't need [i,j] referencing in IDL

; Add directional light to the model to highlight the 3D shape of the
; spheres

oLight2 = obj_new('IDLgrLight', LOCATION=[799,499,12], TYPE=2)
oModel2->Add, oLight2

timestring='!8t_□'+string(t[n-1,0],format='(e12.4)')+
    '!8_□[GM/c!S!E3!R_□]'

titlestring='!8a='+string(a,format='(e12.4)')+
    '!8_□L='+string(L[0],format='(e12.4)')+ '!8_□E='+
    string(E[0],format='(e12.4)')+ '!8_□I!Dc!N'+string$
    (Ic,format='(e21.3)');+'!8, I!Dc!N'+string$
    (Ic,format='(e21.3)')

name_jpg =field+strcompress(Ic,/remove_all)
; preparing the data and plotting:

flat_surface=fltarr(2,2)
xsurf=flat_surface
ysurf=xsurf
xsurf[0,*]=--ranges-1
xsurf[1,*]=ranges+1
ysurf[* ,0]=--ranges-1
ysurf[* ,1]=ranges+1

xr=[-ranges ,ranges]
yr=xr
zr=[-ranges ,ranges]

iplot ,x[* ,0:numpart-1],y[* ,0:numpart-1],z[* ,0:numpart-1], $
    BACKGROUND_COLOR=[0,0,0],COLOR=[240,0,0],xrange=xr,$
    yrange=yr,zrange=zr,XGRIDSTYLE=1,YGRIDSTYLE=1,$
    xstyle=1,ystyle=1,zstyle=1,$
    identifier=1

isurface ,zrs2,xrs2,yrs2,color=[0,240,0],XGRIDSTYLE=1,YGRIDSTYLE=1,$
    BACKGROUND_COLOR=[0,0,0],xrange=xr,yrange=yr,zrange=zr,$
    xstyle=1,ystyle=1,zstyle=1,overplot=1,$
    identifier=2,Name='Outer_□Event_□Horizon'

isurface ,zin,xin,yin,transparency=35,color=[72,72,255], $
    BACKGROUND_COLOR=[0,0,0], $
    XGRIDSTYLE=1, YGRIDSTYLE=1,overplot=2,$
    macro_names=['axis_color'], $
    xrange=xr,yrange=yr,zrange=zr,xstyle=1,ystyle=1,zstyle=1,$
    identifier=3,xtitle='!8x_□[GM/c!S!E2!R_□]', $
    ytitle='!8y_□[GM/c!S!E2!R_□]', ztitle='!8z_□[GM/c!S!E2!R_□]', $
    Name='Ergosphere',/VIEWPLANE_RECT

```

```

isurface,flat_surface,xsurf,ysurf,transparency=35,$
color=[20,20,20],$
BACKGROUND_COLOR=[0,0,0],$
XGRIDSTYLE=1, YGRIDSTYLE=1,$
xrange=xr,yrange=yr,zrange=zr,xstyle=1,ystyle=1,$
zstyle=1,overplot=3,$
macro_names=['axis_color'],$
identifier=4,xtitle='!8x[GM/c!S!E2!R]',,$
ytitle='!8y[GM/c!S!E2!R]',,ztitle='!8z[GM/c!S!E2!R]',,$
Name='Ergosphere',/VIEWPLANE_RECT

ixyouts,strcompress(titlestring,/remove_all), ALIGNMENT=1.0, $
COLOR=[255,255,255], FONT_SIZE=11, $
LOCATION=[0.9, 0.85, 0.0],/normal
ixyouts,timestring, ALIGNMENT=1.0, COLOR=[255,255,255], $
FONT_SIZE=11, LOCATION=[0.9, 0.75, 0.0],/normal

DEVICE,RETAIN=2

itool_write_graphic_kpb,name_jpg,type='jpeg',clobber=1,quality=100

set_plot,'x'
end

```

Routine `veff.pro` plots the effective potential and its contours (Sec. 2.3). The effective potential function is specified by  $V_{\text{effect}}$ . Concerning a magnetized Kerr-Newman black hole, we would have to take into account that the net vector potential is given by the superposition of the dipolar or uniform magnetic fields with the one that corresponds to the Kerr-Newman solution ( $NewmanA_t$ ,  $NewmanA_\phi$ ). The output of this routine can be seen for example in fig. 4.1 for the uniform magnetic field case.

```

pro chniveaux, cmax, cmin, nlevels, ctype, levels
;
; Computation of contour levels
;
; Parameters:  Cmax   Highest contour to be drawn           (input)
;              Cmin   Lowest contour to be drawn           (input)
;              (opt. if linear scaling)
;              nlevels Number of contours to be drawn      (input)
;              CType   Scaling of contour levels           (input)
;                    (1 = linear, 2 = logarithmic base 10)
;              Levels  Array of contour levels              (output)
;
levels = fltarr(nlevels)
If(ctype eq 1.) then begin
  deltaI = cmax/(nlevels-.5) ; Interval between successive
                        ; equidistant contours
  if(cmin ne 0.) then deltaI = (cmax-cmin)/(nlevels-1.)
  levels = cmax-(nlevels-1.-findgen(nlevels))*deltaI
endif else if(ctype eq 2.) then begin
  clmax = alog10(cmax) & clmin = alog10(cmin)
  deltaI = (clmax-clmin)/(nlevels-1.)
  levels = 10.^(clmax - (nlevels-1.-findgen(nlevels))*deltaI)
endif else begin
  Print,'Other nonlinear contour intervals not available'
endif else
return
end

pro veff,L,a,MinVeff,levels,Bo,Qbh,Veffect,xy,z

n=179;+1l ; array size in the dummy
k=2000
k=long(k)

m=1.d0
mpart=0.83631079000000000000000000000000D-58
q=0.92972282038001278947774046315D-40

theta=(dindgen(n)+1)*!dpi/180.d0

```

```

r=(dindgen(k)+1.8*100.d0)/100
S=dblarr(n,k)
D=dblarr(k)
B=dblarr(n,k)
NewmanAt=dblarr(n,k)
NewmanAf=dblarr(n,k)
At=dblarr(n,k)
Af=dblarr(n,k)
alpha=dblarr(n,k)
beta=dblarr(n,k)
gamma0=dblarr(n,k)
Veffect=dblarr(n,k)
xy=dblarr(n,k)
z=dblarr(n,k)

for i=0,n-1 do begin
for j=01,k-11 do begin
S[i,j]=r[j]^2+a^2*cos(theta[i])^2
D[j]=r[j]^2+a^2-2.d0*m*r[j]
B[i,j]=(r[j]^2+a^2)^2-D[j]*a^2*sin(theta[i])^2

NewmanAt[i,j]=Qbh*r[j]/S[i,j]

NewmanAf[i,j]=-Qbh*a*r[j]/S[i,j]*sin(theta[i])^2

At[i,j]=-a*Bo*(1.d0-m*r[j]/S[i,j]*(2.d0-sin(theta[i])^2))+
NewmanAt[i,j]

Af[i,j]=Bo*sin(theta[i])^2/2.d0/S[i,j]*(B[i,j]-4.d0*m*a^2*r[j])$
+NewmanAf[i,j]

alpha[i,j] = B[i,j]-Qbh^2*a^2*sin(theta[i])^2
beta[i,j] = (-q/mpart*At[i,j]*(B[i,j]-Qbh^2*a^2*sin(theta[i])^2) $
+(2.d0*m*r[j]-Qbh^2)*a*(L - q/mpart*Af[i,j]))
gamma0[i,j] = q^2/mpart^2*At[i,j]^2*(B[i,j]-Qbh^2*a^2*$
sin(theta[i])^2)-(4.d0*m*r[j]-2.d0*Qbh^2)*a*$
q/mpart*At[i,j]*(L - q/mpart*Af[i,j]) - $
S[i,j]/sin(theta[i])^2*(L - q/mpart*Af[i,j])^2 *$
(1.d0 - (2.d0*m*r[j]-Qbh^2)/S[i,j]) - (D[j]+Qbh^2)$
*S[i,j]

Veffect[i,j] = (beta[i,j] + Sqrt(beta[i,j]^2 - alpha[i,j]*$
gamma0[i,j]))/alpha[i,j]
xy[i,j]=Sqrt(r[j]^2+a^2+Q^2)*sin(theta[i])
z[i,j]=sqrt(r[j]^2+Q^2)*cos(theta[i])
endfor
endfor

set_plot,'ps'
name='./fig.ps'
DEVICE, BITS_PER_PIXEL=8, COLOR=1,filename=name
TVLCT, [0,255,0,0], [0,0,255,0], [0,0,0,255]
get_lun,ldum
openr,ldum,name
white = 255
black = 0

chniveaux, Max(Veffect), MinVeff, levels, 2, userlevels
Contour, Veffect, xy, z,$ /Fill, C_Colors=Indgen(levels)+3,$
Background=1,Levels=userLevels,c_charsize=1.4,$
charsize=1.8,xrange=[0,10],yrange=[-15,15],xstyle=1,$
ystyle=1,Color=black,$
xtitle=textoidl('sqrt(r^2+a^2) sin\theta'),$
ytitle=textoidl('r cos\theta')

Contour, Veffect, xy, z, /Overplot, Levels=userLevels,$
/Follow,c_charsize=1.4,charsize=1.8;, Color=black

close,ldum
free_lun,ldum
device,/close
set_plot,'x'
device,retain=2,decomposed=0

Window, 1, Title='User Specified Contour Intervals',$
XSize=500, YSize=700

```

```

chniveaux, Max(Veffect), MinVeff, levels, 2, userlevels
Contour, Veffect, xy, z, $
    Levels=userLevels, $
    xtitle=textoid1('sqrt(r^2+a^2)sin\theta'),$
    ytitle=textoid1('r*cos\theta'),xrange=[0,10],$
    yrange=[-15,15],$
    xstyle=1,ystyle=1,c_charsize=1.4,charsize=1.8

Contour, Veffect, xy, z, /Overplot, Levels=userLevels,$
    /Follow,c_charsize=1.4,charsize=1.8

end
;Kerr-Newman-Example
;veff, -0.8, 0.9, 0.9722, 15, 3.309484d-16, 4.d-19

```

Routine `minimum.pro` finds the off-equatorial local minima for the effective potential as we increase the value of the black hole's rotation  $a$ , implementing Powell's method. The output of this routine can be seen for example in fig. 4.4 for the uniform magnetic field case. Plots contain also the projection of the main curve to the  $xy$ -,  $yz$ -,  $xz$ -planes. We have also written similar routines for the calculation of off-equatorial local minima for the effective potential with varying quantities the ratio  $q/m$ , the strength of the magnetic field  $B_o$  (only for the uniform magnetic field) or the ring current  $I_c$  (only for the dipole magnetic field), the net charge of the black hole  $Q_{bh}$  and the angular momentum  $L$  of the charged particle.

```

PRO minimum,xps,yps,Veffs
COMMON mina,a,m,mpart,q,L,Qbh,Bo
n=100
numb=5 ;number of xyouts written on plot
xps=dblarr(n)
yps=dblarr(n)
Veffs=dblarr(n)
a1=dblarr(n)
a0=0.0d0

;Define initial conditions
m=1.d0
mpart=0.836310790000000000000000000000D-58
q=0.92972282038001278947774046315D-40
L=31.9d0
Bo=1.0d-17
Qbh=0.0d0

; Define the starting point:
P = [7.547d0, !dpi-2.292d0]

for i=0,n-1 do begin
; Define the fractional tolerance:
ftol = 1.0d-14

a=a0+double(i)*0.01d0
a1[i]=a

; Define the starting directional vectors in column format:
xi = TRANSPOSE([[1.0, 0.0],[0.0, 1.0]])

; Minimize the function:
POWELL, P, xi, ftol, fmin, 'powfunc'
xy=Sqrt(P[0]^2+a^2)*sin(P[1])
z1=P[0]*cos(P[1])

print,"a: ",a," xy: ", xy," z: ",z1
; Print the solution point:
PRINT, 'Solution_point:', P

xps[i]=Sqrt(P[0]^2+a^2)*sin(P[1])
yps[i]=P[0]*cos(P[1])
Veffs[i]=fmin

; Print the value at the solution point:
PRINT, 'Value_at_solution_point:', fmin
endfor

```

```

set_plot,'ps'
name1='./a_min.ps'
DEVICE, BITS_PER_PIXEL=8, COLOR=1, filename=name1
TVLCT, [0,255,0,0], [0,0,255,0], [0,0,0,255]
plotsym, 0, 1, /FILL,Color= 1
get_lun,ldum3
openr,ldum3,name1
white = 255
black = 0

plot_3dbox,xps,yps,Veffs,psym=8,linestyle=0,$
  xtitle=textoidl('sqrt(r^2+a^2)sin\theta'),$
  ytitle=textoidl('r cos\theta'),ztitle=textoidl('V_{eff}'),$
  title=textoidl('a-Dependence'),/xy_plane,$
  /xz_plane,/yz_plane,$
  xystyle=5,xzstyle=5,yzstyle=5,charsize=1.8,/noerase

plots,xps,yps,Veffs,/continue,color=1,psym=8,linestyle=0,/t3d

for j=0,n-1,numb do begin
  timestring='UUU'+string(a1[j],format='(f4.2)')
  xyouts,xps[j],yps[j],z=Veffs[j],timestring,/data,CHARSIZE = 1.8,/t3d
endfor

close,ldum3
free_lun,ldum3
device,/close
set_plot,'x'
device,retain=2,decomposed=0
TVLCT, [0,255,0,0], [0,0,255,0], [0,0,0,255]

window,xs=500,ys=500

plot_3dbox,xps,yps,Veffs,psym=8,linestyle=0,$
  xtitle=textoidl('sqrt(r^2+a^2)sin\theta'),$
  ytitle=textoidl('r cos\theta'),$
  ztitle=textoidl('V_{eff}'),$
  title=textoidl('a-Dependence'),/xy_plane,$
  /xz_plane,/yz_plane,$
  xystyle=5,xzstyle=5,yzstyle=5,charsize=1.8,/noerase

plots,xps,yps,Veffs,/continue,color=1,psym=8,linestyle=0,/t3d,/data

for i=0,n-1,numb do begin
  timestring='UUU'+string(a1[i],format='(f4.2)')
  xyouts,xps[i],yps[i],z=Veffs[i],timestring,/data,CHARSIZE = 1.8,/t3d
endfor
return
END

FUNCTION powfunc, x
COMMON mina,a,m,mpart,q,L,Qbh,Bo
gamma=sqrt(m^2-a^2)

S=x[0]^2+a^2*cos(x[1])^2
D=x[0]^2+a^2-2.d0*m*x[0]
B=(x[0]^2+a^2)^2-D*a^2*sin(x[1])^2

NewmanAt=Qbh*x[0]/S
NewmanAf=-Qbh*a*x[0]/S*sin(x[1])^2

At=-a*Bo*(1.d0-m*x[0]/S*(2.d0-sin(x[1])^2))+NewmanAt
Af=Bo*sin(x[1])^2/2.d0/S*(B-4.d0*m*a^2*x[0])+NewmanAf

alpha = B-Qbh^2*a^2*sin(x[1])^2
beta = (-q/mpart*At*(B-Qbh^2*a^2*sin(x[1])^2) +$
(2.d0*m*x[0]-Qbh^2)*a*(L - q/mpart*Af))

gamma0 = q^2/mpart^2*At^2*(B-Qbh^2*a^2*sin(x[1])^2) -$
(4.d0*m*x[0]-2.d0*Qbh^2)*a*q/mpart*At*(L -$
q/mpart*Af) -S/sin(x[1])^2*(L - q/mpart*Af)^2*$
*(1.d0 -(2.d0*m*x[0]-Qbh^2)/S) - (D+Qbh^2)*S

```

```
RETURN, (beta + Sqrt(beta^2 - alpha*gamma0))/alpha
END
```

**Automating the procedures - Creating simple movies.** If we want to perform multiple test-runs it would be better to create multiple start files `inirel*.txt` (e.g. `inirel_a_0_9.txt`), and then link them to the file `inirel.txt`. This way we could automate the procedure by creating a bash-script file. The script file will execute programs `findroot.x` and `bh.x` for different initial conditions, namely for different `inirel*.txt`.

To automate the movie-production procedure we have written the following bash-script file (`movies.sh`) which automates the whole procedure and

- links the `inirel*.txt` to file `inirel.txt`,
- compiles and runs `findroot.x`,
- compiles and runs `bh.x`, using the output data of `findroot.x`,
- compiles and runs routine `movies.pro`,
- creates movie file `movie.avi`,
- sends an email when test-run has finished.

The production of simple movies requires the generation of a sequence of numbered images. This is done so by following the same principles as in `testrel.pro`. The only difference between files `movies.pro` and `testrel.pro` is that the former one requires a loop over number of steps. Moreover, file `movies.pro` plots particles' position as scattered points at each timestep. Here, protons are depicted with a red color, while electrons with a green one (Sec. 3.4). Every image produced here, is saved with a different name and answer to the corresponding timestep.

```
pro movies ,x,y,z,xin,yin,zin,xrs2,yrs2,zrs2
  get_lun,ldum
  openr,ldum,'scratch.txt'
  readf,ldum,h1,hmin,eps
  readf,ldum,t1,t2
  readf,ldum,a,mb,Bo
  close,ldum
  free_lun,ldum

  get_lun,ldum
  openr,ldum,'scratch2.txt'
  readf,ldum,n
  close,ldum
  free_lun,ldum

  get_lun,ldum
  openr,ldum,'numofparticles.dat'
  readf,ldum,numpart
  close,ldum
  free_lun,ldum

  n=long(n);+1l ; array size in the dummy
  print,'3-D projective plots'
  file='rtheta.dat'

  q=dblarr(numpart)
  mpart=dblarr(numpart)
  tau=dblarr(n,numpart)
  t=dblarr(n,numpart)
  r=dblarr(n,numpart)
  phi=dblarr(n,numpart)
  theta=dblarr(n,numpart)
  vt=dblarr(n,numpart)
  vr=dblarr(n,numpart)
```

```

vphi=dblarr(n,numpart)
vtheta=dblarr(n,numpart)

get_lun,ldum
openr,ldum,file
for i=0L,n-1L do begin
  for k=0,numpart-1 do begin
    readf,ldum,qi,mparti,taui,ti,ri,thetai,phii,vti,vri,vthetai,vphii
    q[k]=qi
    mpart[k]=mparti
    tau[i,k]=taui
    t[i,k]=ti
    r[i,k]=ri
    phi[i,k]=phii
    theta[i,k]=thetai
    vt[i,k]=vti
    vr[i,k]=vri
    vphi[i,k]=vphii
    vtheta[i,k]=vthetai
  endfor
endfor
close,ldum
free_lun,ldum

x=dblarr(n,numpart)
y=dblarr(n,numpart)
z=dblarr(n,numpart)

x=sqrt(r^2+a^2)*cos(phi)*sin(theta)
y=sqrt(r^2+a^2)*sin(phi)*sin(theta)
z=r*cos(theta)

a_dummy = fltarr(10,10) ; the dummy array to be used
x_dummy = findgen(10) ; the dummy axis vectors
y_dummy = findgen(10)
x_dummy = x_dummy;-x1 ; the axis starts at -n/2, not a 0
y_dummy = y_dummy;-y1
a_dummy=a_dummy

x2=max(x) ; the upper limit of the plot
y2=max(y)
z2=max(z)
x1=min(x) ; min. values of the axes
y1=min(y)
z1=min(z)

rs1=1.d0-sqrt(1.d0^2-a^2)
rs2=1.d0+sqrt(1.d0^2-a^2)

DEVICE,RETAIN=2

ni=21
thetaangle=findgen(ni)
rerg=findgen(ni)
phiangle=findgen(ni)
thetaangle=thetaangle*(180/(ni-1))
phiangle=phiangle*(180/(ni-1))
xin=dblarr(ni,ni)
yin=dblarr(ni,ni)
zin=dblarr(ni,ni)
rin=dblarr(ni,ni)
thetaangle=thetaangle*!dpi/(180.d0)
phiangle=2.d0*phiangle*!dpi/(180.d0)

xrs2=dblarr(ni,ni)
yrs2=dblarr(ni,ni)
zrs2=dblarr(ni,ni)

for j=0,ni-1 do begin
  for i=0,ni-1 do begin
    xrs2[i,j]=sqrt(rs2^2+a^2)*cos(phiangle[i])*sin(thetaangle[j])
    yrs2[i,j]=sqrt(rs2^2+a^2)*sin(phiangle[i])*sin(thetaangle[j])
    zrs2[i,j]=rs2*cos(thetaangle[j])
  endfor
endfor

```

```

for j=0,ni-1 do begin
  rerg[j]=1.d0+sqrt(1.d0-a^2*(cos(thetaangle[j]))^2)
  for i=0,ni-1 do begin
    xin[i,j]=sqrt((rerg[j])^2+a^2)*cos(phiangle[i])*sin(thetaangle[j])
    yin[i,j]=sqrt((rerg[j])^2+a^2)*sin(phiangle[i])*sin(thetaangle[j])
    zin[i,j]=rerg[j]*cos(thetaangle[j])
    rin[i,j]=sqrt(xin[i,j]^2+yin[i,j]^2)
  endfor
endfor

close,ldum
free_lun,ldum

range1=max(x,dimension=1,/absolute,/NAN)
range2=max(y,dimension=1,/absolute,/NAN)
range3=max(z,dimension=1,/absolute,/NAN)
range=[range1,range2,range3]
ranges=max(range,/NAN)
xr=[-ranges,ranges]
yr=[-ranges,ranges]
zr=[-ranges,ranges]

sphereImg1 = obj_new('orb', POS=[0,0,0], $
RADIUS=2.0, COLOR=[240,0,0])

sphereImg2= obj_new('orb', POS=[0,0,0], $
RADIUS=2.0, COLOR=[0,240,0])

oModel1 = obj_new('IDLgrModel')
oModel1->Add, sphereImg1; Don't need [i,j] referencing in IDL

; Add directional light to the model to highlight the 3D shape of the
; spheres

oLight1 = obj_new('IDLgrLight', LOCATION=[799,499,12], TYPE=2)
oModel1->Add, oLight1

oModel2 = obj_new('IDLgrModel')
oModel2->Add, sphereImg2; Don't need [i,j] referencing in IDL

; Add directional light to the model to highlight the 3D shape of the
; spheres

oLight2 = obj_new('IDLgrLight', LOCATION=[799,499,12], TYPE=2)
oModel2->Add, oLight2

titlestring='B!Do!N0=0'+strcompress(Bo,/remove_all)+',$
!!!!!!!!!!!!!!!!!!!!!!$a=0'+strcompress(a,/remove_all)+'0,M=0'+strcompress
$(mb,/remove_all)

cd,'jpg'
for it = 0L,n-1L do begin
  timestring='t0=0'+string(t[it,0],format='(e12.4)')

  name_jpg = '00'+strcompress(100000+it,/remove_all)
; preparing the data and plotting:

  timestring='!8t0=0'+string(t[it],format='(e12.4)')+
  '!80[GM/c!S!E3!R0]'

  iplot,x[it,where(q gt 0)],y[it,where(q gt 0)],$
  z[it, where(q gt 0)],sym_object=oModel1,$
  linestyle=6,sym_color=[255,72,72],sym_thick=10,$
  sym_size=0.2,$
  BACKGROUND_COLOR=[0,0,0],$
  xrange=xr,yrange=yr,zrange=zr,XGRIDSTYLE=1,$
  YGRIDSTYLE=1,xstyle=1,ystyle=1,zstyle=1,$
  identifier=1, /NO_SAVEPROMPT,user_interface='none'

  iplot,x[it,where(q lt 0)],y[it,where(q lt 0)],$
  z[it,where(q lt 0)],sym_object=oModel2,$
  linestyle=6,sym_color=[255,72,72],sym_thick=10,$
  sym_size=0.2,xrange=xr,yrange=yr,zrange=zr,$

```

```

BACKGROUND_COLOR=[0,0,0],XGRIDSTYLE=1,YGRIDSTYLE=1,$
xstyle=1,ystyle=1,zstyle=1,$
overplot=1,identifier=2,/NO_SAVEPROMPT,user_interface='none'

isurface,zrs2,xrs2,yrs2,color=[0,240,0],XGRIDSTYLE=1,YGRIDSTYLE=1,$
BACKGROUND_COLOR=[0,0,0],xrange=xr,yrange=yr,zrange=zr,$
xstyle=1,ystyle=1,zstyle=1,overplot=2,$
identifier=3,$
Name='Outer_Event_Horizon',$
/NO_SAVEPROMPT,user_interface='none'

isurface,zin,xin,yin,transparency=35,color=[72,72,255],$
BACKGROUND_COLOR=[0,0,0],XGRIDSTYLE=1,$
YGRIDSTYLE=1,overplot=3,macro_names=['axis_color'],$
xrange=xr,yrange=yr,zrange=zr,xstyle=1,ystyle=1,zstyle=1,$
identifier=4,xtitle='!8x[GM/c!S!E2!R]',,$
ytitle='!8y[GM/c!S!E2!R]',,ztitle='!8y[GM/c!S!E2!R]',,$
Name='Ergosphere',/NO_SAVEPROMPT,$
user_interface='none',/VIEWPLANE_RECT

ixyouts,titlestring,ALIGNMENT=0.5,COLOR=[255,255,255],$
FONT_SIZE=11,LOCATION=[0.0,0.45,1.0]

ixyouts,timestring,ALIGNMENT=1.0,COLOR=[255,255,255],$
FONT_SIZE=11,LOCATION=[0.45,0.42,1.0]

DEVICE,RETAIN=2

itool_write_graphic_kpb,name_jpg,type='jpeg',clobber=1,quality=100
ixyouts,timestring,ALIGNMENT=1.0,COLOR=[0,0,0],FONT_SIZE=11,$
LOCATION=[0.45,0.42,1.0]

progress=strcompress(it,/remove_all)+'/'+strcompress(n,/remove_all)
print,progress
endfor
cd,'../'

set_plot,'x'

end

```

Images are further processed with `mencoder` and outputted to an `.avi` file. Communication between the four programs (`findroot.x`, `bh.x`, `movies.pro` and `mencoder`) is achieved through an IDL-script (`code/idl/movies.sh`)

```

.r ixyouts.pro
.r itool_write_graphic_kpb.pro
.r movies.pro
movies,x,y,z,xin,yin,zin,xrs2,yrs2,zrs2
exit

```

and a bash-shell script (`code/movies.sh`).

```

echo "info:Running ./bh.x for the uniform_a=0.9 case."
ln -s inirel_uniform_a_0.9.txt inirel.txt
ifort -r16 findroot.f90 funcd.f90 rtbis.f90 open.f90 cstrip.f90 -o findroot.x
echo "info:findroot.f90,funcd.f90,rtbis.f90,open.f90,cstrip.f90,compiled"
./findroot.x
make bh.x
time ./bh.x
cp rtheta.dat ../results/rtheta_uniform_a_0.9.dat
cd ./idl
cp ../scratch.txt ../rtheta.dat ../scratch2.txt ../numofparticles.dat ./
idl movies.sh
cd ..
mencoder "mf://idl/jpg/*.jpg" -mf fps=10 -o movie.avi -ovc lavc -lavcopts vcodec=msmpeg4v2:
vbitrate=800
cp movie.avi ../results/movie_uniform_a_0.9.avi
rm inirel.txt
rm -r ./idl/jpg/*.jpg
echo

```

```
echo "info: Output written in rtheta_uniform_a_0.9.dat"
mail kdioni@physics.auth.gr -s "Test-run(a=0.9) has finished." < /dev/null
```

## A.2 Magnetic Field Lines

### A.2.1 Fortran

Program `field.x` solves the differential equations defined in `derivs.f90` using a 4<sup>th</sup> order Runge-Kutta scheme [29]. The components of the magnetic field are calculated using the derivatives of the vector potential specified in either `uniformB.f90` or `magnetize.f90` subroutines. The user has to define how many field lines are to be plotted, the number of steps for the implementation of the Runge-Kutta algorithm, the position of the ring current  $r_o$  and the rotation  $a$  of the black hole (`init.dat`).

```
program field
implicit none
integer :: n, nstep, numoflines, i, k
parameter (n=3)
double precision :: yrand(n)
double precision, allocatable :: xx(:, :), y(:, :, :), ystart(:, :)
double precision :: x1, x2, pi, Ic, rc, a
parameter (pi=3.14109265359d0)
integer :: i1, i2, i5
external derivs, cstrip

call open(i1, 'scratch.dat', 1, 'unknown')
call cstrip(i2, 'init.dat', i1)
read(i1, *) numoflines, nstep
read(i1, *) a, Ic, rc
close(i1)

Allocate(ystart(numoflines, n), y(numoflines, nstep+1, n), xx &
&(numoflines, nstep+1))

x1=0.d0
x2=36.7d0
call open(i5, "fieldlines.dat", 1, 'unknown')

do i=1, (numoflines)/4
ystart(i, 1)=10.d0
ystart(i, 2)=1.d-5+0.05d0*real(i)
ystart(i, 3)=0.d0
enddo
do i=(numoflines)/4+1, (numoflines)/2
ystart(i, 1)=10.d0
ystart(i, 2)=-pi+1.d-5+0.05d0*real(i-(numoflines)/4)
ystart(i, 3)=0.d0
enddo

do i=1, (numoflines)/2
call rkdumb(Ic, rc, a, i, numoflines, ystart, n, x1, x2, nstep, derivs, xx, y)
do k=1, nstep
print '(2I, 5e10.7)', i, k, y(i, k, 1), y(i, k, 2)
write(i5, '(2I, 4e22.14)') i, k, xx(i, k), y(i, k, 1), y(i, k, 2), y(i, k, 3)
enddo
enddo

do i=(numoflines)/2+1, 3*(numoflines)/4
ystart(i, 1)=10.d0
ystart(i, 2)=-1.d-5+0.05d0*real(i-(numoflines)/2)
ystart(i, 3)=0.d0
enddo
do i=3*(numoflines)/4+1, (numoflines)
ystart(i, 1)=10.d0
ystart(i, 2)=pi-0.05d0*real(i-3*(numoflines)/4)-1.d-5
ystart(i, 3)=0.d0
enddo

Ic=-Ic
```

```

do i=(numoflines)/2+1,numoflines
  call rkdump(Ic,rc,a,i,numoflines,ystart,n,x1,x2,nstep,derivs,xx,y)
  do k=1,nstep
    print '(2I,5e10.7)',i,k,y(i,k,1),y(i,k,2)
    write(i5,'(2I,4e22.14)')i,k,xx(i,k),y(i,k,1),y(i,k,2),y(i,k,3)
  enddo
enddo
close(i5)
deallocate(ystart,y,xx)
end

```

```

subroutine derivs (Ic,rc,a,x,y,dydx)
implicit none
double precision,dimension(3)::Bmag,y,dydx,y1,y2,Bmag1,Bmag2
double precision::x,mu,a,pi,Ic,rc
double precision::m,Atr,Attheta,Afr,Aftheta,grr,gff
double precision::gthetatheta,gtt,gtf,gf1,gffl,gttl
double precision::D,S,B,normB,gamma
parameter (m=1.d0,pi=3.14159265359d0)

  call magnetize(Ic,rc,a,y,Bmag,normB)

  S=y(1)**2+a**2*cos(y(2))**2
  D=y(1)**2+a**2-2.d0*m*y(1)
  B=(y(1)**2+a**2)**2-D*a**2*sin(y(2))**2

  dydx(1)=Bmag(1)/normB
  dydx(2)=Bmag(2)/normB
  dydx(3)=Bmag(3)/normB

  !print*,Bmag(1)/normB,Bmag(2)/normB,Bmag(3)/normB
end subroutine derivs

```

## A.2.2 IDL

This routine reads the data, calculated in program `field.x`, from file `fieldlines.dat` and plots the magnetic field lines. It also plots the ergosphere (blue surface) and outer event horizon (green surface). The output images are the ones illustrated in fig. 2.1 and 2.2.

```

pro field,x,y,z

get_lun,ldum
openr,ldum,"scratch.dat"
  readf,ldum,numofline,nstep
  readf,ldum,a,mu
close,ldum
free_lun,ldum

file="fieldlines.dat"
get_lun,ldum
openr,ldum,file

nstep=long(nstep)
r=fltarr(numofline,nstep)
theta=fltarr(numofline,nstep)
phi=fltarr(numofline,nstep)
x=fltarr(numofline,nstep)
y=fltarr(numofline,nstep)
z=fltarr(numofline,nstep)
s=fltarr(numofline,nstep)
print,nstep
for i=0l,numofline-1l do begin
  for lam=0l,nstep-1l do begin
    readf,ldum,line,numofstep,si,ri,thetai,phii
    s[i,lam]=si
    r[i,lam]=ri
    theta[i,lam]=thetai
    phi[i,lam]=phii
    x[i,lam]=sqrt(r[i,lam]^2+a^2)*sin(theta[i,lam])*cos(phi[i,lam])
  end
end

```

```

    y[i,lam]=sqrt(r[i,lam]^2+a^2)*sin(theta[i,lam])*sin(phi[i,lam])
    z[i,lam]=r[i,lam]*cos(theta[i,lam])
    ;print,line,numofstep,s(i,lam),x(i,lam),y(i,lam),z(i,lam)
  endfor
endfor
close,ldum
free_lun,ldum

rs1=1.d0-sqrt(1.d0^2-a^2)
rs2=1.d0+sqrt(1.d0^2-a^2)

DEVICE,RETAIN=2

ni=21
thetaangle=findgen(ni)
rerg=findgen(ni)
phiangle=findgen(ni)
thetaangle=thetaangle*(180/(ni-1))
phiangle=phiangle*(180/(ni-1))
xin=dblarr(ni,ni)
yin=dblarr(ni,ni)
zin=dblarr(ni,ni)
rin=dblarr(ni,ni)
thetaangle=thetaangle*!dpi/(180.d0)
phiangle=2.d0*phiangle*!dpi/(180.d0)

xrs2=dblarr(ni,ni)
yrs2=dblarr(ni,ni)
zrs2=dblarr(ni,ni)

for j=0,ni-1 do begin
  for i=0,ni-1 do begin
    xrs2[i,j]=sqrt(rs2^2+a^2)*cos(phiangle[i])*sin(thetaangle[j])
    yrs2[i,j]=sqrt(rs2^2+a^2)*sin(phiangle[i])*sin(thetaangle[j])
    zrs2[i,j]=rs2*cos(thetaangle[j])
  endfor
endfor

for j=0,ni-1 do begin
  rerg[j]=1.d0+sqrt(1.d0-a^2*(cos(thetaangle[j]))^2)
  for i=0,ni-1 do begin
    xin[i,j]=sqrt((rerg[j])^2+a^2)*cos(phiangle[i])*sin(thetaangle[j])
    yin[i,j]=sqrt((rerg[j])^2+a^2)*sin(phiangle[i])*sin(thetaangle[j])
    zin[i,j]=rerg[j]*cos(thetaangle[j])
    rin[i,j]=sqrt(xin[i,j]^2+yin[i,j]^2)
  endfor
endfor

window,xs=500,ys=500
range1=max(x,dimension=1,/absolute,/NAN)
range2=max(y,dimension=1,/absolute,/NAN)
range3=max(z,dimension=1,/absolute,/NAN)
range=[range1,range2,range3]
ranges=max(range,/NAN)
;xr=[-ranges,ranges]
;yr=[-ranges,ranges]
;zr=[-ranges,ranges]

xr=[-3,3]
yr=xr
zr=xr

Surface,zin,xin,yin,/SAVE,$
  xstyle=1,ystyle=1,xrange=xr,yrange=yr,$
  zrange=zr,zst=1,$
  ax=30,az=30,$
CHARSIZE=2.0,$
  xtitle='!3x_{G_{\mu}/c!S!E2!R_{\mu}}',ytitle='!3y_{G_{\mu}/c!S!E2!R_{\mu}}',$
  ztitle='!3z_{G_{\mu}/c!S!E2!R_{\mu}}',/noerase

iplot,x[0,*],y[0,*],z[0,*],identifier=1
for i=11,numofline-11 do begin
  plots,x[i,*],y[i,*],z[i,*],/t3d
  iplot,x[i,*],y[i,*],z[i,*],overplot=1,identifier=1;,color=[255,72,72]

```

```
endfor
isurface,zrs2,xrs2,yrs2,color=[0,240,0],XGRIDSTYLE=1,YGRIDSTYLE=1,$
    xrange=xr,yrange=yr,zrange=zr,$
    xstyle=1,ystyle=1,zstyle=1,overplot=1,$
    identifier=1,/NO_SAVEPROMPT,user_interface='none',$
    Name='Outer□Event□Horizon'

isurface,zin,xin,yin,transparency=35,color=[72,72,255],$
    XGRIDSTYLE=1,YGRIDSTYLE=1,overplot=1,$
    xrange=xr,yrange=yr,zrange=zr,xstyle=1,ystyle=1,zstyle=1,$
    identifier=1,xtitle='!8x□[GM/c!S!E2!R□]',$
    ytitle='!8y□[GM/c!S!E2!R□]',$
    ztitle='!8z□[GM/c!S!E2!R□]',$
    Name='Ergosphere',/NO_SAVEPROMPT,user_interface='none',$
    scale_isotropic=1

end
```



# Bibliography

- [1] M. Abramowicz, M. Jaroszynski, and M. Sikora. Relativistic, accreting disks. *A&A*, 63: 221–224, February 1978.
- [2] Milton Abramowitz and Irene A. Stegun. *Handbook of Mathematical Functions with Formulas, Graphs, and Mathematical Tables*. Dover, New York, 1972. ISBN 0-486-61272-4.
- [3] J. M. Aguirregabiria, A. Chamorro, K. R. Nayak, J. Suinaga, and C. Vishveshwara. Equilibrium of a charged test particle in the Kerr-Newman spacetime: force analysis. *Classical and Quantum Gravity*, 13:2179–2189, August 1996.
- [4] A. Beklemishev and M. Tessarotto. Covariant gyrokinetic description of relativistic plasmas. *A&A*, 428:1–19, December 2004.
- [5] A. Beklemishev and M. Tessarotto. Covariant descriptions of the relativistic guiding-center dynamics. *Physics of Plasmas*, 6:4487–4496, December 1999. doi: 10.1063/1.873736.
- [6] J. Bičák, V. Karas, and T. Ledvinka. Black holes and magnetic fields. In V. Karas and G. Matt, editors, *IAU Symposium*, volume 238 of *IAU Symposium*, pages 139–144, April 2007. doi: 10.1017/S1743921307004851.
- [7] R. D. Blandford and R. L. Znajek. Electromagnetic extraction of energy from Kerr black holes. *MNRAS*, 179:433–456, May 1977.
- [8] Z. Budinova, M. Dovciak, V. Karas, and A. Lanza. Magnetic fields around black holes. *ArXiv Astrophysics e-prints*, May 2000.
- [9] Max Camenzind. *Compact Objects in Astrophysics, (White Dwarfs, Neutron Stars and Black Holes)*. A&A Library, Springer. ISBN 9783540257707.
- [10] Sean M. Carroll. *Spacetime and geometry: An introduction to general relativity*. San Francisco, USA: Addison-Wesley (2004). ISBN 0805387323.
- [11] D. K. Chakraborty and A. R. Prasanna. Motion of the charged particles off the equatorial plane of a Kerr black hole in an electromagnetic field. *Pramana*, 19:141–150, 1982.
- [12] S. Chandrasekhar. *The Mathematical Theory of Black Holes (Oxford Classic Texts in the Physical Sciences)*. Oxford University Press, USA, October 1998. ISBN 0198503709.
- [13] Franchis F. Chen. *Introduction to Plasma Physics and Controlled Fusion*. Springer, 1873.
- [14] C. Cremaschini, M. Tessarotto, P. Nicolini, and A. Beklemishev. Generalized covariant gyrokinetic dynamics of magnetoplasmas. *ArXiv e-prints*, June 2008.
- [15] F. de Felice. On the non-existence of non-equatorial circular geodesics with constant latitude in the Kerr metric. *Physics Letters A*, 69:307–308, 1979.

- [16] F. de Felice, F. Sorge, and S. Zilio. Magnetized orbits around a Kerr black hole. *Classical and Quantum Gravity*, 21:961–973, February 2004. doi: 10.1088/0264-9381/21/4/016.
- [17] K. Elsässer. Quasineutral plasma equilibria in a Kerr metric. *Phys.Rev.D*, 65(2):024015–+, January 2002.
- [18] James B. Hartle. *Gravity: An Introduction to Einstein’s General Relativity*. Addison Wesley, December 2002. ISBN 0805386629.
- [19] V. Karas and D. Vokrouhlický. Dynamics of charged particles near a black hole in a magnetic field. *Journal de Physique I*, 1:1005–1012, July 1991.
- [20] R. Khanna. On the magnetohydrodynamic description of a two-component plasma in the Kerr metric. *MNRAS*, 294:673–+, March 1998.
- [21] S. S. Komissarov and J. C. McKinney. Meissner effect and blandford-znajek mechanism in conductive black hole magnetospheres. 2007.
- [22] J. Kovář, Z. Stuchlík, and V. Karas. Off-equatorial orbits in strong gravitational fields near compact objects. *Classical and Quantum Gravity*, 25:5011–+, May 2008. doi: 10.1088/0264-9381/25/9/095011.
- [23] L.-X. Li. Toy model for the Blandford-Znajek mechanism. *Phys.Rev.D*, 61(8):084016–+, April 2000.
- [24] C. W. Misner, K. S. Thorne, and J. A. Wheeler. *Gravitation*. San Francisco: W.H. Freeman and Co., 1973, 1973.
- [25] J. A. Petterson. Stationary axisymmetric electromagnetic fields around a rotating black hole. *Phys. Rev. D*, 12:2218–2225, October 1975.
- [26] A. R. Prasanna and S. Sengupta. Charged particle trajectories in the presence of a toroidal magnetic field on a Schwarzschild background. *Physics Letters A*, 193:25–30, September 1994. doi: 10.1016/0375-9601(94)00563-X.
- [27] A. R. Prasanna and R. K. Varma. Charged particle trajectories in a magnetic field on a curved space-time. *Pramana*, 8:229–244, 1977.
- [28] A. R. Prasanna and C. V. Vishveshwara. Charged particle motions in an electromagnetic field on Kerr background geometry. *Pramana*, 11:359–377, 1978.
- [29] W. H. Press, S. Teukolsky, T. M. Vetterling, and B. P. Flannery. *Numerical Recipes in Fortran 77*. Cambridge University Press, 2nd edition edition, 1996.
- [30] G. Preti. On charged particle orbits in dipole magnetic fields around Schwarzschild black holes. *Classical and Quantum Gravity*, 21:3433–3445, July 2004. doi: 10.1088/0264-9381/21/14/008.
- [31] Richard H. Price and Kip S. Thorne. The membrane paradigm for black holes. 258(4):45–55, April 1988. ISSN 0036-8733.
- [32] D’Inverno Ray. *Introducing Einstein’s Relativity*. Oxford University Press, USA. ISBN 0198596868.
- [33] S. Sengupta. Charged particle trajectories in a toroidal magnetic and rotation-induced electric field around a black hole. *International Journal of Modern Physics D*, 6:591–606, October 1997.
- [34] Nikolaos Spyrou. *Principles of Stellar Evolution (in Greek)*. Mavrogenis and Sons, 1994.

- [35] Carl Mulertz. Stormer. *The Polar aurora*. Clarendon Press, Oxford :, 1955.
- [36] S. A. Teukolsky. Perturbations of a Rotating Black Hole. I. Fundamental Equations for Gravitational, Electromagnetic, and Neutrino-Field Perturbations. *ApJ*, 185:635–648, October 1973.
- [37] Loukas Vlahos. *Plasma Physics (The fourth state of matter) (in Greek)*. Tziolas Publications, 2000.
- [38] D. Vokrouhlicky and V. Karas. Motion of charged particles around a black hole in a magnetic field. *A&A*, 243:165–167, March 1991.
- [39] R. M. Wald. Black hole in a uniform magnetic field. *Phys. Rev. D*, 10:1680–1685, 1974.
- [40] R. L. Znajek. Charged current loops around Kerr holes. *MNRAS*, 182:639–646, March 1978.